INVESTIGATIONS ON COMPACT UNI-PLANAR ANTENNAS FOR WIRELESS COMMUNICATIONS

Thesis submitted by

SREENATH S

in partial fulfillment of the requirements

for the award of the degree of

DOCTOR OF PHILOSOPHY

Under the guidance of

Prof. C. K. AANANDAN

Department of Electronics
Faculty of Technology
Cochin University of Science and Technology
Cochin - 682 022, Kerala, India

November 2016

INVESTIGATIONS ON COMPACT UNI-PLANAR ANTENNAS FOR WIRELESS COMMUNICATIONS

Ph.D. Thesis under the Faculty of Technology

Author:
SREENATH S
Microwave Propagation Research Lab
Department of Electronics
Cochin University of Science and Technology
Cochin - 682 022, Kerala, India.
Email: sreenathatholi@gmail.com

Supervisor:
Dr. C. K. Aanandan
Professor
Microwave Propagation Research Lab
Department of Electronics
Cochin University of Science and Technology
Cochin - 682 022, Kerala, India.
Email:aanandan@gmail.com

Department of Electronics
Cochin University of Science and Technology
Cochin - 682 022, Kerala, India.
www.doe.cusat.edu

November 2016

Dedicated to my family, teachers and dear ones.....

DEPARTMENT OF ELECTRONICS
COCHIN UNIVERSITY OF SCIENCE AND TECHNOLOGY
COCHIN – 682 022

Prof. C. K. Aanandan
(Supervising Guide)
Professor
Department of Electronics
Cochin University of Science and Technology

Certificate

This is to certify that this thesis entitled **"Investigations on compact uni-planar antennas for wireless communications"** is a bonafide record of the research work carried out by Sreenath.S under my supervision in the Department of Electronics, Cochin University of Science and Technology. The results embodied in this thesis or parts of it have not presented for any other degree.

I further certify that the corrections and modifications suggested by the audience during the pre-synopsis seminar and recommended by the Doctoral committee of Mr. Sreenath.S are incorporated in the thesis.

Cochin – 22
November 2016   **Prof. C. K. Aanandan**

Declaration

I hereby declare that the work presented in this thesis entitled "**Investigations on compact uni-planar antennas for wireless communications** "is based on the original research work carried out by me under the supervision and guidance of Prof. C. K. Aanandan, Professor, Department of Electronics, Cochin University of Science and Technology, Cochin-682 022 and has not been included in any other thesis submitted previously for the award of any degree.

Sreenath S
Research scholar,
Department of Electronics,
CUSAT,

Cochin - 22
November 2016

Cochin-22.

Acknowledgments

Abstract

Antenna research and engineering is gaining more and more attention in the modern day world as every human being is carrying a gadget which uses wireless communication. Integration of multiple applications such as WLAN, bluetooth, GPS etc. into a single gadget requires antennas which can operate in all these frequency bands. Short range high data rate communication requires wide bandwidth signals for transmission. UWB communication is gaining more and more interest due to its wide bandwidth and high data rate.

In the Present thesis we are studying various types of uniplanar antennas. These antennas are fed either by Open/Closed ended coplanar strips or co planar waveguide. Four noval antennas based on these transmission lines are discussed in the thesis which includes

1. CPS fed dipole antenna for PCS1900/WLAN applications

2. Slotline fed uniplanar antenna for 2.4 GHz/ 5.8 GHz WLAN applications

3. Slot line coupled wideband slot radiator for 5.2GHZ/5.8GHz WLAN applications

4. CPW fed compact bent monopole antenna for UWB applications

These antenna designs and their evolution are studies using the commercially available simulation tools and verified experimentally. Emperical design equations are formulated and verified for all the four antennas. All the frequency domain parameters such as gain, efficiency , return loss and their radiation pattern are determined experimentally which substantiate the use of these antennas for various wireless bands. The thesis deals with UWB antenna in its fourth chapter.

Even if the antenna has good frequency domain response, for using it in UWB pulse applications, the time domain parameters such as fidelity , group delay and pulse distortion etc have to be estimated. These parameters are analyzed for the proposed antenna and the values are found to be acceptable for UWB applications.

List of Figures

List of Tables

List of Abbreviations

CPW .... Coplanar Waveguide

CPS .... Coplanar Strip

DCS .... Digital Communication System

EMI .... Electro Magnetic Interference

EMC .... Electro Magnetic Coupling

EIRP .... Effective Isotropic Radiated Power

FCC .... Federal Communication Commission

LTI .... Linear Time Invarient

PCB .... Printed Circuit Board

PCS .... Personal Communication System

PIFA .... Planar Inverted- F Antenna

PILA .... Planar Inverted L Antenna

PSD .... Power Spectral Density

Q-factor ...... Quality Factor

UMTS .... Universal Mobile Telecommunications System

UWB .... Ultra Wide Band

VSWR .... Voltage Standing Wave Ratio

WLAN .... Wireless Local Area Network

RFID .... Radio Frequency Identification

GPS .... Global Positioning System

RCS . . . . Radar Crossection System

PBG . . . . Photonic Band Gap

Contents

Chapter 1

Introduction and Review of Literature

> *This chapter briefs the development in antenna engineering. The contributions by eminent researchers in Electromagnetics are discussed with special emphasis on the literature which explains the growth in the area of planar antenna technology. Chapter concludes with a description of the motivation towards the current topic. The organization of the chapters in the thesis are also discussed.*

Contents

1.1   Introduction

Antennas are inevitable component of modern wire free world which is used for transmitting and receiving electromagnetic waves. Antenna converts radiations into current and vice versa [1, 2]. Antenna is a transition between transmission lines to free space. It matches the free space impedance to that

of the transmission line. For an efficient communication system, the antennas have to be designed with care so as to acquire maximum radiation with minimal cost of production and environmental compatibility. An efficient antenna minimizes the system needs thus improving the performance as a whole. The use of the antenna are not only limited to communication but also to various applications like remote sensing, diagnostics and therapeutic applications, radars, GPS etc. Ever since the human evolution, the communication is the rapidly developing area for information interchange.

1.2 Important Milestones in Communication

As we know that the world is changing as Wire free world, it is crucial for us to understand how the transitions and improvement of technology took place. In 1873 the mutual relationship between an electric field and magnetic field was mathematically demonstrated by James Clerk Maxwell. According to him, light is an EM wave. Every electromagnetic wave propagates through vacuum with a speed same as that of light [3]. Maxwells theory was experimentally supported by Heinrich Rudolph Hertz [4,5]. He built the first wireless system using electromagnetic waves in 1886. It used a dipole as a transmitter and a loop as a receiver. A transmission of around 20m was possible.

Guglielmo Marconi did the first commercial wireless transmission over a long distance in 1897 [6]. He started first transatlantic wireless transmission using electromagnetic waves in 1909.

Jagadish Chandra Bose studied the properties of millimeter waves in the same period. The major components used by him for the experiments were polarizers, waveguides, horn antennas, and semiconductors. Horn antenna is one of his major contributions [7,8].

Karl Jansky of Bell Labs used the large antennas designed by him to discover extraterrestrial radio waves [9]. He is known as the father of astronomy. The invention of the Yagi-Uda antenna was in the same period [10].

Second World War witnessed the most important inventions in antennas and radar. Most of the research and development during this period were

associated with military applications. The major inventions during this period were the large reflector array antennas, realization of phased arrays and satellite antennas. The basic ideas of the adaptive array also experimentally demonstrated [11, 12]. The period after world War II two leads towards the developments of the microwave generators such as Magnetron and klystrons. This again accelerated the growth in the field of antennas. The introduction of the Microstrip antenna by Deschamps in 1953 revolutionized the antenna design [13]. The realization and large scale production of microstrip antenna took almost 20 years. Active and Smart antenna arrays were developed during this period [14–17].

1.3 Planar Antennas - Technologies and Developments

This thesis presents the design and development of various uniplanar antennas. The existing planar antenna technologies is reviewed and summarized in the following section.

The commonly used wireless communication bands and their allocated frequency is shown in Fig 1.1. These are the communication bands as per FCC and ITU [18–21].

1.3.1 Microstrip Antennas

The transformation of the large 3D antennas to the compact planar structures started after the invention of microstrip antennas. Microstrip antenna was first realized experimentally in 1970. The significance of Microstrip antennas were low profile and excellent radiation characteristics. One side of a substrate consists of the metal patch, which can be of different shapes. The back side of the substrate is a metal ground plane. Fig 1.2 shows a basic rectangular patch antenna. The length of the patch decides the frequency of operation. The length is equivalent to half the wavelength of the resonance frequency [22–24]. The use of a high-permittivity substrate results in the size reduction of the antenna but results in reduced efficiency and bandwidth. The use of

COMMONLY USED WIRELESS COMMUNICATION BANDS

RFID

865 - 868 MHz

2.446 - 2.454 GHz

GSM 900

890 - 960 MHz

DCS

1710 -1880 MHz

PCS

1850-1990 MHz

IMT2000
1885 -2200 MHz

UMTS 2000
1920-2170 MHz

GPS

1227-1575 MHz

1565-1585 MHz

ISM2.4

2400-2484 MHz

ISM5.2
5150-5350 MHz

ISM5.8
5725-5825 MHz

UWB(Ultra Wide Band)
3.1-10.6(GHz)
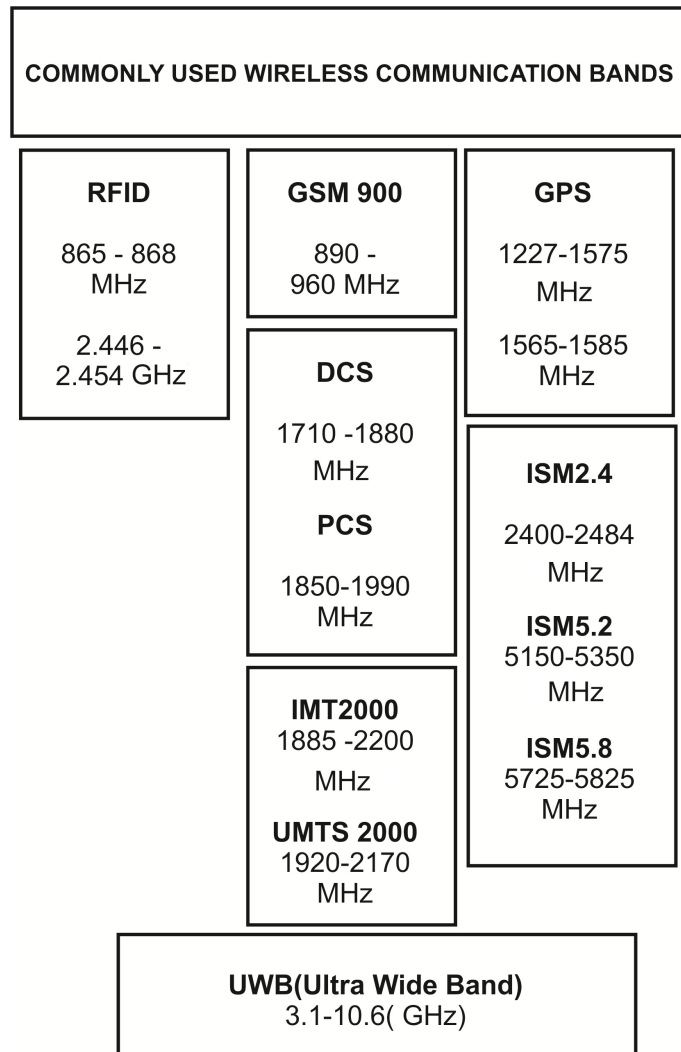
Figure 1.1: Commonly used frequency bands

low permittivity substrates results in enhanced bandwidth but antenna size increases. Low profile, ease of fabrication, less weight, compatibility with conformal and planar antennas is the major advantages of the Microstrip antennas [25, 26]. The significant limitation of the microstrip antenna is its low bandwidth of operation, which is due to the high Q-factor of the antenna. A slight increase in bandwidth can be achieved by increasing the substrate thickness. The surface waves [27, 28] are increased because of this, which in turn deteriorates the efficiency of the antenna.
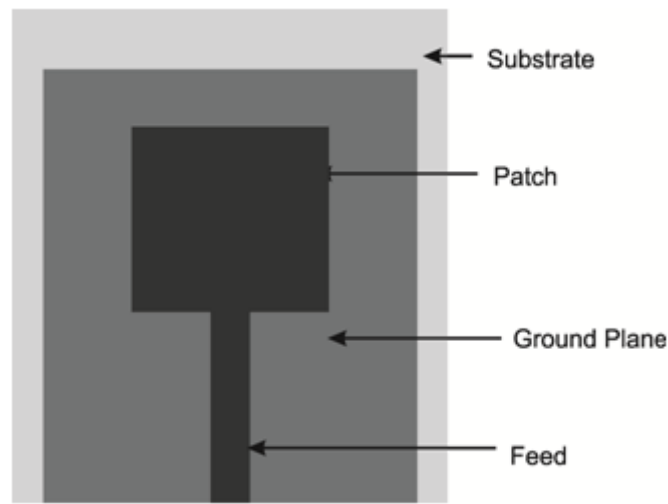
Figure 1.2: Basic microstrip fed rectangular patch antenna

The presence of the ground plane resulted in an unipolar(directional) radiation from the microstrip antenna [29]. Thus the uses of these antennas in applications which require Omni-directional radiation pattern are limited. Many studies have been performed to reduce the disadvantages of microstrip antennas. Mailloux [30] proposed cavity backing for reducing the surface waves. The bandwidth of the microstrip antennas can be increased by staking [31] of the multiple patches. Aperture coupling and slot coupling are also utilized for the bandwidth enhancement [32, 33]. Other methods for increasing the bandwidth includes slot coupling [34], incorporation of parasitic strips [35], using different feed shapes and etching slots with various shapes [36,37]. There are many bandwidth enhancement techniques like Stacking [31], Aperture coupling [32], Proximity coupling [33], Slot coupling [34], the addition of parasitic

elements [35], use of different feed geometries and slots [36–40] etc which can be implemented in microstrip antennas. Integrating multiple frequency bands in a single antenna is a modern day communication demand. The various dual band and multiband microstrip antennas are discussed. An additional resonance is excited by inserting multiple shorting pins in the patch [41]. The metallization from the patch or the ground is peeled off to form the slot, which also excites multiple resonances [42]. Circularly polarized patch antennas are also studied [43]. All these enhancements lead to only a minor increase in bandwidth. The radiation pattern of the microstrip antenna is directional because of the presence of a ground plane. Microstrip monopole configurations are used to overcome these limitations [44]. The next section details truncated ground microstrip antennas.

1.3.2 Microstrip Monopole Antennas

Microstrip-fed monopole antennas are the planar version of the wire monopole antennas. The part of the ground plane which is far from the feed is cut to form the monopole configuration. The monopole configuration is shown in Fig 1.3. The signal strip is extended beyond the truncated ground. The length of the signal strip above the truncated ground plane determines the resonant frequency. Since this antenna is a quarter wave radiator, it will be more compact when compared to the conventional patch antennas. The selectivity (Q-factor) of these antennas will be low.

The attractive features of these antennas are Omni-directional radiation pattern, broad bandwidth and simplicity in production. Monopoles are top loaded with various shapes to enhance the bandwidth. All the usual wireless bands are covered within this bandwidth [45, 46]. Truncation of the ground plane leads to the excitation of a new resonance near to the quarter wave resonance of the monopole. These two resonances are merged to give wideband response [47]. The truncated Microstrip antenna due to inherent wide bandwidth is suitable for designing ultra wideband antennas. Several UWB antennas of this type are there in the literature [48–51]. Plenty of dual band and multiband antennas with microstrip monopole designs are in the literature. [52–56].
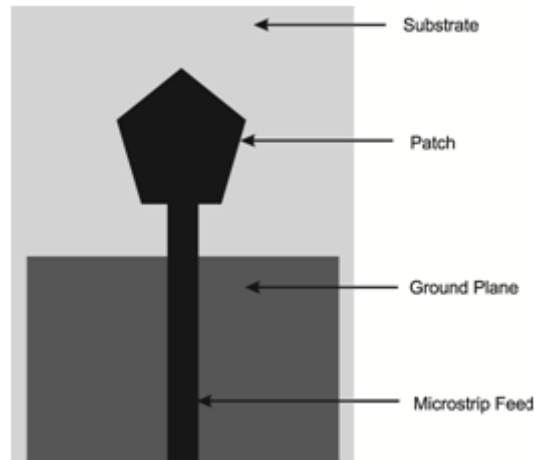
Figure 1.3: Microstrip-fed monopole antenna

Microstrip-fed antennas contain the signal strip at the top layer and the ground plane at the bottom layer. The fabrication process needs extreme care. Integration of active devices is done using drilling holes and connecting vias. This back side processing is complicated and the need for uni-planar antennas is having increased demand in the modern day antenna engineering. The radiating elements of uniplanar antennas are fabricated on the same surface. Integration of the active and passive elements easy. The fabrication process is also simple in this case. Basic uniplanar transmission lines include slotline/Coplanar Strips and coplanar waveguide(CPW). This thesis discusses the developments in antennas fed by uniplanar transmission lines.

1.3.3 CPW Fed Antennas

CPW fed antennas are getting wider interest these days due to its uniplanar unbalanced design. A narrow PEC strip which carries the signal is placed at the center. The ground strips are placed on the either sides of the signal strip. A small gap separates the signal strip and the ground. Fig 1.4 depicts a Pentagon monopole antenna with CPW feed.

The various single band and multiband CPW fed antennas are there in the literature [57–59]. Asymmetric coplanar waveguide fed antennas are also analyzed for making the antennas more compact [60]. CPW feeding is also
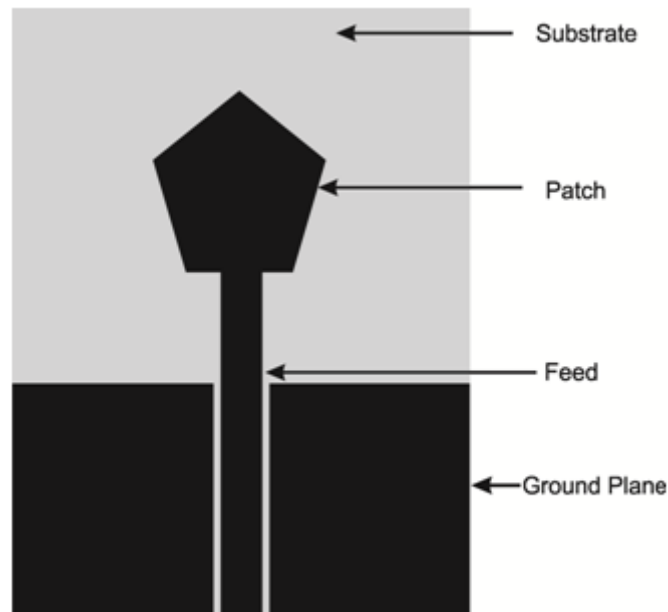
Figure 1.4: CPW fed pentagon monopole antenna

used for designing dielectric resonator antennas which are discussed in the next section. The above mentioned antennas are either half-wave or quarter-wave radiators. Improved compactness is required so as to integrate these antennas in modern gadgets. A variety of methods are adopted for making these antennas more compact. This includes the PBG (photonic band gap) structures, fractal geometry based antennas and metamaterial inspired designs [61–84].

1.3.4   PBG Structures in Antennas

To enhance the bandwidth and gain of the antennas, the most widely used structures are the PBG (Photonic Band Gap). They attenuate the propagation of electromagnetic signals in certain spatial direction and for certain frequencies [61, 62]. In the case of Microstrip antennas bandwidth enhancement without affecting the efficiency of the antenna can be achieved by the use of PBG structures in the ground plane. The surface wave propagation is reduced and the use of PBG enhances the gain of the antenna. Various

PBG designs for enhancing the gain, bandwidth, and harmonic suppression are analyzed [63–66].

1.3.5 Metamaterial-based Antennas

Metamaterials induced a revolutionary change in designing compact antennas and in the field of Electromagnetics. Although the first metamaterial was developed in 1940s, it took 50 long years for the extensive research and development in the area. V.G Veselago proposed Left-Handed media (LHM) for the materials which possess negative permittivity and permeability [67]. All the vectors E, H, k have a negative value that is they are forming a left-hand triplet. The permeability and permittivity functions can be simultaneously converted into negative value by the use of an array of split ring resonators and strips. These types of materials are proposed in the recent literature [68, 69]. Such materials can be used for reducing overall dimensions of the MMIC circuits [70–73].

1.3.6 DRA (Dielectric Resonator Antennas)

Dielectric material cut in a specific shape will act as a microwave frequency resonator with the guided wavelength less than that of the free space wavelength. Since the radiating part is non-metallic, the ohmic loss [74] will be less. Thus the overall efficiency of the antenna will be more. The application of dielectric resonators are not only limited to antennas, but it is also used in filters, oscillators etc. Various modes exist in a DRA. The radiation characteristics of the DRA depend upon the excited mode. The dielectric resonator antennas are fed by CPW or Microstrip transmission lines. Fig 1.5 shows DRA fed by CPW.

The advantages of DRA include the high efficiency, easy coupling from the transmission lines and small size. By varying the dielectric constant and the dimensions of the dielectric material the characteristics such as resonance and bandwidth can be controlled. Various DRAs designed with improved bandwidth, circular polarization and for use in antenna arrays are discussed
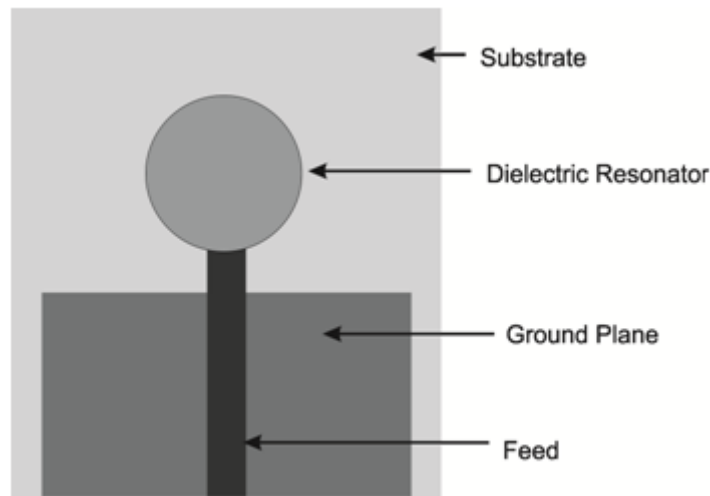
Figure 1.5: Dielectric resonator loaded monopole antenna

in the literature [75–81]. These characteristics make the DRA one of the favorites among the antenna designers.

1.3.7 PIFA (Planar Inverted-F Antennas)

The current mobile communication is not only limited to the voice communications. The number of new mobile users are increasing at an alarming rate, which necessitates a large bandwidth of operation. Modified microstrip and coplanar waveguide configurations are reported in the literature for bandwidth enhancement and multiband operations [82, 83]. The incompatibility of the size of these antennas with the mobile handset led to the development of planar PILA (planar inverted-L) and PIFA. They replaced the conventional monopole antennas in the mobile handsets. Fig 1.6 depicts a basic PIFA antenna.

The PIFA geometry includes a ground plane, a metal patch, the feeding pin and the shorting pin. PIFA resembles the patch antenna but the resonant length is a quarter waves long. A shorting plate that connects the one end of the patch and the ground plane are also available [84, 85]. The size of the PIFA is very low but still it has the limitation of being narrow band. Ground plane modifications and change in feed type are proposed for enhancing the
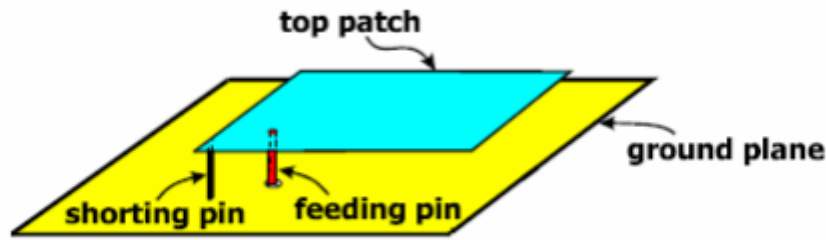
Figure 1.6: PIFA geometry

bandwidth [86, 87]. Various Multiband PIFA antennas are also available in the literature which makes use of the insertion of slits, stalking, etc. [88, 89].

1.3.8   UWB Antennas

UWB technology is promising in the modern day world due to its applications in communication, radar, and medical field. UWB technology transmits pulses with short duration. The qualities of the UWB antenna makes them superior [90–92]. According to FCC, any system which occupies a bandwidth of 500MHz or more can be treated as UWB. The frequency spectrum defined by FCC for commercial UWB systems are from 3.1 GHz to 10.6 GHz [93]. Many researchers contributed towards the development of UWB technology for various applications [94–98].

The comparison of the spectrum utilization by a UWB system to the narrowband system is revealed in Fig 1.7. The PSD in the case of narrow band systems is high. However, in the case of UWB system, it is very low. Because of this low power spectral density, there wont be any interference between the conventional narrow band systems. Ultra wideband antenna design includes a bit of challenge. The design of UWB antenna requires the analysis in time domain and frequency domain since we transmit signal with broad bandwidth, that is short pulses are used for the transmission. Along with the frequency domain parameters, the quality of a UWB antenna is defined by the time domain parameters such as group delay, impulse response, and phase response. Two types of requirements present in the UWB antenna design are the physical requirements and the electrical requirements. There
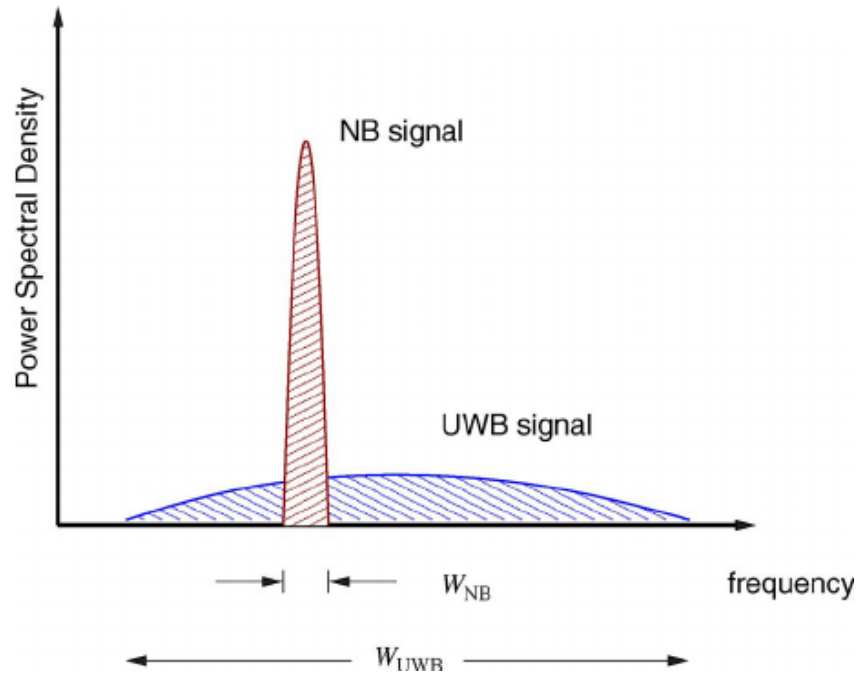
Figure 1.7: UWB signal spectrum utilization over narrow band signal

should be a compromise between these two requirements. The antenna size, profile, the cost of design and fabrication and the integration with MMIC element are some of the physical constraints. The electrical constraints include gain stability in the whole band, the radiation pattern according to the requirements, and constant polarization over the entire band etc. UWB antennas are mainly three types according to these design constraints. They are multi-resonant antennas, frequency independent antennas and traveling wave antennas. The ultra wideband characteristics in a multi-resonant antenna are formed by using more than one narrowband radiating lengths. Examples of these types of the antenna include Yagi antenna and log periodic antenna. These antennas have UWB characteristics but they are not useful for impulse radio UWB systems due to the dispersion of the pulses which arise since the phase centers of the antenna are not fixed in frequency. Travelling wave antennas are good contenders for UWB applications. Tapered slot antenna and the horn antennas are examples of this type. Horn antennas are high gain directional UWB antennas which are commonly used as standards in radiation

measurements and feed for reflectors. These antennas possess same polarization over the entire band, constant group delay, and very low dispersion. Vivaldi antennas also come under this classification [99, 100]. Bowtie antenna (biconical), spiral and conical antennas are structures which are frequency independent [101, 102]. Fractal antennas and log spiral antennas, which are considered as complementary antennas characterized by self-complementary characterization [103–105]. Log periodic antennas are also this type [106–108]. Electrically small antennas are exceptional candidates for UWB applications as the antenna size is small compared to the wavelength. Monopole antennas can be modified for this purpose [109–116]. UWB antennas with notched WLAN bands from 5 to 6 GHz are reported [117–120]. Plenty of literature on directional UWB antennas is available. Applications of the directional UWB antennas are in ground penetrating radars, medical applications such as microwave imaging. Vivaldi antennas and exponentially tapered slot antennas come under these types of antennas which is of large size. The radiation characteristics will not be same over the entire bandwidth. [121–127].

1.4   Motivation Towards the Present Work

Antennas are indispensable part of any communication system. Antennas play a vital role in day to day living of every human being. Every human being carries an antenna knowingly or unknowingly in the form of electronic gadgets. The design procedure of an antenna has to meet several goals which have to be achieved considering certain constraints. The basic theory of antenna design is to create a discontinuity in the transmission line by structural changes. The uniplanar antennas are significant in the antenna design due to the less complexity in design and fabrication, low cost and the lack of backside processing. The uniplanar transmission lines considered here is the Slotline/Coplanar strip and the coplanar waveguide.

A coplanar strip or the slot line is an inefficient transmission line when they are fabricated on a low permittivity substrate. For transmitting power through CPS transmission lines we have to use dielectric substrates with high permittivity for confining the electric field across the slot. However, this

property of the slot line can be effectively utilized in designing antennas with high efficiency, enhanced gain, and good radiation properties. Open ended CPS can be effectively transformed into an efficient radiator. The CPS can also be converted into a half wavelength radiator when one end is shorted. The closed-ended CPS configuration can be modified to make it an excellent radiator, by using it as a feeding element through electromagnetic coupling to the adjacent slots made in the metal plane. The number of research works on CPS antennas or the slot line antennas is very few [128–132]. Another uniplanar transmission line is the coplanar waveguide. The ground and the signal strip can be modified to make it as an efficient radiator. UWB antennas and their applications are widespread in the modern day world. All the UWB antenna designs are mainly the monopole antenna. The efforts to make a simple UWB antenna from the basic quarter wave monopole are analyzed and done in the present thesis. How can antenna design be made simple? This question is tried to be answered in the present thesis. The transformation of the transmission line to the antenna with simple geometrical modifications for various microwave communication bands are studied. developments of antennas with less geometrical parameters and simple structure transformed from the basic uniplanar transmission lines is the main theme of the thesis.

1.5   Organisation of the Thesis

The Thesis is organized into six chapters.

Chapter 1 focuses on the historical developments in the wireless technologies and evolution of the planar antennas. Antennas in literature for various applications are reviewed and motivation towards the present work is also discussed.

Chapter 2 Basic Antenna parameters and their measurement techniques are discussed briefly in this chapter. Instruments used and the tools for simulations are also discussed. Time domain antenna parameters and their measurements are discussed in detail.

Chapter 3 explains the Open ended slotline antennas. Various transmission lines are reviewed and the detailed study of Open ended slot line with reduced length is performed. How to create radiation from an open ended slot line is investigated and the analysis of the single band antenna is done. The evolution of the dual band antenna for PCS/WLAN applications from a basic OES is discussed and its characteristics are studied. The design equations of the antenna are formed and validated on different substrates.

Chapter 4 gives a detailed analysis of the closed ended slot line antennas. Advantages of the closed ended slot line over the open ended slot line are discussed. The characteristics of a basic closed-ended slotline are studied. The evolution of the Slot line fed uniplanar antenna for 2.4/5.8 GHz WLAN bands from the basic closed ended slot line are explained. Radiation characteristics of this antenna are analyzed and the design equations are formed and validated.

Chapter 5 deals with designing UWB antenna using CPW feed. Various methods available for designing UWB antennas are discussed. The evolution of the CPW fed compact bent monopole antenna for UWB applications from a quarter wave monopole antenna is discussed. Radiation characteristics of the antenna are analyzed in the frequency domain. Pulse handling capacity of the antenna is studied. The design equations of the antenna are formed and validated on different substrates.

Chapter 6 concludes the highlights of the works in the thesis. Scope for future work on the Slot line fed antenna and the CPW fed UWB antennas are discussed.

REFERENCES

[1] "IEEE Standard for Definitions of Terms for Antennas," *IEEE Std 145-2013 (Revision of IEEE Std 145-1993)*, pp. 1–50, March 2014.

[2] "The antenna theory website." [Online]. Available: http:// www. antenna-theory.com/, (Accessed on 21-12-2012)

[3] J. C. Maxwell, *A treatise on electricity and magnetism.* Clarendon press, 1881, vol. 1.

[4] P. S. Carter and H. H. Beverage, "Early history of the antennas and propagation field until the end of world war i, part i - antennas," *Proceedings of the IRE*, vol. 50, no. 5, pp. 679–682, May 1962.

[5] J. D. Kraus and R. J. Marhefka, "Antenna for all applications," *Upper Saddle River, NJ: McGraw Hill*, 2002.

[6] J. Kraus, "Antennas since hertz and marconi," *IEEE Transactions on Antennas and Propagation*, vol. 33, no. 2, pp. 131–137, February 1985.

[7] J. F. Ramsay, "Microwave antenna and waveguide techniques before 1900," *Proceedings of the IRE*, vol. 46, no. 2, pp. 405–415, Feb 1958.

[8] G. L. Pearson and W. H. Brattain, "History of semiconductor research," *Proceedings of the IRE*, vol. 43, no. 12, pp. 1794–1806, Dec 1955.

[9] T. K. Sarkar and D. L. Sengupta, "An appreciation of j.c. bose's pioneering work in millimeter waves," *IEEE Antennas and Propagation Magazine*, vol. 39, no. 5, pp. 55–62, Oct 1997.

[10] K. G. Jansky, "Electrical disturbances apparently of extraterrestrial origin," *Proceedings of the Institute of Radio Engineers*, vol. 21, no. 10, pp. 1387–1398, Oct 1933.

[11] M. Skolnik, "Radar: From hertz to the 21st century," *IEEE Antennas and Propagation Society Newsletter*, vol. 30, no. 5, pp. 13–18, October 1988.

[12] S. Uda, "Wireless beam of short electric waves," *Iet Software/iee Proceedings - Software*, pp. 273–282, March 1926.

[13] A. C. Schell, "Antenna developments of the 1950s to the 1980s," in *Antennas and Propagation Society International Symposium, 2001. IEEE*, vol. 1. IEEE, 2001, pp. 30–33.

[14] Deschamps G. A, "Microstrip microwave antennas," *III rd USAF Symposium on Antennas*, 1953.

[15] W. A. Imbriale, "Evolution of the large deep space network antennas," *IEEE Antennas and Propagation Magazine*, vol. 33, no. 6, pp. 7–19, Dec 1991.

[16] O. Edvardsson, "Recent advances in handset antennas for satellite communication," in *Antennas and Propagation Society International Symposium, 2001. IEEE*, vol. 4.   IEEE, 2001, pp. 553–556.

[17] Y. Qian and T. Itoh, "Progress in active integrated antennas and their applications," *IEEE Transactions on Microwave Theory and Techniques*, vol. 46, no. 11, pp. 1891–1900, Nov 1998.

[18] Binu Paul, "Development and analysis of microstrip antennas for dualband microwave communication," *Ph.D. thesis, Cochin University of Science and Technology*, 2005.

[19] T. K. Sarkar, R. Mailloux, A. A. Oliner, M. Salazar-Palma, and D. L. Sengupta, *History of wireless*.   John Wiley & Sons, 2006, vol. 177.

[20] "Itu: Committed to connecting the world." [Online]. Available: http://www.itu.int/, (Accessed on 10-10-2012)

[21] "Federal communications commission — the united states of america." [Online]. Available: http://www.fcc.gov/ (Accessed on 10-10-2012)

[22] C. A. Balanis, *Antenna theory: analysis and design*.   John Wiley & Sons, 2016.

[23] D. M. Pozar, "Microstrip antennas," *Proceedings of the IEEE*, vol. 80, no. 1, pp. 79–91, Jan 1992.

[24] David M. Pozar, "Microstrip antennas: The analysis and design of microstrip antennas and arrays," *Wiley-IEEE Press*, May 1995.

[25] S. D. A. Fonseca and A. Giarola, "Microstrip disk antennas, part i: Efficiency of space wave launching," *IEEE Transactions on Antennas and Propagation*, vol. 32, no. 6, pp. 561–567, Jun 1984.

[26] S. D. A. Fonseca and A. Giarola, "Microstrip disk antennas, part i: Efficiency of space wave launching," *IEEE Transactions on Antennas and Propagation*, vol. 32, no. 6, pp. 561–567, Jun 1984.

[27] J. Huang, "The finite ground plane effect on the microstrip antenna radiation patterns," *IEEE Transactions on Antennas and Propagation*, vol. 31, no. 4, pp. 649–653, Jul 1983.

[28] C A Balanis, "Advanced engineering electromagnetics," *John Wiley & Sons, New York*, 1989.

[29] Ramesh Garg, Prakash Bhartia , Inder Bahl, "Microstrip antenna design handbook," *1st ed. MA Artech House*, 2001.

[30] R. Mailloux, "On the use of metallized cavities in printed slot arrays with dielectric substrates," *IEEE Transactions on Antennas and Propagation*, vol. 35, no. 5, pp. 477–487, May 1987.

[31] S. Long and M. Walton, "A dual-frequency stacked circular-disc antenna," *IEEE Transactions on Antennas and Propagation*, vol. 27, no. 2, pp. 270–273, Mar 1979.

[32] C. Tsao, Y. Hwang, F. Kilburg, and F. Dietrich, "Aperture-coupled patch antennas with wide-bandwidth and dual-polarization capabilities," in *Antennas and Propagation Society International Symposium, 1988. AP-S. Digest.* IEEE, 1988, pp. 936–939.

[33] D. M. Pozar and B. Kaufman, "Increasing the bandwidth of a microstrip antenna by proximity coupling," *Electronics Letters*, vol. 23, no. 8, pp. 368–369, April 1987.

[34] A. Ittipiboon, B. Clarke, and M. Cuhaci, "Slot-coupled stacked microstrip antennas," in *Antennas and Propagation Society International Symposium, 1990. AP-S. Merging Technologies for the 90's. Digest.* IEEE, 1990, pp. 1108–1111.

[35] C. K. Aanandan, P. Mohanan, and K. G. Nair, "Broad-band gap coupled microstrip antenna," *IEEE Transactions on Antennas and Propagation*, vol. 38, no. 10, pp. 1581–1586, Oct 1990.

[36] S. Mridula, S. K. Menon, B. Lethakumary, B. Paul, C. K. Aanandan, and P. Mohanan, "Planar l-strip fed broadband microstrip antenna," *Microwave and Optical Technology Letters*, vol. 34, no. 2, pp. 115–117, 2002.

[37] J. George, K. Vasudevan, P. Mohanan, and K. G. Nair, "Dual frequency miniature microstrip antenna," *Electronics Letters*, vol. 34, no. 12, pp. 1168–1170, Jun 1998.

[38] B. Lethakumary, S. K. Menon, C. K. Aanandan, and P. Mohanan, "A wideband rectangular microstrip antenna using an asymmetric t-shaped feed," *Microwave and Optical Technology Letters*, vol. 37, no. 1, pp. 31–32, 2003.

[39] B. Paul, S. Mridula, C. K. Aanandan, and P. Mohanan, "A new microstrip patch antenna for mobile communications and bluetooth applications," *Microwave and Optical Technology Letters*, vol. 33, no. 4, pp. 285–286, 2002.

[40] M. Paulson, S. O. Kundukulam, C. K. Aanandan, P. Mohanan, and K. Vasudevan, "Compact microstrip slot antenna for broadband operation," *Microwave and Optical Technology Letters*, vol. 37, no. 4, pp. 248–250, 2003.

[41] S. I. Latif, L. Shafai, and S. K. Sharma, "Bandwidth enhancement and size reduction of microstrip slot antennas," *IEEE Transactions on Antennas and Propagation*, vol. 53, no. 3, pp. 994–1003, March 2005.

[42] S. O. Kundukulam, M. Paulson, C. K. Aanandan, and P. Mohanan, "Slot-loaded compact microstrip antenna for dual-frequency operation," *Microwave and Optical Technology Letters*, vol. 31, no. 5, pp. 379–381, 2001.

[43] Nasimuddin, K. P. Esselle, and A. K. Verma, "Wideband circularly polarized stacked microstrip antennas," *IEEE Antennas and Wireless Propagation Letters*, vol. 6, pp. 21–24, 2007.

[44] Z. N. Chen, M. J. Ammann, X. Qing, X. H. Wu, T. S. p. See, and A. Cai, "Planar antennas," *IEEE Microwave Magazine*, vol. 7, no. 6, pp. 63–73, Dec 2006.

[45] M. J. Ammann and M. John, "Optimum design of the printed strip monopole," *IEEE Antennas and Propagation Magazine*, vol. 47, no. 6, pp. 59–61, Dec 2005.

[46] M. N. Suma, R. K. Raj, M. Joseph, P. C. Bybi, and P. Mohanan, "A compact dual band planar branched monopole antenna for dcs/2.4-ghz wlan applications," *IEEE Microwave and Wireless Components Letters*, vol. 16, no. 5, pp. 275–277, May 2006.

[47] M. N. Suma, P. C. Bybi, and P. Mohanan, "A wideband printed monopole antenna for 2.4-ghz wlan applications," *Microwave and Optical Technology Letters*, vol. 48, no. 5, pp. 871–873, 2006.

[48] Y. Ge, K. P. Esselle, and T. S. Bird, "A spiral-shaped printed monopole antenna for mobile communications," in *2006 IEEE Antennas and Propagation Society International Symposium*. IEEE, 2006, pp. 3681–3684.

[49] J. S. Row and S. W. Wu, "Monopolar square patch antennas with wideband operation," *Electronics Letters*, vol. 42, no. 3, pp. 139–140, Feb 2006.

[50] J. I. Kim and Y. Jee, "Design of ultrawideband coplanar waveguide-fed li-shape planar monopole antennas," *IEEE Antennas and Wireless Propagation Letters*, vol. 6, pp. 383–387, 2007.

[51] Y.-L. Kuo and K.-L. Wong, "Printed double-t monopole antenna for 2.4/5.2 ghz dual-band wlan operations," *IEEE Transactions on Antennas and Propagation*, vol. 51, no. 9, pp. 2187–2192, Sep 2003.

[52] R. K. Raj, M. Joseph, C. K. Aanandan, K. Vasudevan, and P. Mohanan, "A new compact microstrip-fed dual-band coplanar antenna for wlan applications," *IEEE Transactions on Antennas and Propagation*, vol. 54, no. 12, pp. 3755–3762, Dec 2006.

[53] M. Joseph, R. K. Raj, M. N. Suma, C. K. Aanandan, K. Vasudevan, and P. Mohanan, "Microstrip-fed dual band folded dipole antenna for dcs/pcs/2.4 ghz wlan applications," *International Journal on Wireless & Optical Communications*, vol. 04, no. 01, pp. 43–51, 2007.

[54] D.-C. Chang, M.-Y. Liu, and C.-H. Lin, "A cpw-fed u type monopole antenna for uwb applications," in *2005 IEEE Antennas and Propagation Society International Symposium*, vol. 2. IEEE, 2005, pp. 512–515.

[55] W.-S. Lee, D.-Z. Kim, K.-J. Kim, and J.-W. Yu, "Wideband planar monopole antennas with dual band-notched characteristics," *IEEE Transactions on Microwave Theory and Techniques*, vol. 54, no. 6, pp. 2800–2806, June 2006.

[56] W. C. Liu and C. F. Hsu, "Dual-band cpw-fed y-shaped monopole antenna for pcs/wlan application," *Electronics Letters*, vol. 41, no. 7, pp. 390–391, March 2005.

[57] K. F. Jacob, M. N. Suma, R. K. Raj, M. Joseph, and P. Mohanan, "Planar branched monopole antenna for uwb applications," *Microwave and Optical Technology Letters*, vol. 49, no. 1, pp. 45–47, 2007.

[58] H.-D. Chen and H.-T. Chen, "A cpw-fed dual-frequency monopole antenna," *IEEE Transactions on Antennas and Propagation*, vol. 52, no. 4, pp. 978–982, April 2004.

[59] W. C. Liu and H. J. Liu, "Compact triple-band slotted monopole antenna with asymmetrical cpw grounds," *Electronics Letters*, vol. 42, no. 15, pp. 840–842, July 2006.

[60] [60] R. Garg, P. Bhartia, and I. Bahl, "Microstrip antenna design handbook," *, 1st ed. Boston, MA: Artech House*, vol. 1, p. 790795, 2001.

[61] I. Chang and B. Lee, "Design of defected ground structures for harmonic control of active microstrip antenna," in *Antennas and Propagation Society International Symposium, 2002. IEEE*, vol. 2.   IEEE, 2002, pp. 852–855.

[62] V. Radisic, Y. Qian, R. Coccioli, and T. Itoh, "Novel 2-d photonic bandgap structure for microstrip lines," *IEEE Microwave and Guided Wave Letters*, vol. 8, no. 2, pp. 69–71, Feb 1998.

[63] P. Salonen, M. Keskilammi, and L. Sydanheimo, "A low-cost 2.45 ghz photonic band-gap patch antenna for wearable systems," in *Antennas and Propagation, 2001. Eleventh International Conference on (IEE Conf. Publ. No. 480)*, vol. 2.   IET, 2001, pp. 719–723.

[64] Y. J. Sung and Y. S. Kim, "An improved design of microstrip patch antennas using photonic bandgap structure," *IEEE Transactions on Antennas and Propagation*, vol. 53, no. 5, pp. 1799–1804, May 2005.

[65] H. Liu, Z. Li, X. Sun, and J. Mao, "Harmonic suppression with photonic bandgap and defected ground structure for a microstrip patch antenna," *IEEE Microwave and Wireless Components Letters*, vol. 15, no. 2, pp. 55–56, Feb 2005.

[66] D. Guha, M. Biswas, and Y. M. M. Antar, "Microstrip patch antenna with defected ground structure for cross polarization suppression," *IEEE Antennas and Wireless Propagation Letters*, vol. 4, no. 1, pp. 455–458, 2005.

[67] V. G. Veselago, "the Electrodynamics of Substances With Simultaneously Negative Values of and ," *Soviet Physics Uspekhi*, vol. 10, no. 4, pp. 509–514, 1968.

[68] J. B. Pendry, A. J. Holden, D. J. Robbins, and W. J. Stewart, "Magnetism from conductors and enhanced nonlinear phenomena," *IEEE Transactions on Microwave Theory and Techniques*, vol. 47, no. 11, pp. 2075–2084, Nov 1999.

[69] D. R. Smith, W. J. Padilla, D. C. Vier, S. C. Nemat-Nasser, and S. Schultz, "Composite medium with simultaneously negative permeability and permittivity," *Phys. Rev. Lett.*, vol. 84, pp. 4184–4187, May 2000.

[70] A. Lai, T. Itoh, and C. Caloz, "Composite right/left-handed transmission line metamaterials," *IEEE Microwave Magazine*, vol. 5, no. 3, pp. 34–50, Sept 2004.

[71] F. Bilotti, A. Alu, and L. Vegni, "Design of miniaturized metamaterial patch antennas with μ -negative loading," *IEEE Transactions on Antennas and Propagation*, vol. 56, no. 6, pp. 1640–1647, June 2008.

[72] D. H. Werner and S. Ganguly, "An overview of fractal antenna engineering research," *IEEE Antennas and Propagation Magazine*, vol. 45, no. 1, pp. 38–57, Feb 2003.

[73] J. Kim, C. S. Cho, and J. W. Lee, "5.2 ghz notched ultra-wideband antenna using slot-type srr," *Electronics Letters*, vol. 42, no. 6, pp. 315–316, March 2006.

[74] S. A. Long and E. M. O'Connor, "The history of the development of the dielectric resonator antenna," in *Electromagnetics in Advanced Applications, 2007. ICEAA 2007. International Conference on.* IEEE, 2007, pp. 872–875.

[75] P. W. Tang and P. F. Wahid, "Hexagonal fractal multiband antenna," *IEEE Antennas and Wireless Propagation Letters*, vol. 3, no. 1, pp. 111–112, Dec 2004.

[76] A. Okaya and L. F. Barash, "The dielectric microwave resonator," *Proceedings of the IRE*, vol. 50, no. 10, pp. 2081–2092, Oct 1962.

[77] S. Long, M. McAllister, and L. Shen, "The resonant cylindrical dielectric cavity antenna," *IEEE Transactions on Antennas and Propagation*, vol. 31, no. 3, pp. 406–412, May 1983.

[78] J. T. H. S. Martin, Y. M. M. Antar, A. A. Kishk, A. Ittipiboon, and M. Cuhaci, "Dielectric resonator antenna using aperture coupling," *Electronics Letters*, vol. 26, no. 24, pp. 2015–2016, Nov 1990.

[79] G. Drossos, Z. Wu, and L. E. Davis, "Theoretical and experimental investigation of cylindrical dielectric resonator antennas," *Microwave and Optical Technology Letters*, vol. 13, no. 3, pp. 119–123, 1996.

[80] A. Ittipiboon, R. K. Mongia, Y. M. M. Antar, P. Bhartia, and M. Cuhaci, "Aperture fed rectangular and triangular dielectric resonators for use as magnetic dipole antennas," *Electronics Letters*, vol. 29, no. 23, pp. 2001–2002, Nov 1993.

[81] D. Guha and Y. M. M. Antar, "New half-hemispherical dielectric resonator antenna for broadband monopole-type radiation," *IEEE Transactions on Antennas and Propagation*, vol. 54, no. 12, pp. 3621–3628, Dec 2006.

[82] Y. Liu, Z. Shen, and C. L. Law, "A compact dual-band cavity-backed slot antenna," *IEEE Antennas and Wireless Propagation Letters*, vol. 5, no. 1, pp. 4–6, Dec 2006.

[83] Z. N. Chen and M. Y. W. Chia, "Broadband planar inverted-l antennas," *IEE Proceedings - Microwaves, Antennas and Propagation*, vol. 148, no. 5, pp. 339–342, Oct 2001.

[84] Y. J. Cho, Y. S. Shin, and S. O. Park, "Internal pifa for 2.4/5 ghz wlan applications," *Electronics Letters*, vol. 42, no. 1, pp. 8–10–, Jan 2006.

[85] L. M. Feldner, C. T. Rodenbeck, C. G. Christodoulou, and N. Kinzie, "Electrically small frequency-agile pifa-as-a-package for portable wireless devices," *IEEE Transactions on Antennas and Propagation*, vol. 55, no. 11, pp. 3310–3319, Nov 2007.

[86] B. C. Kim, J. H. Yun, and H. Do Choi, "Small wideband pifa for mobile phones at 1800 mhz," in *IEEE Vehicular Technology Conference*, 2004, pp. 27–29.

[87] F. Wang, Z. Du, Q. Wang, and K. Gong, "Enhanced-bandwidth pifa with t-shaped ground plane," *Electronics Letters*, vol. 40, no. 23, pp. 1504–1505, Nov 2004.

[88] B. Sanz-Izquierdo, J. C. Batchelor, R. J. Langley, and M. I. Sobhy, "Single and double layer planar multiband pifas," *IEEE Transactions on Antennas and Propagation*, vol. 54, no. 5, pp. 1416–1422, May 2006.

[89] D. M. Nashaat, H. A. Elsadek, and H. Ghali, "Single feed compact quad-band pifa antenna for wireless communication applications," *IEEE Transactions on Antennas and Propagation*, vol. 53, no. 8, pp. 2631–2635, Aug 2005.

[90] H. G. Schantz, "A brief history of uwb antennas," *IEEE Aerospace and Electronic Systems Magazine*, vol. 19, no. 4, pp. 22–26, April 2004.

[91] W. Wiesbeck, G. Adamiuk, and C. Sturm, "Basic properties and design principles of uwb antennas," *Proceedings of the IEEE*, vol. 97, no. 2, pp. 372–385, Feb 2009.

[92] F. Sabath, E. L. Mokole, and S. N. Samaddar, "Definition and classification of ultra-wideband signals and devices," *Radio Science bulletin, No.313*, pp. 12–26, June 2005.

[93] European Union, "Commission decision on allowing the use of the radio spectrum for equipment using ultra-wideband technology in a harmonised manner in the community," *Official Journal*, pp. 1–4, February 2007.

[94] Y. Shi, S. Aditya, and C. L. Law, "Time domain responses of printed uwb antennas," in *2005 5th International Conference on Information Communications & Signal Processing*. IEEE, 2005, pp. 153–156.

[95] A. Shlivinski, E. Heyman, and R. Kastner, "Antenna characterization in the time domain," *IEEE Transactions on Antennas and Propagation*, vol. 45, no. 7, pp. 1140–1149, Jul 1997.

[96] B. Levitas, "Uwb time domain measurements," in *Antennas and Propagation, 2007. EuCAP 2007. The Second European Conference on.* IET, 2007, pp. 1–8.

[97] D. Ghosh, A. De, M. C. Taylor, T. K. Sarkar, M. C. Wicks, and E. L. Mokole, "Transmission and reception by ultra-wideband (uwb) antennas," *IEEE Antennas and Propagation Magazine*, vol. 48, no. 5, pp. 67–99, Oct 2006.

[98] Y. Duroc, A. Ghiotto, T. P. Vuong, and S. Tedjini, "Uwb antennas: Systems with transfer function and impulse response," *IEEE Transactions on Antennas and Propagation*, vol. 55, no. 5, pp. 1449–1451, May 2007.

[99] A. Z. Hood, T. Karacolak, and E. Topsakal, "A small antipodal vivaldi antenna for ultrawide-band applications," *IEEE Antennas and Wireless Propagation Letters*, vol. 7, pp. 656–660, 2008.

[100] L. Ying and C. Ai-xin, "Design and application of vivaldi antenna array," in *Antennas, Propagation and EM Theory, 2008. ISAPE 2008. 8th International Symposium on.* IEEE, 2008, pp. 267–270.

[101] K. Kiminami, A. Hirata, and T. Shiozawa, "Double-sided printed bow-tie antenna for uwb communications," *IEEE Antennas and Wireless Propagation Letters*, vol. 3, no. 1, pp. 152–153, Dec 2004.

[102] Y. Ito, M. Ameya, M. Yamamoto, and T. Nojima, "Unidirectional uwb array antenna using leaf-shaped bowtie elements and flat reflector," *Electronics Letters*, vol. 44, no. 1, pp. 9–11, January 2008.

[103] M. Naghshvarian-Jahromi, "Novel wideband planar fractal monopole antenna," *IEEE Transactions on Antennas and Propagation*, vol. 56, no. 12, pp. 3844–3849, Dec 2008.

[104] M. Karlsson and S. Gong, "An integrated spiral antenna system for uwb," in *2005 European Microwave Conference*, vol. 3. IEEE, 2005, pp. 4–pp.

[105] S. y. Chen, P. h. Wang, and P. Hsu, "Uniplanar log-periodic slot antenna fed by a cpw for uwb applications," *IEEE Antennas and Wireless Propagation Letters*, vol. 5, no. 1, pp. 256–259, Dec 2006.

[106] J. Dyson, "The equiangular spiral antenna," *IRE Transactions on Antennas and Propagation*, vol. 7, no. 2, pp. 181–187, April 1959.

[107] A. Calmon, G. Pacheco, and M. Terada, "A novel reconfigurable uwb log-periodic antenna," in *2006 IEEE Antennas and Propagation Society International Symposium*. IEEE, 2006, pp. 213–216.

[108] R. Pantoja, A. Sapienza, and F. M. Filho, "A microwave printed planar log-periodic dipole array antenna," *IEEE Transactions on Antennas and Propagation*, vol. 35, no. 10, pp. 1176–1178, Oct 1987.

[109] D. Valderas, R. Alvarez, J. Melendez, I. Gurutzeaga, J. Legarda, and J. I. Sancho, "Uwb staircase-profile printed monopole design," *IEEE Antennas and Wireless Propagation Letters*, vol. 7, pp. 255–259, 2008.

[110] D. Schaubert, E. Kollberg, T. Korzeniowski, T. Thungren, J. Johansson, and K. Yngvesson, "Endfire tapered slot antennas on dielectric substrates," *IEEE Transactions on Antennas and Propagation*, vol. 33, no. 12, pp. 1392–1400, Dec 1985.

[111] G. M. Yang, R. H. Jin, G. B. Xiao, C. Vittoria, V. G. Harris, and N. X. Sun, "Ultrawideband (uwb) antennas with multiresonant split-ring loops," *IEEE Transactions on Antennas and Propagation*, vol. 57, no. 1, pp. 256–260, Jan 2009.

[112] N. Behdad and K. Sarabandi, "A compact antenna for ultrawideband applications," *IEEE Transactions on Antennas and Propagation*, vol. 53, no. 7, pp. 2185–2192, July 2005.

[113] W. Wiesbeck, G. Adamiuk, and C. Sturm, "Basic properties and design principles of uwb antennas," *Proceedings of the IEEE*, vol. 97, no. 2, pp. 372–385, Feb 2009.

[114] C.-C. Lin, Y.-C. Kan, L.-C. Kuo, and H.-R. Chuang, "A planar triangular monopole antenna for uwb communication," *IEEE Microwave and Wireless Components Letters*, vol. 15, no. 10, pp. 624–626, 2005.

[115] J. Y. Sze, C. I. G. Hsu, and J. Y. Shiu, "Small cpw-fed band-notched ultrawideband rectangular aperture antenna," *IEEE Antennas and Wireless Propagation Letters*, vol. 7, pp. 513–516, 2008.

[116] D. Valderas, R. Alvarez, J. Melendez, I. Gurutzeaga, J. Legarda, and J. I. Sancho, "Uwb staircase-profile printed monopole design," *IEEE Antennas and Wireless Propagation Letters*, vol. 7, pp. 255–259, 2008.

[117] Q. X. Chu and Y. Y. Yang, "A compact ultrawideband antenna with 3.4/5.5 ghz dual band-notched characteristics," *IEEE Transactions on Antennas and Propagation*, vol. 56, no. 12, pp. 3637–3644, Dec 2008.

[118] C. Marchais, G. LeRay, and A. Sharaiha, "Stripline slot antenna for uwb communications," *IEEE Antennas and Wireless Propagation Letters*, vol. 5, no. 1, pp. 319–322, Dec 2006.

[119] A. M. Abbosh, "Miniaturized microstrip-fed tapered-slot antenna with ultrawideband performance," *IEEE Antennas and Wireless Propagation Letters*, vol. 8, pp. 690–692, 2009.

[120] M. Gopikrishna, D. D. Krishna, C. K. Aanandan, P. Mohanan, and K. Vasudevan, "Compact linear tapered slot antenna for uwb applications," *Electronics Letters*, vol. 44, no. 20, pp. 1174–1175, September 2008.

[121] J. Y. Siddiqui, Y. M. M. Antar, A. P. Freundorfer, E. C. Smith, G. A. Morin, and T. Thayaparan, "Design of an ultrawideband antipodal tapered slot antenna using elliptical strip conductors," *IEEE Antennas and Wireless Propagation Letters*, vol. 10, pp. 251–254, 2011.

[122] Y. Che, K. Li, X. Hou, and W. Tian, "Simulation of a small sized antipodal vivaldi antenna for uwb applications," in *2010 IEEE International Conference on Ultra-Wideband*, vol. 1. IEEE, 2010, pp. 1–3.

[123] C. R. Medeiros, J. R. Costa, and C. A. Fernandes, "Compact tapered slot uwb antenna with wlan band rejection," *IEEE Antennas and Wireless Propagation Letters*, vol. 8, pp. 661–664, 2009.

[124] T.-G. Ma and S.-K. Jeng, "A printed dipole antenna with tapered slot feed for ultrawide-band applications," *IEEE Transactions on Antennas and Propagation*, vol. 53, no. 11, pp. 3833–3836, Nov 2005.

[125] S. Nikolaou, G. E. Ponchak, J. Papapolymerou, and M. M. Tentzeris, "Conformal double exponentially tapered slot antenna (detsa) on lcp for uwb applications," *IEEE Transactions on Antennas and Propagation*, vol. 54, no. 6, pp. 1663–1669, June 2006.

[126] N. Gupta, "Material selection of ltcc based microstrip patch antenna substrate using ashby's approach," *Computer, Consumer and Control (IS3C), 2014 International Symposium on*, pp. 1018–1021, 2014.

[127] X. Chen, J. Liang, S. Wang, Z. Wang, and C. Parini, "Small ultra wideband antennas for medical imaging," *Antennas and Propagation Conference, 2008. LAPC 2008. Loughborough*, pp. 28–31, March 2008.

[128] S. X. Ta, B. Kim, H. Choo, and I. Park, "Slot-line-fed quasi-yagi antenna," *Antennas Propagation and EM Theory (ISAPE), 2010 9th International Symposium on*, pp. 307–310, Nov 2010.

[129] V. Deepu, S. Mridula, R. Sujith, and P. Mohanan, "Slot line fed dipole antenna for wide band applications," *Microwave and Optical Technology Letters*, vol. 51, no. 3, pp. 826–830, 2009.

[130] V. Deepu, K. R. Rohith, J. Manoj, M. N. Suma, K. Vasudevan, C. K. Aanandan, and P. Mohanan, "Compact uniplanar antenna for wlan applications," *Electronics Letters*, vol. 43, no. 2, pp. 70–72, January 2007.

[131] S. M. Nair, S. V.A, N. C.M, C. Aanandan, K. Vasudevan, and P. Mohanan, "Compact slotline fed enhanced gain dipole antenna for 5.2 ghz/5.8-ghz applications," *International Journal of RF and Microwave Computer-Aided Engineering*, vol. 23, no. 1, pp. 40–46, 2013.

[132] T. K. Roshna, U. Deepak, R. Sujith, and P. Mohanan, "A high gain compact coplanar stripline fed antenna for wireless applications," *General Assembly and Scientific Symposium (URSI GASS), 2014 XXXIth URSI*, pp. 1–4, Aug 2014.

Chapter 2

ANTENNA DESIGN, METHOD-OLOGY AND MEASUREMENT TECHNIQUES

This chapter describes the methods employed in antenna design, fabrication, and measurements. The CAD modeling and optimization of the antenna are done using the simulation software CST Microwave Studio. The fabrication technique used here is the photolithography. Measurements of the frequency domain antenna parameters are done using network analyzers(HP8510C, Agilent PNA 8362B, and R&S ZVB20). Time domain analysis of the UWB antenna is also discussed.

Contents

2.1 Simulation Tools and Antenna Optimization.

CST Microwave Studio is an efficient electromagnetic solver used for modeling and analyzing antennas, RCS, EMI and EMC of the multi-layered structures and devices etc. Biomedical Simulations are also possible with CST. The antenna is modeled in the CST and for solving the structure transient solver of the antenna is run which is fast as well as well suited for multiband and wideband applications [1].

The antenna is modeled using the GUI available in CST. Once the structure is modeled, the port has to be assigned to the antenna for excitation. There is a discrete port as well as waveguide port available for this purpose. The desired frequency range is selected before running the transient solver. Once the transient solver completes the simulation, results can be displayed or exported into .csv or .txt file for future use. The optimization and the parametric sweep and analysis tool enable us to optimize the parameter for a specific value either the dimension or the position. The values of the properties of the materials used can also be varied and optimized. The antenna geometry can be optimized for a certain specific set of goals. The transient response of the antenna can also be calculated using farfield probes placed around the antenna, by taking the time domain signals. Normalized cross correlation of two pulses can be calculated which shows the similarity in pulses.

2.2 Fabrication Technique for Antennas

Photolithography is the technique used for making the prototype of the antennas presented in this thesis. The fabrication process of the various antennas involves the realization of the CAD design into a prototype. For this a suitable substrate is to be identified. The antenna fabrication using photolithographic technique is explained in the following section.
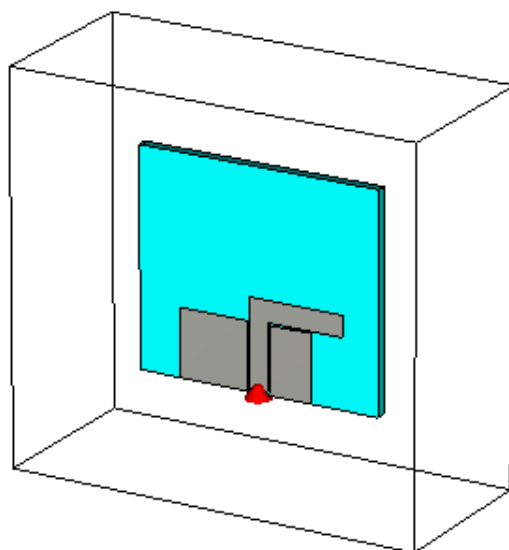
Figure 2.1: Antenna modeled in CST Microwave Studio

2.2.1   Substrate Materials: Characteristics

Advances in MMIC industry demands superior quality materials with microwave properties for the use of substrates and IC packaging applications. The signal propagation speed in these materials should be high. The materials with low dielectric loss will have minimum propagation delay. Dimensional strength, homogeneity, high thermal conductivity and the isotropicity are the other important features to be taken care of while choosing a substrate [2–5]. Choosing the dielectric substrates depends on the frequency of operation and the radiation properties of the antenna. Bandwidth is limited, and the excitation of the surface waves occurs if we are using a substrate with higher permittivity. The frequency of operation increases as the substrate permittivity increases which result in an increase in loss tangent of the substrate hence the antenna efficiency is decreased. The increase in the substrate thickness enhances the bandwidth of the antenna on the expense of efficiency. This is due to the surface waves. Various dielectric measurement techniques are available in the literature [6–8]. Cavity perturbation technique is the most commonly used one for measuring the dielectric permittivity for low loss material samples. A rectangular waveguide cavity is used for the measurements.

The Q factor and the resonance frequency were measured for the cavity only for various cavity modes. A thin sample of the substrate is positioned at the E-field cavity where the E-field is maximum. The resulting resonance frequency and the Quality factor are measured after placing the sample, and the complex dielectric constant of the materials are measured using the following expressions.

$$\epsilon_r^{'} = 1 + \frac{V_c(f_0 - f_s)}{2V_s f_s} \tag{2.1}$$

$$\epsilon_r^{"} = \frac{V_c(Q_0 - Q_s)}{4V_s Q_0 C_s} \tag{2.2}$$

where,

$f_o = cavities resonant frequency,$

$f_s = samples resonant frequency,$

$V_c = cavity volume,$

$V_s = Sample volume,$

$Q_0 = Quality factor for empty cavity,$

$Q_s = Quality factor for cavity loaded with sample.$

2.2.2 Fabrication Method

The fabrication method used here is photolithography. A suitable substrate is selected for the fabrication process. The layout is made using CAD tools and print out of the negative mask of the design is made on a transparent or a semitransparent sheet. To remove impurities from the metallization of the substrate, it is cleaned with acetone.

A mixture of photoresist and thinner in the ratio 1:1 is made and coated over the substrate. After drying, the mask is placed above the substrate and is exposed to the UV light. The exposed substrate is then dipped in the developer solution for hardening the photoresist in the exposed portion. The masked portion has to be removed. The substrate is dipped in the dye so as to get a better visibility of the exposed photoresist and washed using water. The unwanted copper portions are removed using the etching process using Ferric

chloride. FeCl3 dissolves the unexposed copper coating. Photolithography process is detailed in Fig 2.2
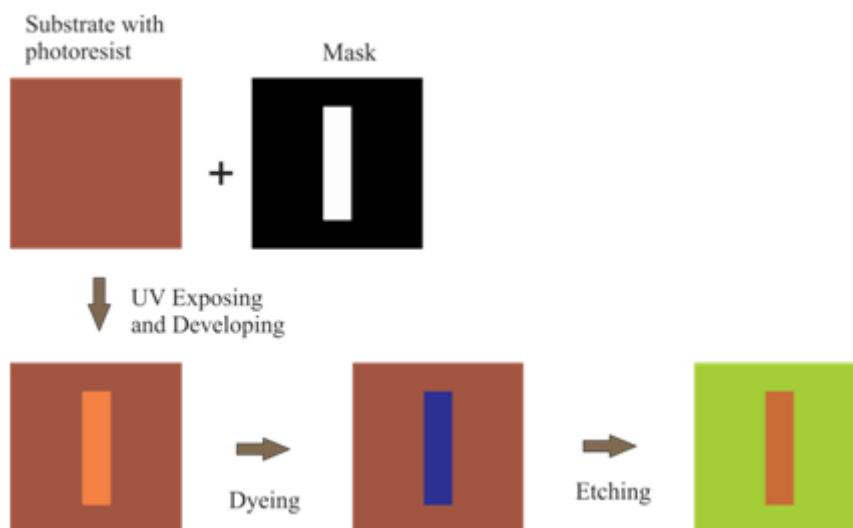
Figure 2.2: Antenna Fabrication Steps

2.3   Facilities for Antenna Measurements

The details of the measurement of various antenna parameters and the experimental facilities are outlined in the following sections. Network analyzers are used to measure the antenna radiation characteristics along with automated antenna positioner and the double ridged UWB horn antenna.

2.3.1   HP8510C VNA

HP8510C is a versatile equipment for measuring all the S parameters such as $S_{11}, S_{12}, S_{21}, S_{22}$ and group delay. Time domain and frequency domain measurements can be done. Both the magnitude and phase of these parameters can be measured [9]. A Matlab-based application developed in the lab named CREMASOFT is used to set up the measurement and saving the results in .CSV format. A basic measurement setup schematic for the reflection characteristics is given in Fig. 2.3

2.3.2 Agilent E8362B Network Analyzer(PNA)

Frequency domain measurements with high rate and accuracy can be done using this analyzer up to 20 GHz [10]. This can make measurements at more number of points than VNA. It is equipped with Windows operating system and has 32 measurement channels with 16001 points per channel with $< 26\mu sec$ point measurement speed.
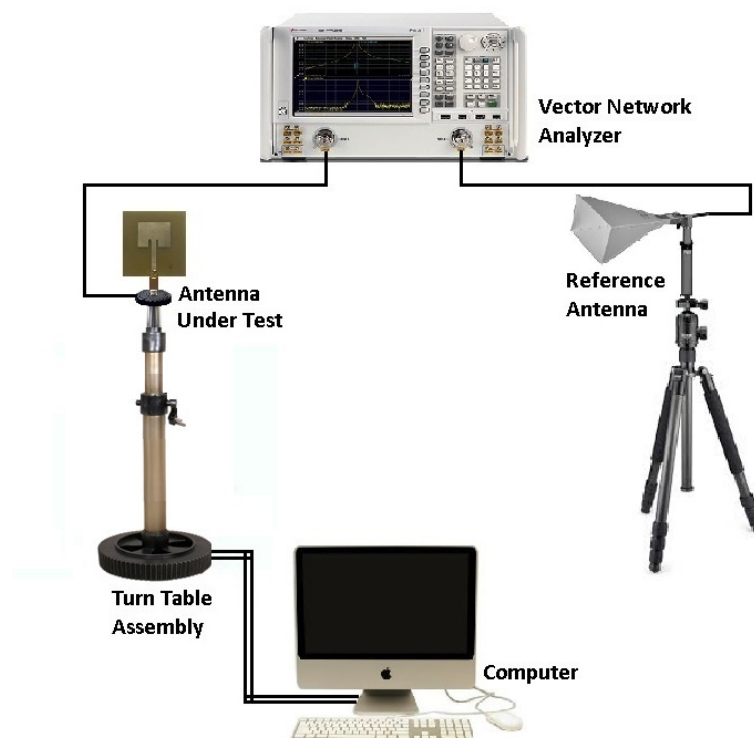
Figure 2.3: Antenna Measurement arrangement using VNA

2.3.3 Rohde and Schwarz ZVB20 PNA

The Rohde and Schwarz ZVB20 is a programmable network analyzer with improved measurement speed. The configuration capabilities and the system characteristics are also enhanced in this PNA. Parallel measurement facility

with high speed is available in RS ZVB20 because the signal from the generator can be given to the ports simultaneously. Capturing of the data from these ports and their display can also be done at the same time. We can measure two port device under test simultaneously in the four port version of PNA. The features of this PNA include a good user interface, wide dynamic range, parallel measurements, high output power, etc. its maximum frequency of operation is 20 GHz.

2.3.4   Anechoic Chamber

For better measurement results the effect of the unwanted reflections of electromagnetic waves has to be eliminated. Anechoic chambers are used to remove the reflections caused by objects which are near to the measurement set up. All measurements are carried inside the chamber. One entire room is set with absorbers on the wall floor and ceiling so as to avoid the multipath signals. The photograph of the anechoic chamber in the research lab appears in Fig 2.4.

The pyramidal shape of the absorbers increases the absorption of the incident microwave power on it. All the walls and roofs are covered with Aluminum sheets so as to avoid the entry of electromagnetic interference from the adjacent rooms.

2.3.5   Turn Table Assembly

Turntable assembly is used for mounting the antenna under test. It consists of a microcontroller based stepper motor driven platform which rotated as per the commands received from the Matlab based front end software(CREMA Soft) installed in the computer.A UWB horn antenna with a large aperture is used for measuring purpose.

2.4   Antenna Measurement Techniques

The subsequent sections explain the measurement techniques and procedures of the antenna radiation characteristics. AUT is connected to any one of
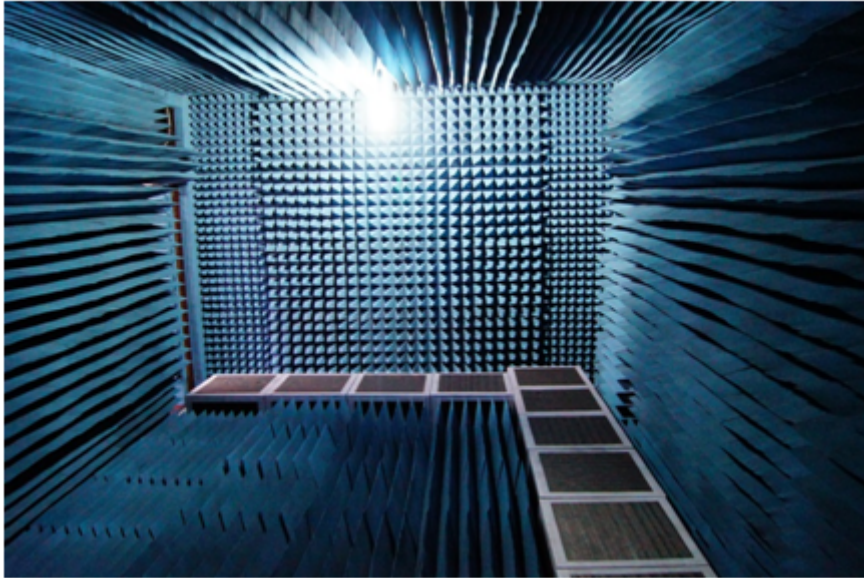
Figure 2.4: Anechoic Chamber for conducting Measurements

the ports of the analyzer so as to input the signal. The cables and connectors used for this purpose are likely to be lossy at higher frequencies. For obtaining accurate S-parameter results, calibration of the analyzer is required which is done by the conventional open, short and matched load technique. Single port calibration methods can be adopted for measuring the S_{11}, $VSWR$, and the Z_{in}.

Since the emphasis of the antenna engineering and research is on building more compact and efficient antennas which are of the order of a quarter of the wavelength, different aspects has to be considered for the accuracy of measurements. One major concern is the spurious cable current caused by the coaxial feed cable. Return loss characteristics and its impedance matching are varied because of this. One method for suppressing the spurious cable current is developed in [11]. The low electric field regions are predicted by the simulation software for attaching the measurement cables safely. The simulated and measured results are compared and the spurious cable radiation can be accounted. The quarter wave sleeve balm serves to suppress the feed cable current. The ferrite beads can also be use for this, but the complete elimination of the feed cable current is not practically possible [12].

2.4.1 Resonant Frequency, Bandwidth and Return Loss

The port which we are connecting the antenna is calibrated initially for the desired frequency range. For measuring the antenna reflection characteristics, it is connected to any one of the calibrated ports of the network analyzer in S_{11}/S_{22} mode. The measured result with respect to the frequency is stored in .csv file format using the computer interface software CremaSoft .

The frequency with lowest S_{11} is taken as the resonance frequency. The bandwidth of the AUT is taken as the range of frequencies with S_{11} value less than $-10dB$, which indicates a VSWR value of 2. Bandwidth of the antenna is expressed in percentage as,

$$\%Bandwidth = \frac{f_h - f_l}{f_c} * 100 \qquad (2.3)$$

Where f_h is the higher frequency with -10 dB point and f_1 is the lower -10 dB point and f_c is the center frequency with minimum S_{11}. The percentage bandwidth is also called 2:1 VSWR bandwidth.

2.4.2 Radiation Pattern

The measurement is set up in the reflection free anechoic chamber . The AUT is placed on the antenna holder and connected to a port of the network analyzer, kept in the S_{21} mode. The number of points in the frequency is set as per our need. The angular parameters for controlling rotations are entered in the software. Antenna positioner is placed in the direction of maximum radiation. The calibration used for pattern measurement is the THRU calibration for the desired frequency range. They are saved in the analyzer calibration set. Time gating is provided for removing any unwanted spurious radiations. CremaSoft automatically measures the radiation pattern, and the results are stored in a CSV file.

2.4.3   Measurement of Antenna Gain

Gain transfer method [13–15] is used for antenna gain measurement. An antenna with a standard gain is used as the reference antenna. The reference antenna is attached on the antenna positioner. The port is THRU calibrated for the chosen frequency. The Antenna under test is connected to the antenna positioner after removing the standard antenna. The fabricated antenna has to be aligned with the measuring horn antenna in the direction of maximum radiation. The change in S_{21} is recorded, which is the gain of the antenna related to the reference antenna. This relative gain is added with the gain of the reference antenna to get the reference antenna to get the gain of the test antenna. The gain of the horn antenna is added with the relative gain of the AUT to obtain the absolute gain.

2.4.4   Measurement of Radiation Efficiency

One of the primary antenna parameters is the radiation efficiency. It explains how efficiently an antenna can convert the time varying currents fed to it into radiation. The most common method for measuring the efficiency of a resonant antenna is Wheeler cap method [16, 17]. AUT is placed in a cylindrical cavity with a conducting cap. The resistance of the antenna with and without a cap is measured using PNA, and these values are substituted in the following expression to calculate the efficiency.

$$Efficiency, \eta = \frac{R_{nocap} - R_{cap}}{R_{nocap}} \tag{2.4}$$

Where, R_{cap} and R_{nocap} are the input resistance with and without a cap. The method explained above is suitable well for narrow band antennas. For wideband antennas , efficiency is measured using the modified Wheeler Cap method [18]. Three power fractions are used to represent the losses occurs in an antenna (Power budget). They are radiation losses($\eta = P_{rad}/P_{in}$), reflection losses ($m = P_{refl}/P_{in}$) and dissipation losses($l = P_{loss}/P_{in}$) . The sum of the above fractions gives a maximum value of one according to the energy conservation.

$$l + m + \eta = 1 \tag{2.5}$$

A spherical shell surrounds AUT. The structural scattering will be minimum, and the miss match fraction ($m = |S_{11} - F_S|^2$) will be the antenna mode scattering term. By reciprocity, the transmit efficiency and the receiving efficiency are same (η). Then the scattering coefficient in the shell becomes:

$$\begin{aligned} |S_{11} - F_s|^2 &= m + \eta^2 + \eta^2 m^2 + \eta^2 m^2 + \eta^2 m^2 + \ldots \\ &= |S_{11} - F_s|^2 + \eta^2 \sigma_{n=0} |S_{11} - F_s|^{2n} \\ &= |S_{11} - F_s|^2 + \eta^2 \frac{1}{1 - |S_{11} - F_s|^2} \end{aligned} \tag{2.6}$$

$$\eta = \sqrt{(1 - |S_{11} - F_s|^2)((|S_{11} - W_c|^2) - |S_{11} - F_s|^2)} \tag{2.7}$$

A metallic chamber which is oblate with a diameter of $70cm$ is used for the efficiency measurements. Return loss ($S_{11} - F_s$)of the antenna in the open space is measured. The return loss is measured for the antenna placed in a metallic chamber ($S_{11} - W_c$). These measured values are substituted into the above equation to obtain the efficiency.

2.5 UWB Antenna Characteristics Analysis in Time Domain

As the thesis investigates on the UWB antennas, the analysis of various time domain parameters is compulsory. The UWB systems use short transient pulses for the transmission of the information. The shape of the transmitted and received pulse has to be same for distortionless transmission of the information. In the practical cases, the received pulse will be distorted in shape and sometimes there will be a long tail for the pulse which is called "ringing effect" . Thus the design of the antenna should be done carefully so as to remove these distortions.

2.5.1 UWB Antenna System Model

A typical UWB transmitter-receiver antenna system [19, 20] is shown in Fig 2.5.
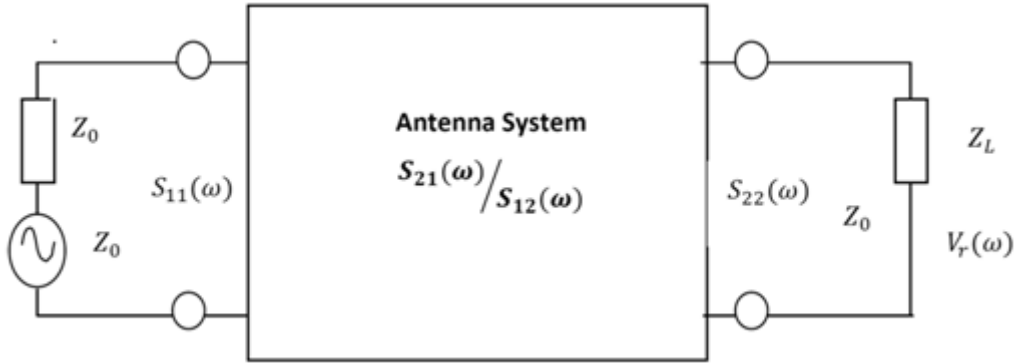
Figure 2.5: UWB antenna system

The transmitted and received power in a system of two antennas are given by the Friss transmission equation, as given in Eqn 2.8

$$\frac{P_r}{P_f} = (1 - |\tau_t|^2)(1 - |\tau_r|^2) G_r G_t |\widehat{P}_t \widehat{P}_r|^2 \left(\frac{\lambda}{4\pi d}\right)^2 |\widehat{P}_t \widehat{P}_r|^2 \qquad (2.8)$$

Where P_t is the input power given to transmitting antenna and P_r is the output power measured from the receiving antenna. Both theses values are taken after time averaging. G_t and G_r represent the transmitter and receiver antenna gains. d represents the distance between the two antennas. All the parameters in the equation 2.8 are frequency reliant for a wideband system. The formula for a wideband system is shown below.

$$\frac{P_r(\omega)}{P_f(\omega)} = (1 - |\tau_t(\omega)|^2)(1 - |\tau_r(\omega)|^2) G_t(\omega) G_r(\omega) |P_t(\omega) P_r(\omega)|^2 \left(\frac{\lambda}{4\pi d}\right)^2 \quad (2.9)$$

In the case of two similar antennae with polarization and reflection matching aligned for maximum directional reception and radiation, the above equation reduces to

$$\frac{P_r(\omega)}{P_f(\omega)} = \left(\frac{\lambda}{4\pi d}\right)^2 G_r(\omega)G_t(\omega) \tag{2.10}$$

The transfer function defines the input /output relationship of a system. From Fig 2.5,

$$\frac{V_t^2(\omega)}{2} = P_t(\omega)Z_0$$
$$\frac{V_t^2(\omega)}{2} = P_r(\omega)Z_0 \tag{2.11}$$

Then S_{21} can be written as

$$\begin{aligned} S_{21}(\omega) &= \frac{V_r(\omega)}{V_t(\omega)} \\ &= \left|\sqrt{\frac{P_r(\omega)Z_L}{P_t(\omega)4Z_L}}\right| e^{-j\varphi(\omega)} \\ &= |S_{21}(\omega)| e^{-j\varphi(\omega)} \end{aligned} \tag{2.12}$$

$$\varphi(\omega) = \varphi_t(\omega) + \varphi_r(\omega) + \frac{wd}{c} \tag{2.13}$$

d gives the separation between the two antennas. The terms, $\varphi_t(\omega)$ and $\varphi_r(\omega)$ is the phase deviation associated with the Tx and Rx antennas. The transfer function of an antenna system depends on various antenna characteristics. This includes the gain, matching, and polarization. The distance of separation, d between the two antennas also has to be considered. S_{21} is an important parameter in the antenna engineering since we can calculate even path loss and phase delay.

2.5.2   Group Delay

Negative frequency derivative of signal phase is what we call as group delay. Both phase and amplitude distortions are encountered when a signal propagates through a medium. The properties of the medium/device determine the

amount of distortion. A pulse hitting a device or material will have many frequency components, and each frequency component undergoes different phase shifts. Group delay measures the dispersive nature of the device.

The group delay is mathematically related to the system response as:

$$H(f) = A(\omega)e^{j\theta(\omega)} \qquad (2.14)$$

And

$$\tau_g = \frac{-d\theta(\omega)}{d\omega} \qquad (2.15)$$

The nonlinearity of the phase response gives rise to the variation of group delay. That is the input signal will have different delays with respect to the frequency, and because of that the output signal will be highly distorted. The phase response of a filter has to satisfy the following relationships to have a constant group delay [21].

$$\theta(\omega) = -\alpha\omega \quad \text{OR} \quad \theta(\omega) = \beta - \alpha\omega \qquad (2.16)$$

UWB antenna is considered similar to that of a band pass filter. It has certain phase and magnitude response. The group delay is used to determine the phase linearities. The group delay is related to antenna gain response. The nonlinearities present in the phase can be efficiently analyzed using group delay plot. The input given to the UWB antenna is short pulses with large bandwidth. So if there exists a variation of the group delay in the passband of the transmitted pulse, it will distort the pulse. Two similar antennas are placed face to face and side by side orientations for measuring the group delay.

2.5.3 Selection of Source Pulse

The selection of the input pulse for the UWB antenna systems is the prime factor which has to be considered in the transient analysis. The chosen pulse width should be minimum and should contain all the frequency components of the required band. Various waveforms proposed for the UWB systems in the literature are the Laplacian pulse , cubic pulse, and Rayleighs pulse and

Gaussian pulses which are non-damped waveforms. If the width of these pulses is in order of nanoseconds, it satisfies the spectral requirements.

The spectrum of the chosen pulse should be uniform over the entire frequency range. The presence of DC components should not be there in the spectrum [22]. According to FCC any pulses with a bandwidth of $500MHz$ or greater can be used as UWB signals. FCC has limited the power of the signal to be transmitted. Thus the Pulse shape becomes significant in considering SNR, the effective bandwidth, and power utilization [23]. A suitable candidate is a Gaussian pulse, but the presence of the DC offset in the power spectral density leads to improper radiation [24]. A novel prolate spheroid wave functions are proposed as pulse shapes for use in impulse radio(ultra wideband) communications which yield orthogonal pulses and have a constant pulse width regardless of the pulse order which eliminates inter symbol interference [25]. Numerical generation of the pulses that fits in the FCC UWB mask is also studied [26, 27]. Although the pulses generated using this method are mutually orthogonal, it requires high sampling rates that lead to large memory requirements and thus implementation difficulties.

Signal bandwidth can be changed by pulse width variation and modulate with a sinusoid. There are UWB applications like impulse radio which uses carrier less transmission which cannot use the above method. The properties of the Hermite orthogonal polynomials [28] are changed so as to shape the pulse according to our needs. The most commonly used method is the use of the higher order Gaussian derivatives pulses [29] . Various differentiated Gaussian pulses have exceptional temporal and spectral properties. These are similar to that of a sinusoid modulated by Gaussian envelope.

$$V_n(t) = \frac{d^n}{dt^n}\left[e^{-2\pi(\frac{t}{\sigma})^2}\right] \tag{2.17}$$

Where n is the order of differentiation and represents the time in radians when $V_0(\sigma) = e^{-1}$, as shown in Fig 2.6(a). Certain higher order Gaussian derivatives pulses match the UWB band directly. Fourth order Rayleigh pulse is an example for the same. To peak the pulse spectrum at 5.5 GHz, σ value is chosen properly. This is the input pulse template used in this thesis for the analysis of the UWB antennas. Fig 2.6(a) shows the Gaussian pulse and their

derivatives. For a better distinction the figures are shifted in X-axis in Fig 2.6(a) and their power spectral densities in Fig 2.6 (b).
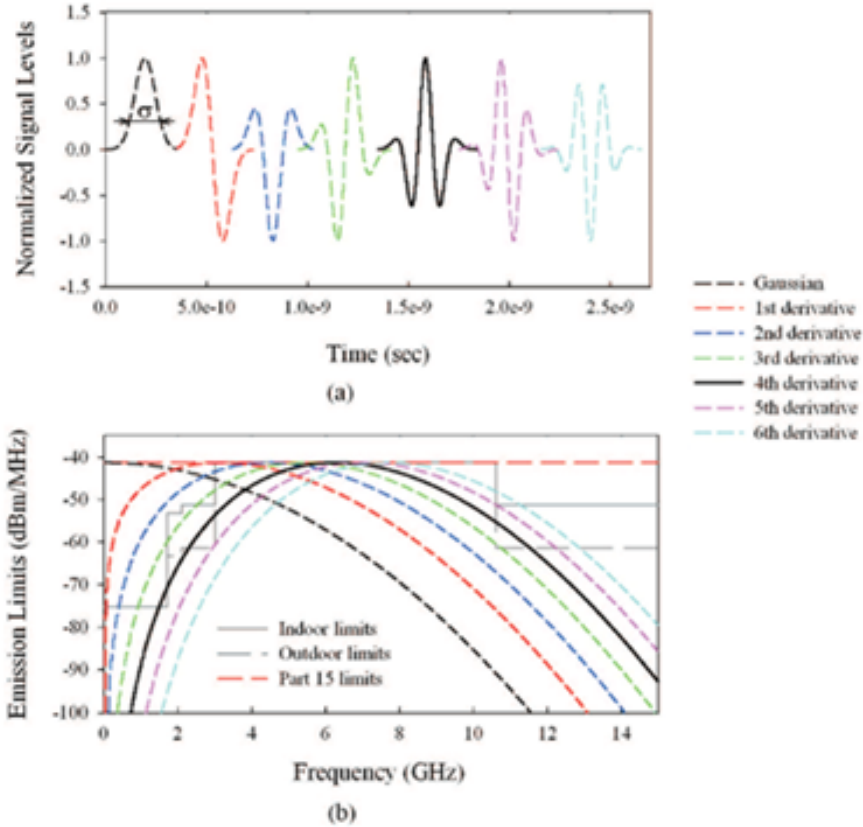
Figure 2.6: Gaussian Pulse and their Derivatives (a) Time domain (b) Power spectral densities

2.5.4 UWB antenna Transfer function Determination

Two similar antennas are used for determining the system transfer function. The $S_2 1$ is measured for these antennas in various orientations. These measured values are substituted into the equation given below to calculate the transfer function ($H(\omega)$).

$$H(\omega) = \sqrt{\frac{(2\pi R_c S_{21}(\omega) e^{\frac{j\omega R}{c}})}{j\omega}} \qquad (2.18)$$

The two antennas are placed at a distance of R and c represents the free space velocity.

2.5.5   Impulse Response

The impulse response is deduced by taking the IFFT of the transfer function. The measurement is taken over a frequency range of 3 to 12 GHz. Zero padding is done at the frequencies starting from $0 - 3$ GHz and 12 to f_{max}. This is done to so as to eliminate the response of the antenna to the noise signals in the out of band frequencies [30]. The conjugate of the zero padded signal is taken and reflected to the negative frequencies. This results in a symmetric pattern around DC. The IFFT of this signal gives the time domain impulse response.

2.5.6   UWB Antenna Received Signal Response

In the case of a UWB system, the received pulse waveforms should be same as for that of the transmitted waveforms with minimal distortions. The pulse received can be calculated from the source pulse and the system transfer function measured using a similar set of antennas.

The transfer function is the system response in frequency domain. It is measured using a VNA. The transfer function has to be transformed into the time domain. This is done by Hermitian Processing [31]. Zero padding is done to the transfer function from the lowest frequency down to DC. The zero padded signal is then conjugated and reflected to the negative frequencies. This results in the impulse response of the system in the frequency domain. It is then converted to the time domain using IFFT. The time domain impulse response is convolved with the input signal to obtain the output signal.

2.5.7   Fidelity Factor and Pulse Distortion Analysis

In the ideal condition, a UWB antenna should replicate the input pulse at the receiver end. However, in real-world changes in the radiation characteristics

and the position of the phase centers changes the transmitted pulse properties. This leads to non-linear phase response of the antenna resulting in pulse dispersion. Distortions of the signals in the frequency domain result in pulse dispersion hence the shape of the pulse is changed. Complex detection schemes have to be used at the receiver to recover a distorted pulse. Constant gain over the entire bandwidth is an important criterion for UWB antennas. This eliminates the frequency dependent distortions of the pulse transmitted. The received pulse shows spatial dependencies as the antenna gain varies with angles [32]. The spatiotemporal impulse responses account for the Pulse deformations introduced by the antenna along the various point of references. Fidelity factor is a term used to represent the similarity in the input pulse and the received pulse. It is the measure of how faithfully an antenna reproduces the shape of an input pulse. The commonly employed UWB receivers are mainly based on the correlation with the template waveform or based on the pulse energy detection. So the fidelity factor has to be calculated for finding the pulse distortions [33]. The fidelity factor, F is expressed as

$$FidelityFactor(F) = MAX \frac{\int X(t). \int Y(t-\tau)d\tau}{\sqrt{\int |X(t)^2|.dt \int |Y(t)|^2dt}} \qquad (2.19)$$

Here τ is the delay that is varied so as to maximize the numerator. The fidelity factor compares only the shape of the waveforms. The amplitudes of the waveforms are not compared. For different antenna orientations the fidelity factor is computed taking $y(t)$ as the input waveform and $x(t)$ as the received one [34].

In order to identify how a UWB system performs, two similar planar antennas are taken assuming one as the transmitting antenna and other as the receiving antenna. Both the antennas are placed in the free space 120cms apart, to be in the far field of each other.

2.5.8 EIRP

UWB communication is intended for short range high speed wireless indoor communication. Study of the antenna characteristics is most important because of this. The FCC spectral mask limits the EIRP of the antenna. So

advance study on the effect of the UWB antenna on the input pulse is required. The gain of the isotropic antenna is similar in all directions which imply

$$G_T(f, \theta, \phi) = G_T(f) \tag{2.20}$$

Where G_T is the transmitter antenna gain, θ and ϕ represents the azimuth and elevation angles in the spherical coordinates respectively. The radiated power density of the antenna over a sphere of radius d is given as,

$$\rho(f) = \frac{P_T(f)G_T(f)}{4\pi d^2} \tag{2.21}$$

Isotropic Radiated power is given as

$$IRP(f) = d_{ref}^2 \int_0^{2\pi} \int_0^\pi \frac{P_T(f)G_T(f)sin\theta d\theta d\phi}{4\pi d_{ref}^2} \tag{2.22}$$

Where d_{ref} is the distance of separation between the antennas. In the case of any practical UWB antennas, FCC requirement is that on any point of the sphere at a distance of d_{ref}, the power radiated must not go beyond that of the isotropic antenna, so the name effective isotropic radiated power(EIRP).

$$\begin{aligned} IRP(f) &= max_{\phi,\theta} P_T(f)G_T(f, \phi, \theta) \\ &= P_T(f)G_T(f, \phi_0, \theta_0) \end{aligned} \tag{2.23}$$

Where (ϕ_0, θ_0) represents the maximal gain direction in the spherical coordinates. Let $G_T(f)$ be maximum gain at a frequency f then,

$$EIRP(f) = P_T(f)G_T(f) \tag{2.24}$$

Friis transmission formula in its simple form is used to calculate the EIRP in watts per unit bandwidth. In this case, both the antennas are assumed to be polarization and impedance matched [35].

$$EIRP(f) = P_T(f)G_R(f)\left(\frac{c}{4\pi df}\right)^2 \tag{2.25}$$

In the equation 2.25 $P_T(f)$ is the transmitted power density, $G_R(f)$ is the gain of the antenna at the receiving side, d is the far field separation of the transmit and receive antenna, c is the velocity of light and f is the desired frequency of operation. This equation is only valid if we place the antennas in their far fields. The separation between the antennas should be greater than that of the maximum dimensions of the antenna used for transmission$(d > 2D_{max}^2/\lambda)$. When $D_{max} >> \lambda$, the field strength at the farfield will be very low. Near field, measurements are taken in those cases for estimating the EIRP [36].

As far as UWB antenna is concerned, the maximum antenna dimension is always less than the distance between the transmit and receive antenna, and the 10 GHz is the highest frequency of interest. There will be sufficient farfied distance in our case, and the equation 2.25 will be valid. Similar receive and transmit antennas are used for measuring the EIRP using the network analyzer.

$$H_{CH}(f) = \frac{P_R(f)}{P_T(f)} \tag{2.26}$$

Where H_{CH} is the channel response and which is determined by the transmitting and receive antenna responses in the free space. The orientation of the antennas is to be adjusted with care for maximum reception of transmitted power. The gain of the transmitter antenna and receiver antenna is the same. Then we can write it as a common term $G(f) = G_T(f) = G_R(f)$and from Eqn 2.23 and Eqn 2.25 we have

$$H_{CH}(f) = \frac{P_R(f)}{P_T(f)} \tag{2.27}$$

$$EIRP(f) = \sqrt{H_{CH}(f)}\left(\frac{4\pi df}{c}\right) \tag{2.28}$$

This expression was derived under the assumption that, there is no multipath reflection in the Friss transmission formula. Practically this condition may be created by RF absorbers around the antenna while measuring H_{CH} which will absorb all the major unwanted reflections. The remaining reflections caused due to the multipath signal can be eliminated by the truncation

of channel impulse response. The truncated impulse response is then transformed into frequency domain using fourier transform so as to use in eqn 2.28.

REFERENCES

[1] "Antenna design and simulation." [Online]. Available: http://www.antenna-theory.com/, (Accessed on 10-10-2016)

[2] I. Youngs, G. Stevens, and A. Vaughan, "Trends in dielectrics research: an international review from 1980 to 2004presented at the 2005 annual conference of the dielectrics group of the institute of physics." *Journal of Physics D: Applied Physics*, vol. 39, no. 7, p. 1267, 2006.

[3] M. Pecht, R. Agarwal, F. P. McCluskey, T. J. Dishongh, S. Javadpour, and R. Mahajan, "Electronic packaging materials and their properties," 1998.

[4] T. Hu, J. Juuti, H. Jantunen, and T. Vilkman, "Dielectric properties of bst/polymer composite," *Journal of the European Ceramic Society*, vol. 27, no. 13, pp. 3997–4001, 2007.

[5] D. Chung, *Materials for electronic packaging.* Butterworth-Heinemann, 1995.

[6] Chung, Deborah, *Materials for electronic packaging.* Butterworth-Heinemann, 1995.

[7] Y. Rao, J. Qu, T. Marinis, and C. Wong, "A precise numerical prediction of effective dielectric constant for polymer-ceramic composite based on effective-medium theory," *IEEE Transactions on Components and Packaging Technologies*, vol. 23, no. 4, pp. 680–683, 2000.

[8] A. Parkash, J. Vaid, and A. Mansingh, "Measurement of dielectric parameters at microwave frequencies by cavity-perturbation technique," *IEEE Transactions on microwave theory and techniques*, vol. 27, no. 9, pp. 791–795, 1979.

[9] "HP8510C Network Analyzer operating and programming manual," *Hewlett Packard*, 1991.

[10] "Antenna design and simulation." [Online]. Available: http://www.home.agilent.com (Accessed on 15-12-2009)

[11] P. Massey and K. Boyle, "Controlling the effects of feed cable in small antenna measurements," in *Antennas and Propagation, 2003.(ICAP 2003). Twelfth International Conference on (Conf. Publ. No. 491)*, vol. 2. IET, 2003, pp. 561–564.

[12] K. S. Leong, M. L. Ng, and P. H. Cole, "Investigation of rf cable effect on rfid tag antenna impedance measurement," in *2007 IEEE Antennas and Propagation Society International Symposium*. IEEE, 2007, pp. 573–576.

[13] C. A. Balanis, *Antenna theory: analysis and design*. John Wiley & Sons, 2016.

[14] J. D. Kraus, R. J. Marhefka, and A. S. Khan, *Antennas and wave propagation*. Tata McGraw-Hill Education, 2006.

[15] J. Anguera, A. Sanz, Y.-J. Ko, C. Borja, C. Puente, and J. Soler, "Theoretical and practical experiments for a single antenna gain testing method: Application to wireless communication devices," *Microwave and optical technology letters*, vol. 49, no. 8, pp. 1781–1785, 2007.

[16] H. Wheeler, "The radiansphere around a small antenna," *in Proc. IRE*, vol. 49, no. 8, pp. 1325–1331, 1959.

[17] H. Choo, R. Rogers, and H. Ling, "On the wheeler cap measurement of the efficiency of microstrip antennas," *IEEE transactions on antennas and propagation*, vol. 53, no. 7, pp. 2328–2332, 2005.

[18] H. G. Schantz, "Radiation efficiency of uwb antennas," in *IEEE Conference on Ultra Wideband Systems and Technologies*, vol. 2002, 2002, pp. 351–355.

Department of Electronics

[19] L. Guo, J. Liang, C. Parini, and X. Chen, "A time domain study of cpw-fed disk monopole for uwb applications," in *2005 Asia-Pacific Microwave Conference Proceedings*, vol. 1. IEEE, 2005, pp. 4–pp.

[20] Y. J. Cho, K. H. Kim, D. H. Choi, S. S. Lee, and S.-O. Park, "A miniature uwb planar monopole antenna with 5-ghz band-rejection filter and the time-domain characteristics," *IEEE transactions on antennas and propagation*, vol. 54, no. 5, pp. 1453–1460, 2006.

[21] E. C. Ifeachor and B. W. Jervis, *Digital signal processing: a practical approach*. Pearson Education, 2002.

[22] B. Allen, M. Dohler, E. Okon, W. Malik, A. Brown, and D. Edwards, *Ultra wideband antennas and propagation for communications, radar and imaging*. John Wiley & Sons, 2006.

[23] Z. N. Chen, X. H. Wu, H. F. Li, N. Yang, and M. Y. W. Chia, "Considerations for source pulses and antennas in uwb radio systems," *IEEE Transactions on Antennas and Propagation*, vol. 52, no. 7, pp. 1739–1748, 2004.

[24] J. D. Taylor, *Ultrawideband Radar: Applications and Design*. CRC press, 2012.

[25] R. S. Dilmaghani, M. Ghavami, B. Allen, and H. Aghvami, "Novel uwb pulse shaping using prolate spheroidal wave functions," in *Personal, Indoor and Mobile Radio Communications, 2003. PIMRC 2003. 14th IEEE Proceedings on*, vol. 1. IEEE, 2003, pp. 602–606.

[26] B. Parr, B. Cho, K. Wallace, and Z. Ding, "A novel ultra-wideband pulse design algorithm," *IEEE Communications Letters*, vol. 7, no. 5, pp. 219–221, 2003.

[27] H. Zhang and R. Kohno, "Ssa realization in uwb multiple access systems based on prolate spheroidal wave functions," in *Wireless Communications and Networking Conference, 2004. WCNC. 2004 IEEE*, vol. 3. IEEE, 2004, pp. 1794–1799.

[28] M. Ghavami, "Hermite function based orthogonal pulses for uwb communications," in *Proc. Wireless Personal Multimedia Conference 2001, Aalborg, Denmark, Sept.*, 2001.

[29] H. Sheng, P. Orlik, A. M. Haimovich, L. J. Cimini, and J. Zhang, "On the spectral and power requirements for ultra-wideband transmission," in *Communications, 2003. ICC'03. IEEE International Conference on*, vol. 1. IEEE, 2003, pp. 738–742.

[30] J. S. McLean, R. Sutton, and H. Foltz, "The effect of source pulse shape on the energy and correlation patterns of uwb antennas," in *Wireless Technology, 2004. 7th European Conference on*, Oct 2004, pp. 113–116.

[31] J. Liang, L. Guo, C. Chiau, and X. Chen, "Time domain characteristics of uwb disc monopole antennas," in *The European Conference on Wireless Technology*, 2005.

[32] N. Fortino, J.-Y. Dauvignac, G. Kossiavas, and R. Staraj, "Design optimization of uwb printed antenna for omnidirectional pulse radiation," *IEEE Transactions on Antennas and Propagation*, vol. 56, no. 7, pp. 1875–1881, 2008.

[33] D. Lamensdorf and L. Susman, "Baseband-pulse-antenna techniques," *IEEE Antennas and Propagation Magazine*, vol. 36, no. 1, pp. 20–30, 1994.

[34] M. Klemm, I. Z. Kovcs, G. F. Pedersen, and G. Troster, "Novel small-size directional antenna for uwb wban/wpan applications," *IEEE Transactions on Antennas and Propagation*, vol. 53, no. 12, pp. 3884–3896, 2005.

[35] G. D. Vendelin, A. M. Pavio, and U. L. Rohde, *Microwave circuit design using linear and nonlinear techniques.* John Wiley & Sons, 2005.

[36] J. D. Brunett, R. M. Ringler, and V. V. Liepa, "On measurements for eirp compliance of uwb devices," in *2005 International Symposium on Electromagnetic Compatibility, 2005. EMC 2005.*, vol. 2. IEEE, 2005, pp. 473–476.

Chapter 3

OPEN ENDED SLOTLINE FED ANTENNAS

> *The chapter gives a bright idea on the open-ended slot line/CPS and their characteristics. CPS fed dipole antenna for PCS1900/5.2 GHz WLAN bands is presented and analyzed. The suitability of the open ended slot line is analyzed for building an efficient radiator. The characteristics of the antenna are studied, and empirical design equations are developed and validated on different substrates.*

Contents

3.1   Introduction

The antenna may be treated as an electromagnetic field to current and current to field converter. Antenna generates radiation from the electromagnetic

current fed to it using the different feeding mechanisms and vice versa. Maximum power is transferred from source to load only if the feed point impedance matches the source impedance. Hence the role of feed in the design of compact efficient antennas is significant.

Antennas have undergone rapid evolution from the huge three-dimensional structures to the small planar ones. Different feeding mechanisms used in the planar antenna technologies are discussed in the chapter. The suitability of open-ended slot line for designing an antenna is also discussed. A dual band antenna evolved from the basic open ended slot line is presented and exhaustively studied using simulation tools and experimentally verified.

3.2 Printed Transmission Lines

Studies of planar transmission lines are crucial as far as the planar antenna design is concerned. Different planar feeding techniques are presented in the present section. One of the most commonly used planar transmission lines is Microstrip line which is a dual-layered structure. Coplanar waveguide and the slotline/coplanar strips are the uniplanar transmission lines discussed here.

3.2.1 Microstrip Line

The structure of microstrip line is depicted in Fig 3.1. Micro Strip Line has a narrow metal signal strip fabricated on a low loss dielectric substrate backed by a metallic ground plane. The parameters determining the characteristic impedance of the microstrip are the signal strip width (w), the substrate height (h) and the dielectric constant of the substrate (ϵ_r) [1].
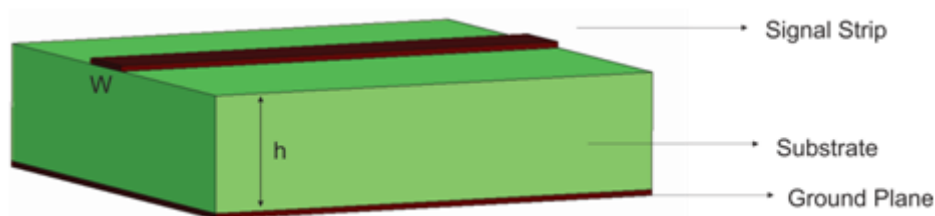

Figure 3.1: Microstrip line

Since the structure is a two-sided one, the integration of microwave components, both active and passive is difficult. Uniplanar antennas are mostly preferred for solving this problem. The commonly used transmission lines in this category include coplanar waveguide and slotlines/coplanar Strips .

3.2.2 CPW Transmission Line

The structure of a coplanar waveguide is shown in Fig 3.2. It consists of a central conductor and parallel ground planes separated by a small gap at both the sides. The width of the central conductor and the gap determines the characteristic impedance for a chosen substrate with height (h) and dielectric constant (ϵ_r) [2]. Integration of the circuit elements is easy since the structure is uniplanar
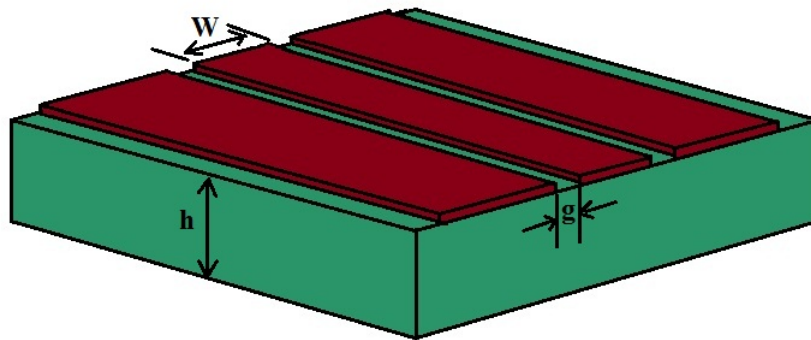
Figure 3.2: CPW Transmission Line

3.2.3 Co-Planar Strip(CPS)/Slotline

A slot line is a uniplanar transmission line proposed by Cohn in 1968 for use in microwave integrated circuits [3]. A slot line consists of a narrow gap etched out from metallization fabricated on a dielectric substrate as shown in Fig 3.3. The other side of the substrate is not having metallization. The uniplanar nature of the slot line makes it suitable for the use in the MMIC circuits.

Slotline may be treated as the complementary structure of the CPW in with the center strip replaced with a slot, and the gaps are substituted with metallization. The basic structure consists of two metal plates separated with a gap g. Slotline may be treated as a planar version of parallel wire transmission line. Active and passive elements can be connected easily in the series mode or the shunt mode which make the slot line an attractive choice for MMIC circuits. Since both the signal strips used in slot line are having the same surface area, the surface current distributions will also be same on both strips. The feed is connected between the two metal strips out of which one acts as a signal strip and other serves as the ground.

CPS is a good transmission line when it is fabricated on a substrate with high permittivity. But for substrates, with lower permittivity, the use of CPS is lossy due to the non-confinement of the field in the gap. Slot line on a low permittivity substrate has interesting applications in the antenna engineering.
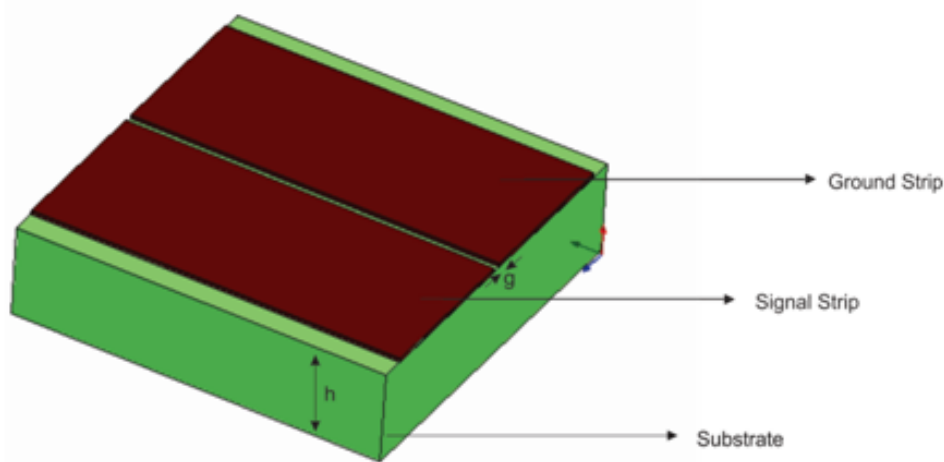

Figure 3.3: CPS/Slotline Transmission Line

The characteristic impedance of the slotline is determined by the gap g and the permittivity of the substrate. The characteristic impedance is obtained by curve-fitting the numerical results obtained from Galerkins method in Fourier transform domain [4].

For $0.0015 < g/\lambda_0 < 0.075$ and $3.8 < \epsilon_r < 9.8$ the characteristic impedance

of the slotline is given by the following equation.

$$Z_0 = 73.76 - 2.15\epsilon_r + (638.9 - 31.37\epsilon_r)\left(\frac{g}{\lambda_0}\right)^{0.6}$$
$$+ (36.23\sqrt{\epsilon_r^2 + 41} - 225)\frac{\frac{g}{h}}{\frac{g}{h} + 0.876\epsilon_r - 2}$$
$$+ 0.51(\epsilon_r + 2.12)\left(\frac{g}{h}\right)ln\left(\frac{100h}{\lambda_0}\right) - 0.753\epsilon_r(h/\lambda_0)/\sqrt{g/\lambda_0} \quad (3.1)$$

3.3 Open Ended Slot line(OES)

As already mentioned Slot line is a good transmission line when fabricated on high dielectric permittivity substrates ($\epsilon_r > 10$). In the case of high permittivity substrates, the slot mode wavelength will be very much smaller than the free space wavelength. In the case of low permittivity substrates, radiation losses occur from the slot line since the slot mode wavelength will be greater than the free space wavelength. So the fields are not confined to the slot. So we usually dont use slot line as a transmission line with low permittivity substrates but for an antenna designer to generate radiation from slotline transmission line is relatively easy. This is the motivation for designing slot line fed antennas in the present work. Since the chapter deals with CPS fed dipole antenna the detailed study of open-ended slot line is required. Slot line with open ends is analyzed here. An open ended slot line with reduced dimensions is shown in the Fig 3.4.
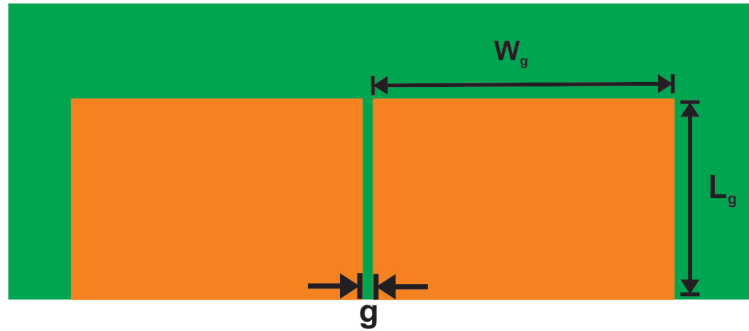

Figure 3.4: Slotline with open end ($L_g = 13$ mm, $W_g = 14.75$ mm, $g = 0.5$ mm, $h = 1.6$ mm, $\epsilon_r = 4.4$)

In order to understand the radiation properties of the open ended slotline, the structure is simulated on an FR4 substrate ($\epsilon_r = 4.4$, $h = 1.6$ mm and $tan\delta = 0.016$) with the dimensions $L_g = 13$ mm, $W_g = 14.75$ mm and $g = 0.5$ mm. The simulation was done using CST Microwave Studio , and the result is plotted in Fig 3.5. A resonance at 4 GHz is observed with poor impedance matching from the figure.
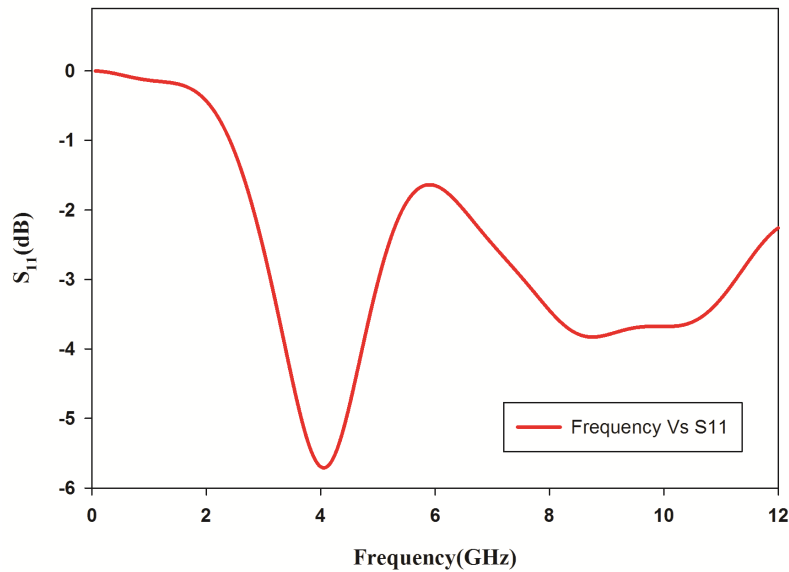

Figure 3.5: *Reflection Characteristics of Open ended Slotline ($L_g = 13$ mm, $W_g = 14.75$ mm, $g = 0.5$ mm, $h = 1.6$ mm, $\epsilon_r = 4.4$)*

The simulated efficiency of this design is 71% with a gain of $1.8 dBi$

3.3.1 Parametric Analysis

To obtain a vivid view of the characteristics of the antenna, the parametric analysis of the antenna is performed. The following section describes the effects of various parameters on the resonant frequency.

Effect of Parameter L_g on Reflection Characteristics.

Reflection characteristics of the short open-ended CPS with respect to the variation of the parameter L_g is shown in Fig 3.6. The shift in resonance is

negligible with the parameter variation as shown in the figure. As L_g increases the resonant frequency slightly shifts to a higher value, which is caused by the confinement of the fringing field close to the gap and the surface current density at the far end of the strips from gap are very low. That is, in the case of an open-ended CPS with higher values of L_g, the resonance current is maximum near the gap, and the average resonance length is reduced which causes the resonance to shift to a higher value.If we increase L_g above $0.6W_g$ the resonance shifts to a lower value, which is shown in fig 3.6(b). This is due to the formation of a new resonant path along the slot length. This resonant path is utilized in the dual band antenna design. As L_g increases the input impedance becomes more and more inductive causing the reduction in matching.

(a)   *(b)*
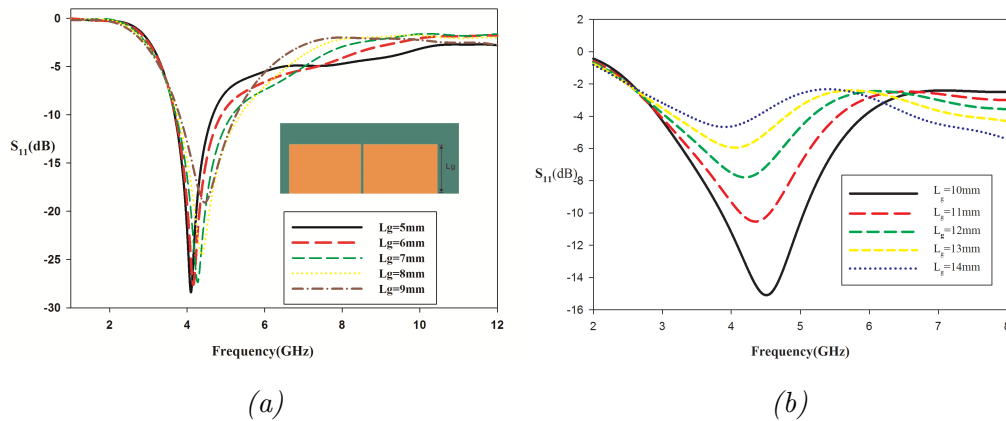
Figure 3.6: Variation of Reflection Characteristics with L_g (a)L_g <10 mm (b)L_g >10 mm
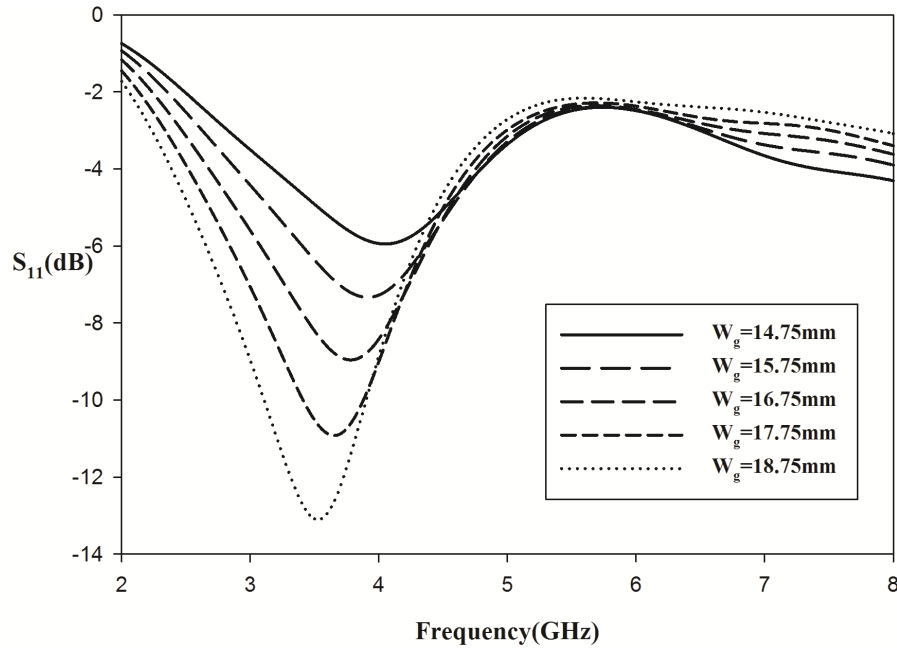
Figure 3.7: Variation of Reflection Characteristics with W_g

Effect of W_g on Reflection Characteristics

Fig 3.7 shows the variation of the S_{11} with the change in the width of the strips W_g. It is seen that as W_g increases the resonance shifts to a lower frequency. This shows W_g is an important parameter in determining the resonance. Average resonance length increases with the increase in W_g. Impedance matching is affected by the variation of this parameter due to the change in input impedance at resonance.

Variation in Reflection Coefficient with Substrate Thickness (h)

Variation of S_{11} with the change in substrate thickness is studied, and the results are plotted in Fig 3.8. As the substrate thickness increases, the only noticeable difference is in the impedance matching. Resonant frequencies are not affected by this parametric change.
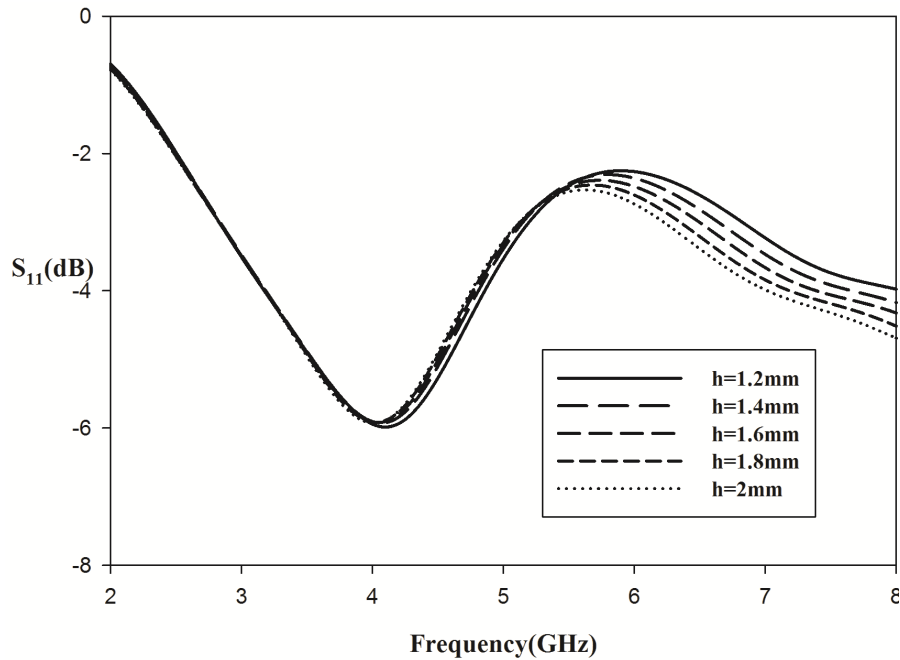
Figure 3.8: Variation of Reflection Characteristics with h

Effect of ϵ_r on the Reflection Characteristics.

Four different substrates are chosen so as to study the dependency of S_{11} on the ϵ_r. The results of the analysis are shown in Fig 3.9. The resonant frequency shift to a lower value with the increase in permittivity. Impedance matching is reduced as we increase ϵ_r.

3.3.2 Analysis of OES Using Surface Current Distributions

The surface current distribution of an open ended slot line at 4.2 GHz is shown in the Fig 3.10. It is seen from the figure that the surface current is aligned as in a dipole antenna along the strips. Half wave variations are seen along the width of the antenna. The polarization of the antenna is along the x-direction. From the parametric analysis, it is seen that as the length of the slotline increases the resonance shifts to a higher value. To investigate into

this problem, the absolute surface current distributions of open-ended slotline
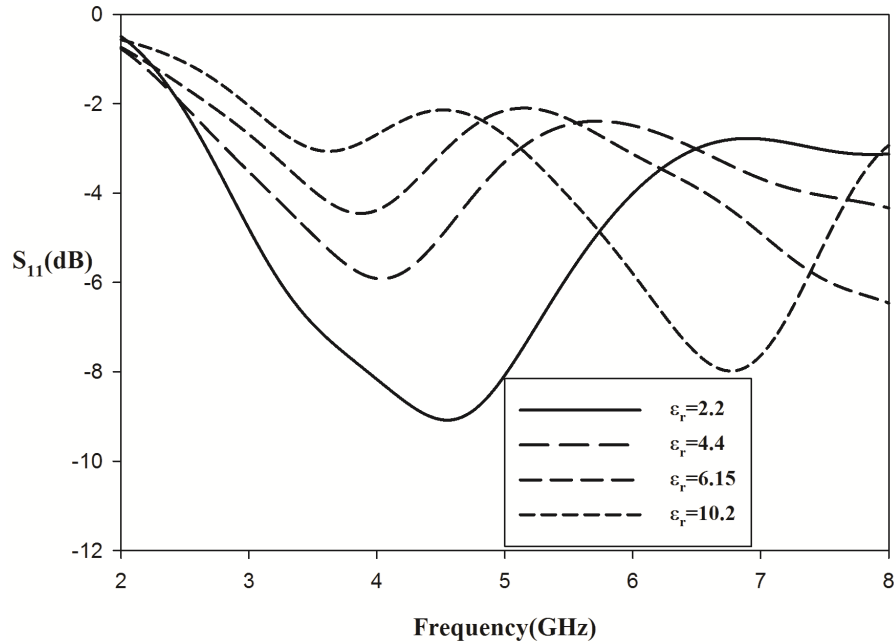
Figure 3.9: Reflection characteristics of OES on different substrates
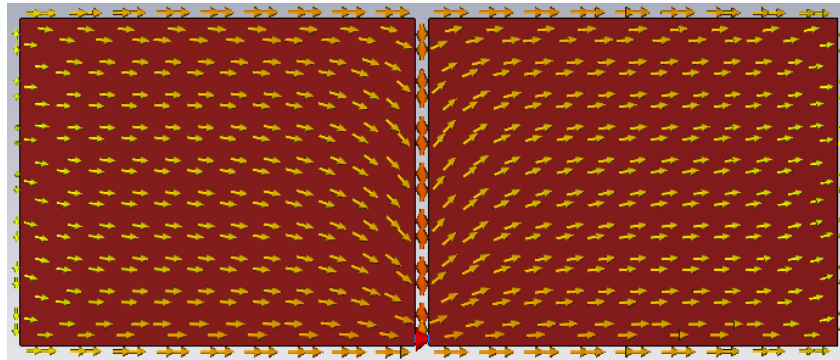

Figure 3.10: Surface current distribution of OES at 4.03 GHz

with different lengths are analyzed. The results are shown in Fig 3.11. From the figure, it is clear that the surface current density of CPS with reduced length is seen at the conducting part of the CPS. As length increases the surface current density tends to confine near the slot. The current densities

at the far end are very low, resulting in the reduction of effective resonant length. This substantiates the reason for the abnormal behavior of resonance with the increase in parameter L_g.
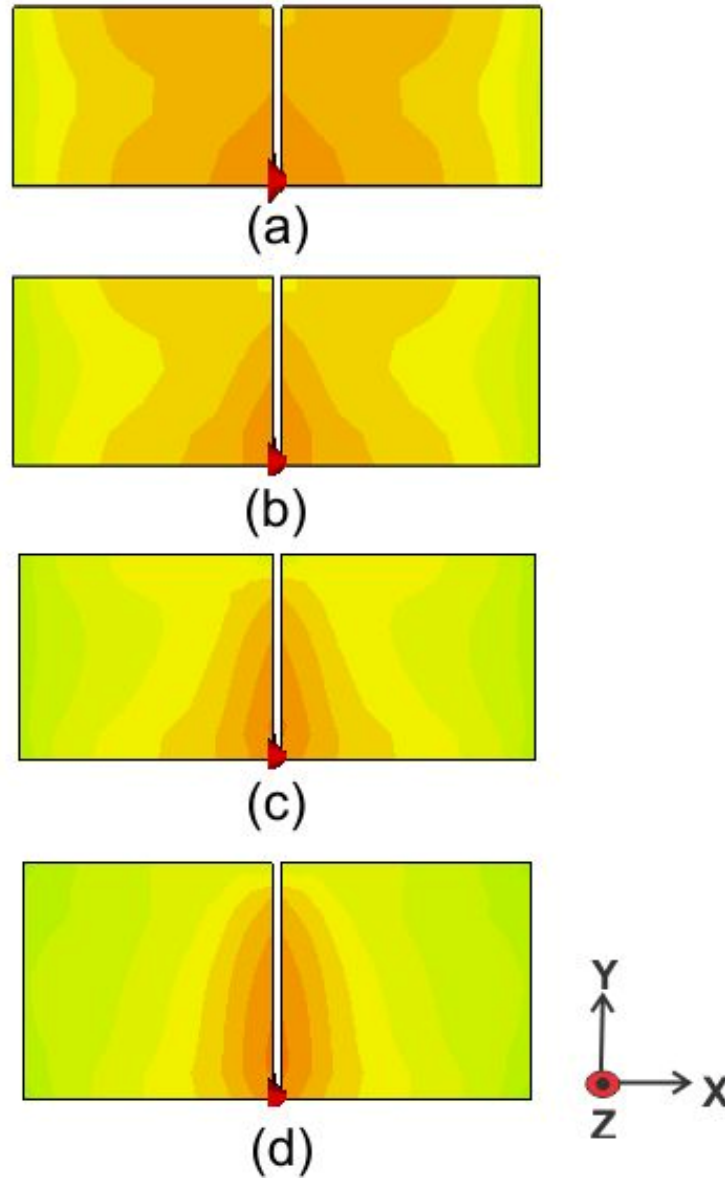
Figure 3.11: Absolute Surface current distribution of OES at 4.03 GHz for (a)$L_g = 6$ mm (b) $L_g = 8$ mm (c) $L_g = 10$ mm (d)$L_g = 12$ mm
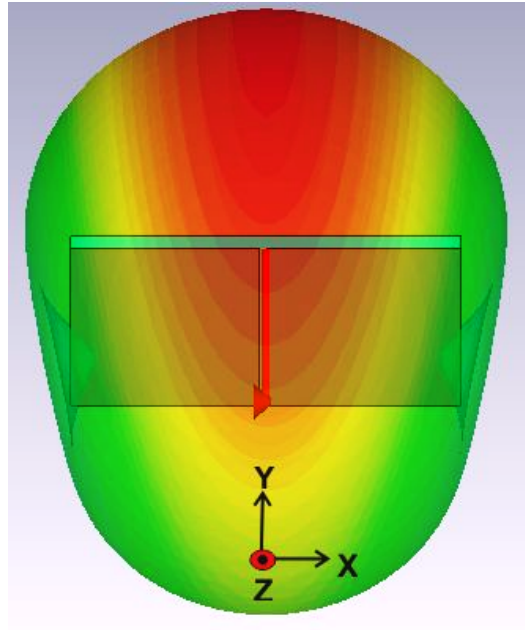
Figure 3.12: Simulated 3D Radiation Pattern of OES at 4.03 GHz

3.4 Open Ended CPS Fed Single Band Radiator

From the parametric studies done in section 3.3, it is clear that the CPS can be transformed as an efficient radiator. The following sections describe the evolution of CPS fed dipole antenna for dual band applications. The evolution of the antenna begins with a basic open-ended slotline, from which a single band radiator is formed, which is then converted into a dual band antenna.

3.4.1 Single Band OES Radiator

A basic open-ended CPS/Slotline with reduced length has a surface current distribution similar to that of a dipole antenna as shown in Fig 3.10. Extending a strip from the top edge of OES results the increase of inductive reactance which improves the impedance matching. Effective resonant length

is increased due to this extension. . The geometry of the proposed single band design is shown in Fig 3.13a and the simulated
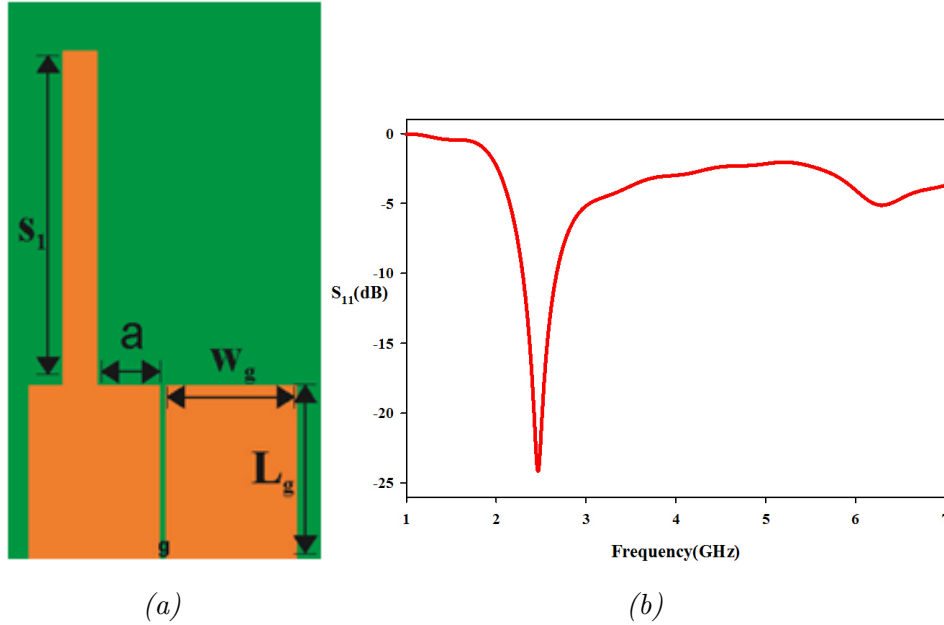

(a)   (b)

Figure 3.13: Single band OES antenna design ($S_1 = 25$ mm, $W_g = 9.75$ mm, $L_g = 13$ mm, $a = 4.65$ mm, $g = 0.5$ mm) (a) Geometry (b) Reflection Characteristics

reflection characteristics is shown in the Fig 3.13b.Resonance is observed at 2.43 GHz with proper impedance matching. The deciding length for this resonance is $(S_1 + a + W_g)$ which is approximately half the guided wavelength long. Parametric analysis is performed so as to study the cause of resonance and radiation.

3.4.2 Effect of Strip S_1 on the Reflection Characteristics of the Antenna

The variational study of the parameter S_1 on the reflection characteristics is shown in Fig 3.14. It is seen that the resonant frequency shifts to a lower value with the increase in S_1. As S_1 increases, the effective resonance length

is increased causing resonance to come to a lower value. It is observed that the impedance matching is decreased slightly with the increase in S_1.
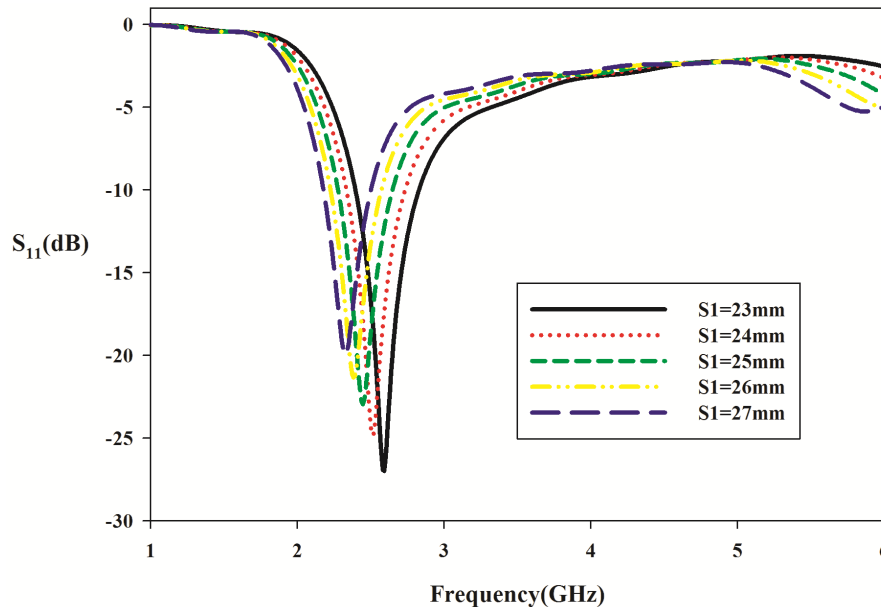

Figure 3.14: Effect of Strip S_1 on the reflection characteristics of the antenna.

3.4.3 Effect of Strip Width W_s on the Reflection Characteristics of the Antenna

The effect of the width of the strip on the reflection characteristics is analyzed using CST Microwave studio, and the results are plotted in Fig 3.15. It is seen that resonant frequency shifts to a higher value as we increase in strip width, this is due to the reduction of the effective resonant length that is, as W_s increases the length a is reduced which is the part of the effective resonant path which contributes to radiation. The impedance matching of the antenna is decreased as the width of the strip increases; this is due to the change in input impedance. The real part of the impedance increases with the increase in strip width.
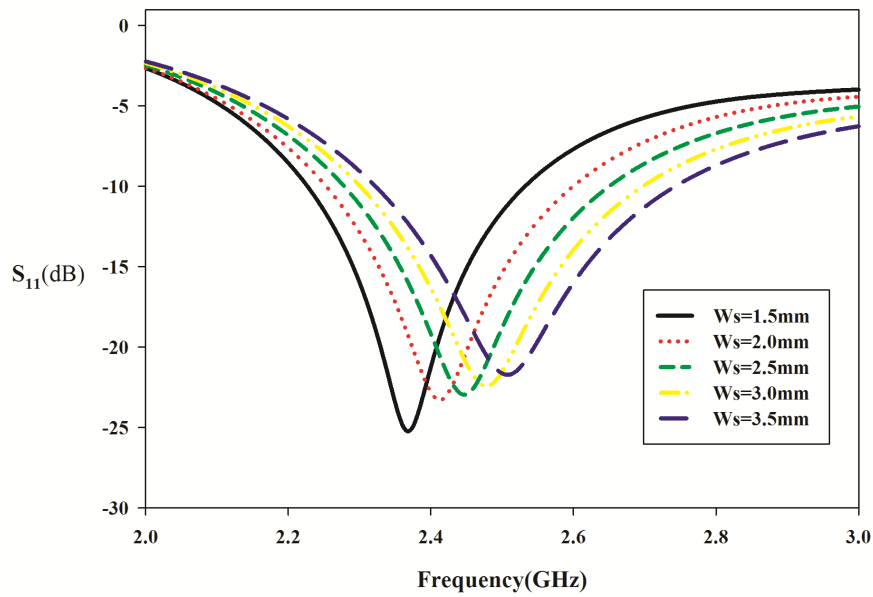
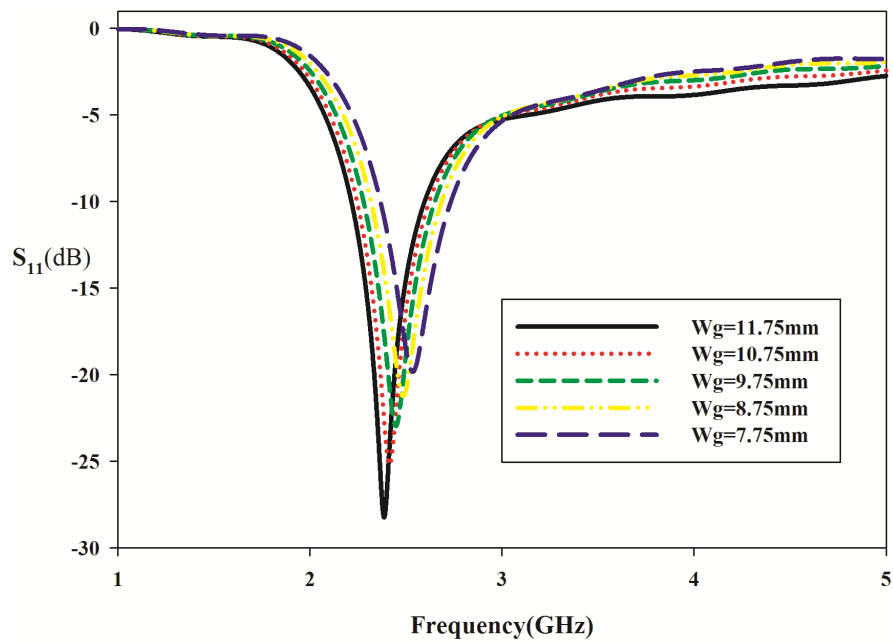*Figure 3.15: Effect of strip width W_s on the reflection characteristics*

Figure 3.16: Effect of W_g on the reflection characteristics

3.4.4 Effect of W_g on the Reflection Characteristics of the Antenna

As W_g increases the resonance come to a lower value which indicates that W_g is a determinant factor for the resonance and radiation which is shown in Fig 3.16. Impedance matching also improves with the increase in W_g. This is because of the increase in distributed capacitance which leads to the reduction in reactive part of the input impedance which approaches towards zero. Thus the impedance matching is improved. As the strip width increases the real part of the input impedance increases and it approaches towards 50Ω.

3.4.5 Surface Current Distribution and 3D Radiation Pattern of the Antenna

The surface current distribution of the antenna is plotted in figure 3.17. A half wave variation is seen across the points ABC with A and C being the minima points and B is the point where the maximum surface current density is perceived. It substantiates the parametric analysis and the reason for resonance. The resonance length is contributed by the parameters S_1, W_g and a. As the strips are extended, the surface current density is distributed along the strip length. The simulated 3D radiation pattern of the OES antenna is shown in Fig 3.18. It is seen that the maximum radiation is along the X direction and the nulls are located on the Y axis. The antenna is linearly polarized along the Y axis.
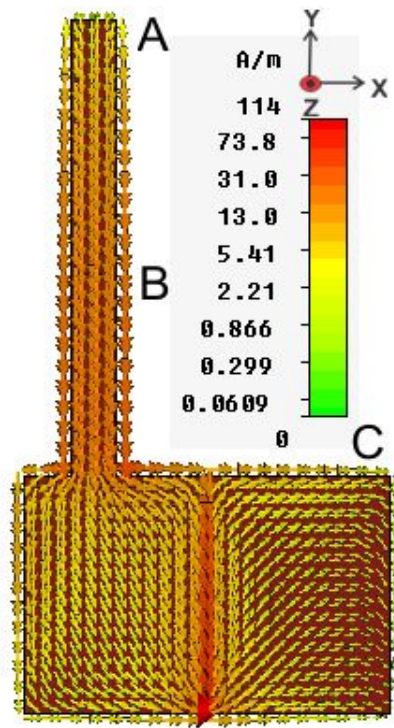
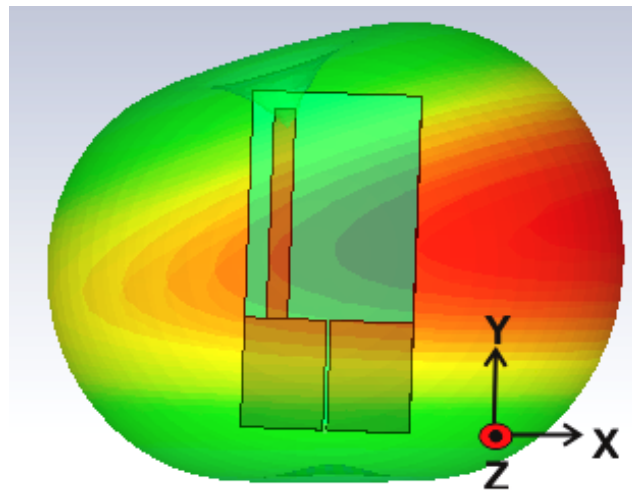*Figure 3.17: Simulated surface current distributions at 2.43 GHz*

Figure 3.18: Simulated 3D radiation pattern at 2.43 GHz

3.5   OES Dual Band Radiator

Section 3.3 is the first stage of evolution of the OES dual band antenna. For obtaining a single band resonance, we extended the left strip of CPS which resulted in an efficient radiator. In order to get an additional resonance, another strip is extended from the right side of CPS.
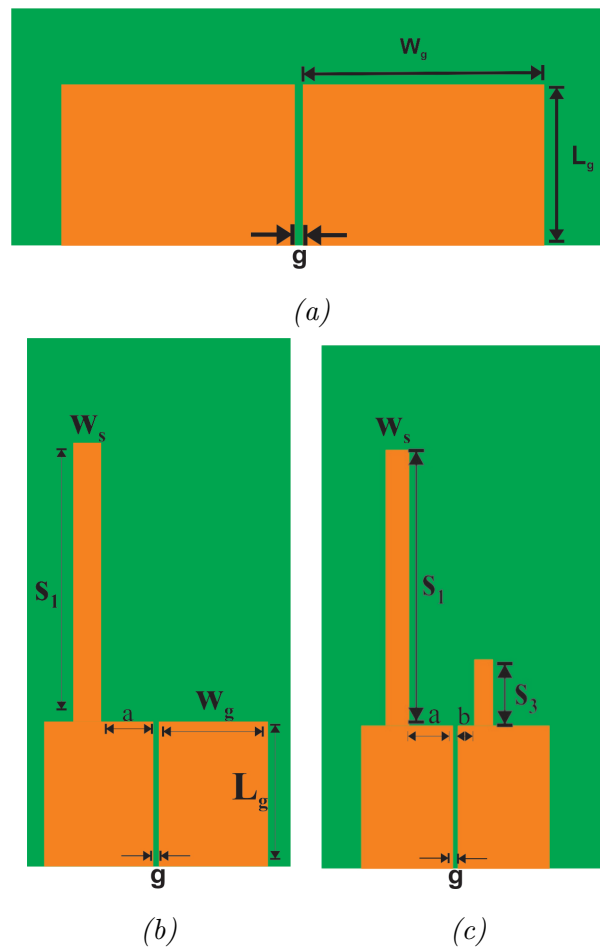

Figure 3.19: Evolution of the dual band antenna (a) Basic OES (b) CPS fed single band antenna (c) Basic dual band design

3.5.1 Evolution of OES Dual Band Radiator

Evolution of OES dual band radiator is depicted in Fig 3.19. The design is emerged from a basic open-ended slot line radiator. In order to excite an additional resonance, the right strip of the CPS is extended slightly which resulted in resonance near 6 GHz the design is shown in Fig 3.19(c), and the corresponding simulated S_{11} is given in Fig 3.20.
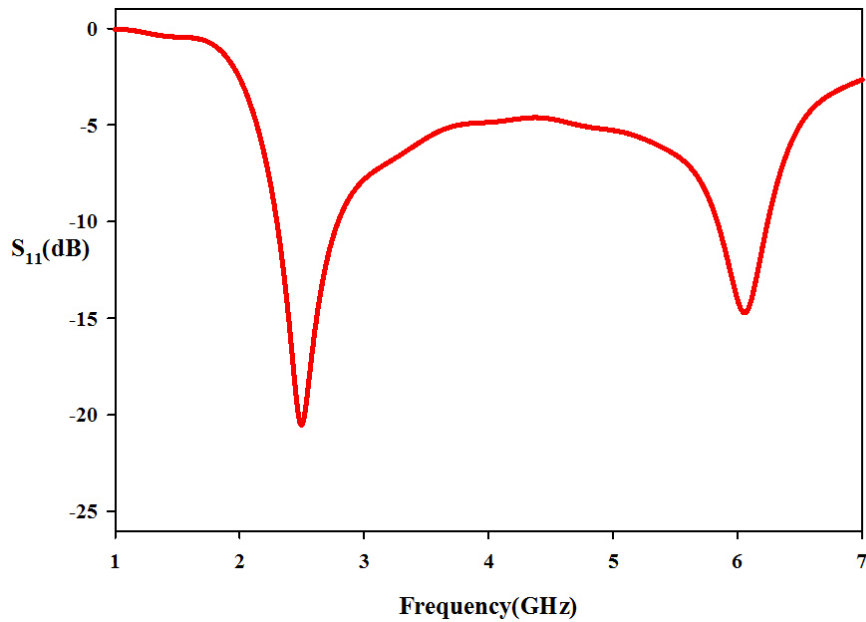

Figure 3.20: Reflection characteristics of the dual band antenna

3.5.2 CPS Fed Dipole Antenna for PCS/WLAN Applications

CPS fed dipole antenna with asymmetric arm lengths is proposed in the present section. The design is obtained by bending the strip S_1 shown in Fig 3.19(c) into an inverted L form so as to bring down the resonant frequency to cover the PCS band. The higher resonance at 6 GHz shown in Fig 3.20 is also bought down to 5.2 GHz which covers the WLAN band. The detailed analysis of the final dual band antenna is done in the following sections. The

antenna radiates both in the PCS1900 band and 5.2 GHz WLAN bands. The geometry of the evolved design is shown in Fig 3.21. The design is fabricated on an FR4 substrate with $\epsilon_r = 4.4$, $h = 1.6$ mm and $tan\delta = 0.016$. The gap g of the slotline is designed for obtaining 50 Ω impedance. Variational studies of the antenna parameters are performed in the next section so as to get a clear idea of the radiation mechanism .
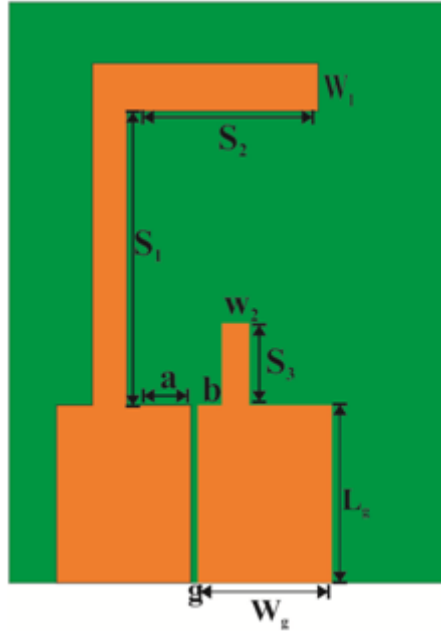

Figure 3.21: Geometry of the PCS/WLAN antenna ($S_1 = 21.5$ mm, $S_2 = 13.9$ mm,$S_3 = 6$ mm, $a = 4.65$ mm, $b = 1.75$ mm, $L_g = 13$ mm, $\epsilon_r = 4.4$, $W_g = 9.75$ mm, $g = 0.5$ mm)

Effect of the Parameter S_2 on the Reflection Characteristics

The dependence of the parameter S_2 on the resonances is shown in Fig 3.22. It is seen that as the parameter S_2 increases both the resonances are shifted to a lower value, which gives us the indication that S_2 is an important parameter which contributes towards the effective resonant lengths at both the frequencies. The separate parametric studies of S_1 are not required since S_1
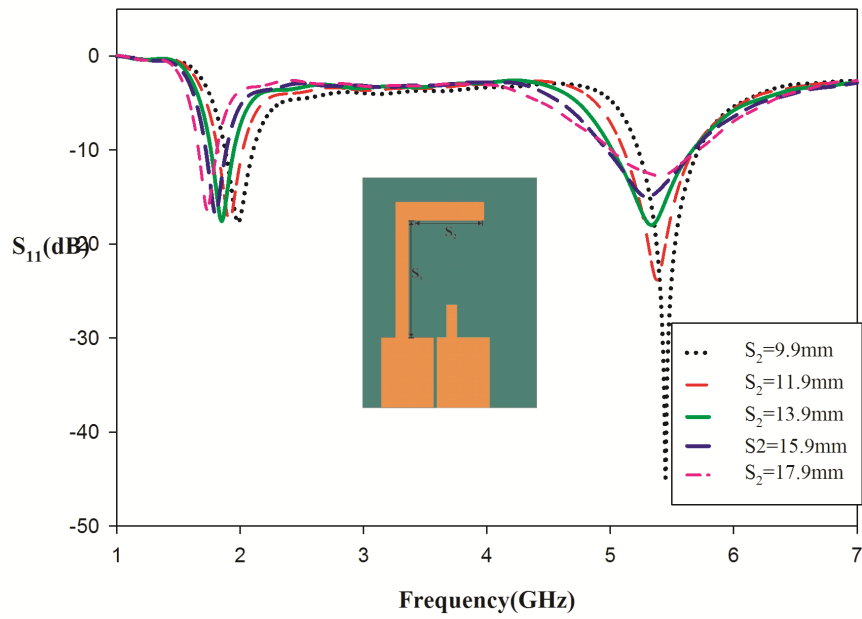
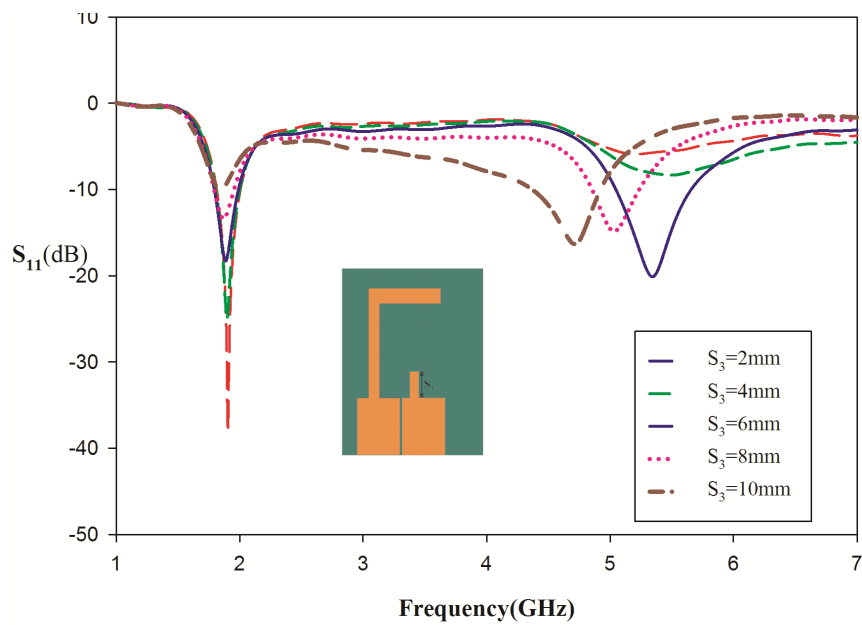*Figure 3.22: Effect of the parameter S_2 on reflection characteristics*

Figure 3.23: Effect of the parameter S_3 on reflection characteristics

and S_2 are the part of a continuous resonant path. Thus the effect of S_1 and S_2

can be taken together for analysis. Impedance matching and the bandwidth at the lower resonance remains unchanged. Whereas at higher resonance it is observed that the impedance matching decreases with increase in the length S_2.

Effect of the Parameter S_3 on the Reflection Characteristics

The dependence of the parameter S_3 that is the length of the second extension strip from the top end of the other strip on the reflection characteristics is analyzed and the result is shown in the Fig 3.23.

From the Figure, it is seen that both the resonances are affected by the variation of the parameter S_3. Both the resonances shift to a lower value as the length S_3 increases. However, the effect is more predominant for the higher resonance where the wavelength becomes comparable with the length S_3. Impedance matching at the first resonance increases with increase in length S_3.
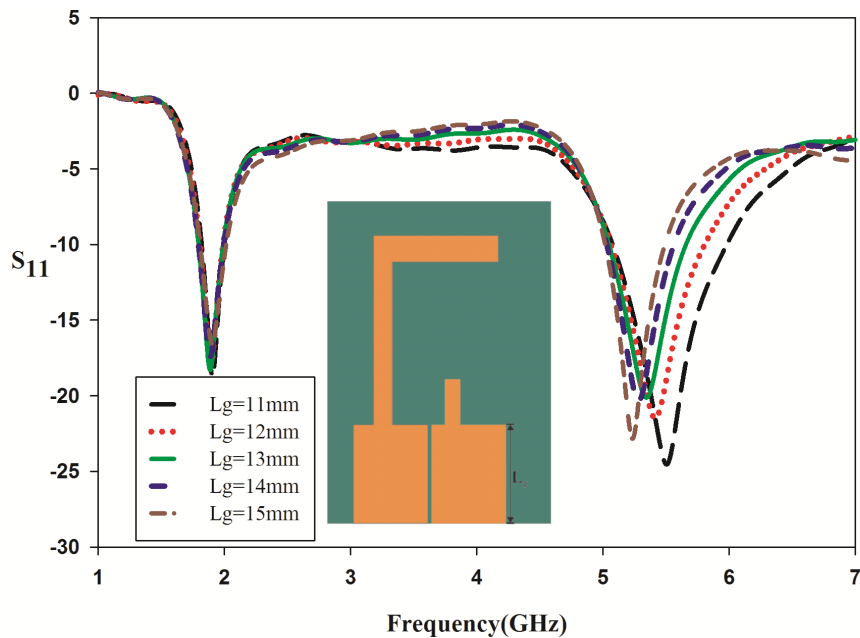

Figure 3.24: Effect of the parameter L_g on reflection characteristics

Effect of the Parameter L_g on the Reflection Characteristics

The effect of L_g on the reflection characteristics is studied, and the results are plotted in Fig 3.24. From the Figure, it is seen that as the value of L_g increases, the second resonance is shifted to a lower value. The first resonance is unaffected by the variation of L_g. So the second resonance can be tuned independently by changing the length L_g.

3.5.3 Analysis of Surface Current Distribution

To identify the resonant path and radiation mechanism, surface current distributions are analyzed. Surface current distribution for the resonance 1.88 GHz is shown in the Fig 3.25. From the Figure, a half wave variation is seen across the path ABC which includes the inner edge of the length $(S_1 + S_2)$, a, b and S_3. A and C are the points where minimum surface current densities are seen, and maximum surface current density is seen at B.
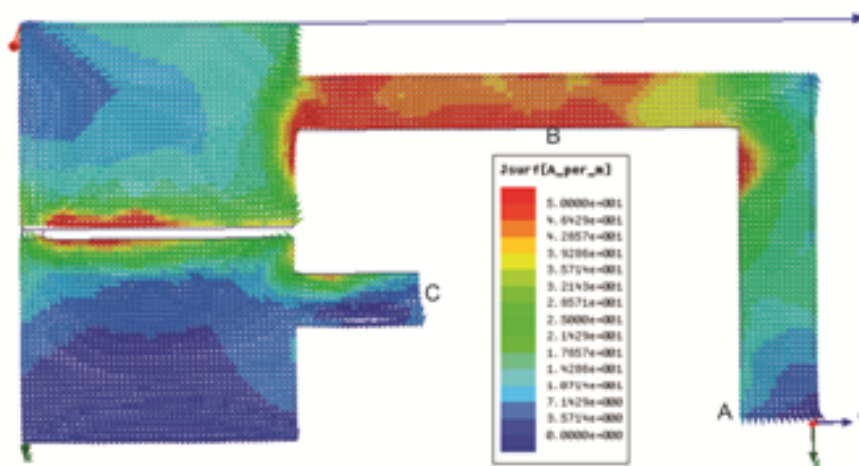

Figure 3.25: Simulated surface current distribution at 1.88 GHz

The surface current distributions at 5.2 GHz are shown in the Fig 3.26. Four half wave variations can be seen along the path ABCDEFG. One along ABC with B is the maxima point, one along CDE, D being the maxima point, one along the EFG, F being the maxima point and the final one from G to
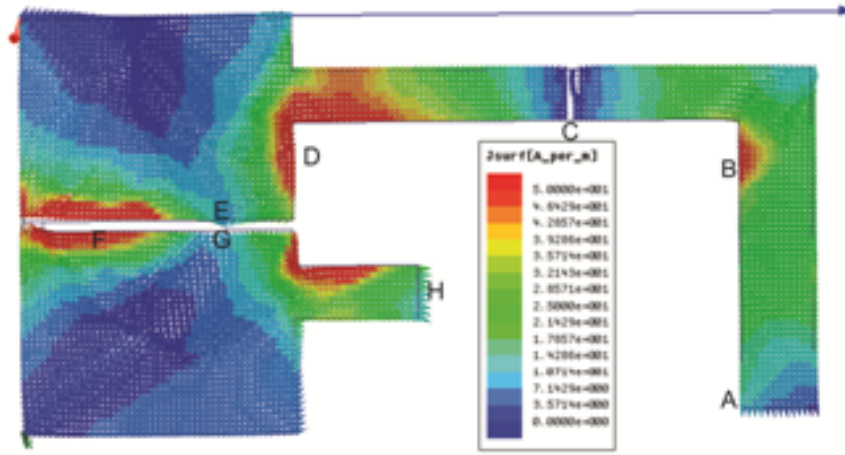
Figure 3.26: Simulated surface current distribution at 5.2 GHz

H with the maxima point in between them. It is seen that an anti-parallel current path exists at the both ends of the gap which cancels at the far field, but it contributes towards the second resonance.

Thus it is seen from the surface current distributions both the resonance can be varied by a similar set of parameters. The length L_g contributes towards the second resonance but non-radiating. Since L_g is the path which includes the SMA connector also, the spurious feed radiation can be avoided in the proposed design. The advantage of the proposed design is both same parameters can control the resonances. Polarization is linear along the Y axis in both the bands.

3.5.4 Antenna Design

From the parametric analysis, the deciding factors for both the resonance are investigated. The effects of these parameters are verified using the surface current distributions. Approximate design equations are derived from the above studies, as given below.

$$L_{S1} + L_{S2} = 0.51\lambda_{g1} \tag{3.2}$$

$$L_{S1} + L_{S2} + 2L_g = 2.2\lambda_{g2} \tag{3.3}$$

$$L_{S1} = S_1 + S_2 + a \qquad (3.4)$$

$$L_{S2} = S_2 + b \qquad (3.5)$$

$$\lambda_{g1} = \lambda_{g01}/\sqrt{\epsilon_{reff}} \qquad (3.6)$$

$$\epsilon_{reff} = \frac{\epsilon + 1}{2} \qquad (3.7)$$

Optimal parameters computed based on these design equations for the antenna are given in Table 3.1

Table 3.1: Computed antenna parameters

(All lengths in mm)	ANT1	ANT2	ANT 3
Substrate	Rogers 5880	FR4 EPOXY	Rogers RO 3006
h(mm)	1.57	1.6	1.28
ϵ_r	2.2	4.4	6.15
g	0.30	0.5	0.75
S_1	27.02	21.5	18.69
S_2	18.05	13.9	12.08
S_3	7.79	6	5.21
a	6.04	4.65	4.04
b	2.27	1.75	1.72
L_g	16.86	13	11.30
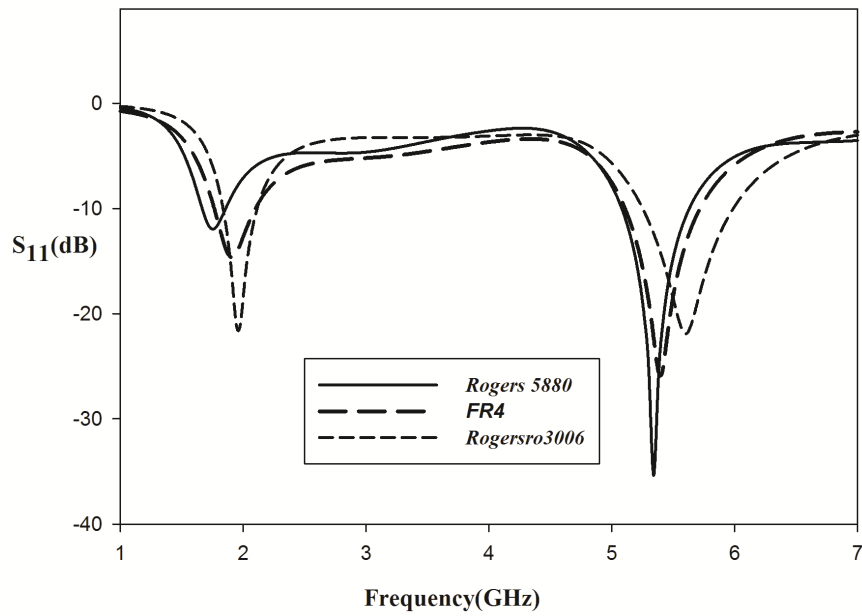
Figure 3.27: Reflection characteristics verification on different substrates
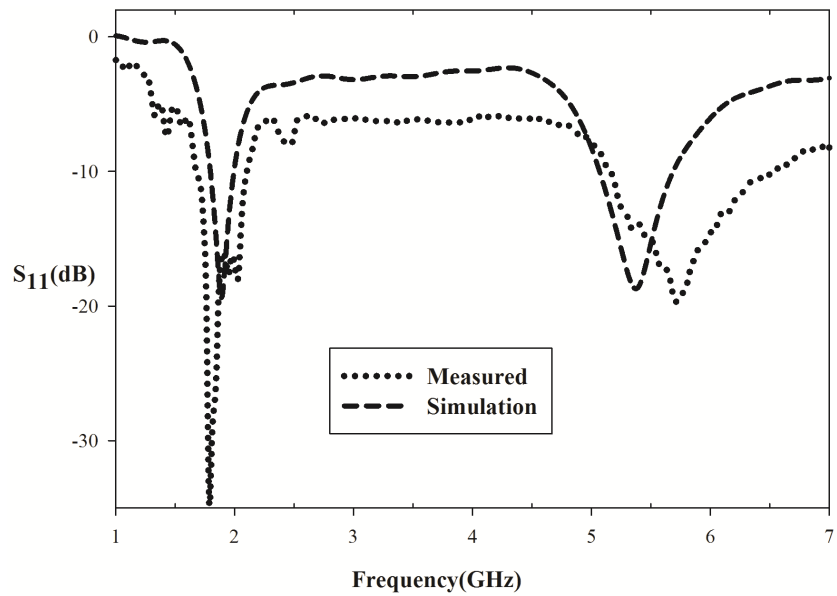

Figure 3.28: Reflection Characteristics Measured and Simulated

3.5.5 Experimental Results

The proposed antenna is fabricated on the FR4 substrate, and its characteristics are measured using vector network analyzer. The measured reflection characteristics are compared with the simulation results in Fig 3.28, where there is an agreement within tolerable limits. Two resonances, one at 1.88 GHz and the other at 5.4 GHz which covers the PCS1900 and WLAN bands. The gain of the antenna measured is found to be $2.38dBi$ and $3.4dBi$ for lower and higher band respectively. Measured efficiency is determined to be 88.6% and 92% respectively. The measured radiation pattern of the antenna is shown in Fig 3.29 and Fig 3.30 for 1.88 GHz and 5.2 GHz respectively.Both the bands shows almost similar radiation patterns which are omnidirectional.
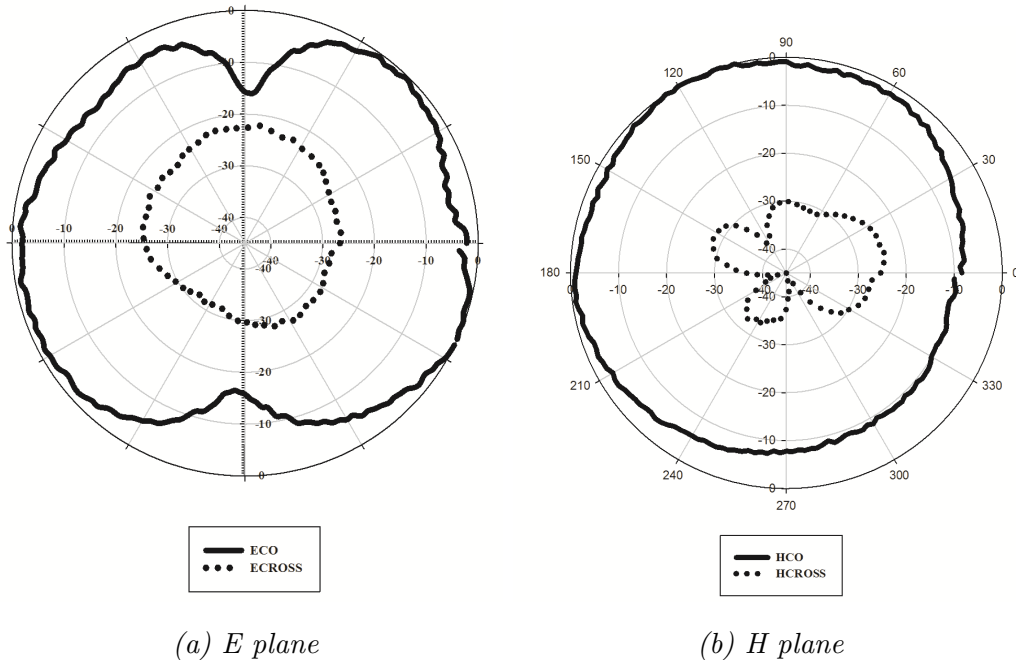

(a) E plane   *(b) H plane*

Figure 3.29: Measured Radiation pattern at 1.88 GHz
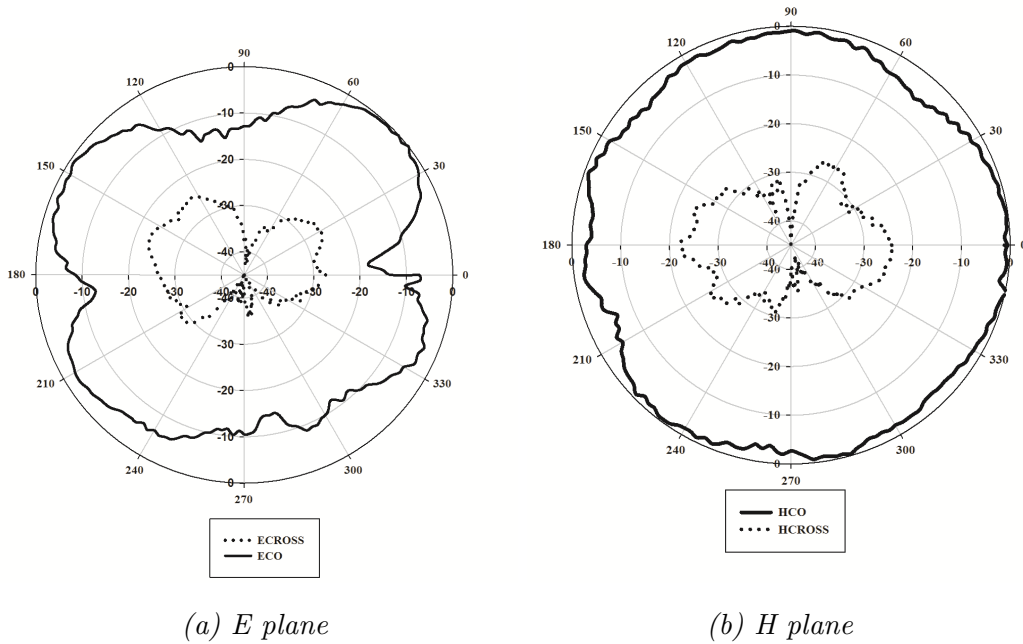
(a) E plane

(b) H plane

Figure 3.30: Measured Radiation pattern at 5.2 GHz

3.6   Chapter Conclusions

The chapter gave a detailed analysis for various available planar feeding techniques. The analysis of the open ended slot lines with reduced length is analyzed. The evolution of the dual band radiator from a basic open ended slot line is discussed in detail. The dual band antenna designed for PCS/WLAN applications possess good radiation characteristics. The fabricated prototype of the antenna is shown in Fig 3.31.

Table 3.2: Comparison of proposed antenna with Literature antennas

Parameter	ANT1 [5]	ANT2 [6]	ANT3 [7]	Proposed Design
Resonance Frequencies	1.9 GHz, 3.5 GHz, 5.5 GHz	2.5 GHz, 3.5 GHz, 5.2 GHz	2.1 GHz, 5.9 GHz	1.88 GHz, 5.4 GHz
Size	40 mm × 36mm	28 mm × 32 mm	58 mm × 62 mm	25 mm × 20 mm
Gain	0.3dBi, 2.2 dBi	2.77 dBi, 2.98 dBi, 2.78 dBi	2 dBi, 2.7 dBi	2.38 dBi, 3.4 dBi
Efficiency	85%	–	90%, 80%	88.6%, 92%
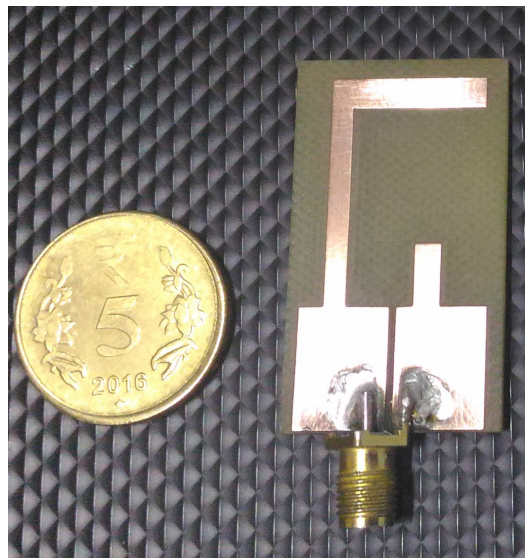
Figure 3.31: Fabricated Prototype of the antenna

REFERENCES

[1] R. Garg, "Microstrip antenna design handbook," *Artech House antennas and propagation library*, pp. 761–762, 2001.

[2] R. Garg, I. Bahl, and M. Bozzi, "Microstrip lines and slotlines," *Artech house*, 2013.

[3] "Slot Line on a Dielectric Substrate," *IEEE Trans. Microwave Theory Tech.*, vol. 17, no. 10, pp. 768–778, 1969.

[4] E. Mariani, C. Heinzman, J. Agrios, and S. Cohn, "Slot Line Characteristics," *IEEE Transactions on Microwave Theory and Techniques*, vol. 17, no. 12, 1969.

[5] A. Dadgarpour, A. Abbosh, and F. Jolani, "Planar multiband antenna for compact mobile transceivers," *IEEE Antennas and Wireless Propagation Letters*, vol. 10, pp. 651–654, 2011.

[6] W. Hu, Y. Z. Yin, P. Fei, and X. Yang, "Compact triband square-slot antenna with symmetrical l-strips for wlan/wimax applications," *IEEE Antennas and Wireless Propagation Letters*, vol. 10, pp. 462–465, 2011.

[7] B. Yildirim, E. Basaran, and B. Turetken, "Dielectric-loaded compact wlan/wcdma antenna with shorted loop and monopole elements," *IEEE Antennas and Wireless Propagation Letters*, vol. 12, pp. 288–291, 2013.

Chapter 4

CLOSED ENDED SLOTLINE ANTENNAS

The chapter highlights the creation of efficient radiation from the closed-ended slotline and the impedance and radiation characteristics of these antennas. Slot line fed uniplanar antenna for 2.4/5.8GHz WLAN applications is derived from a basic closed ended slot line with a transition from slot line to the rectangular slot with proper tapering. The subsequent sections discuss the slotline coupled wideband slot radiator which investigates slotline to slot coupling technique for efficient radiation. The antenna is designed to radiate a bandwidth of 4.8 to 6.2GHz covering both the 5.2/5.8 GHz WLAN bands. The design equations for both the antennas are derived and validated on three different substrates, which resulted in a similar response.

Contents

4.1   Basic Closed Ended Slotline

The characteristics of the open ended slot lines are discussed in section 3.2. Closed-ended slot lines are formed by shorting the one end of the slotline. A better understanding of the closed ended slot line is necessary so as to
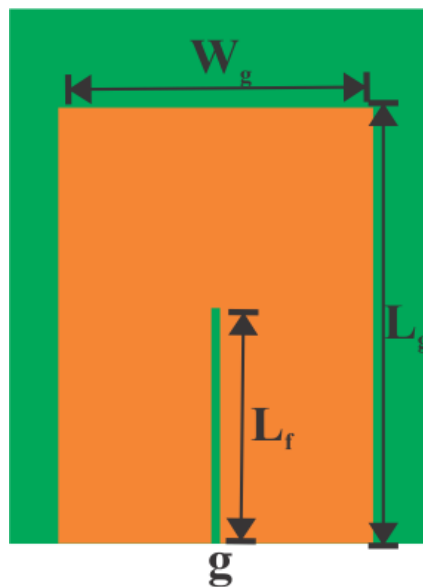

Figure 4.1: Basic closed-ended slotline geometry

analyze the antennas with the closed end. A basic closed end slotline antenna has the properties of a slot antenna, where the resonance is determined only by the slot length thus extending the circuit ground to the metallization does not affect the resonance frequency. A basic closed ended slot line is shown in the Fig 4.1 with parameters, $g = 0.5$ mm, $L_g = 25$ mm, $W_g = 18$ mm, and $L_f = 13.5$ mm. FR4 ($\epsilon_r = 4.4$, $h = 1.6$ mm, $tan\delta = 0.016$) substrate is chosen for designing the closed-ended slotline. The gap g is optimized so as to obtain nearly 50Ω input impedance. The simulated reflection characteristics obtained in CST microwave studio is shown in the Fig 4.2. A resonance with poor matching is observed near 6 GHz. Since our aim is to use it as an
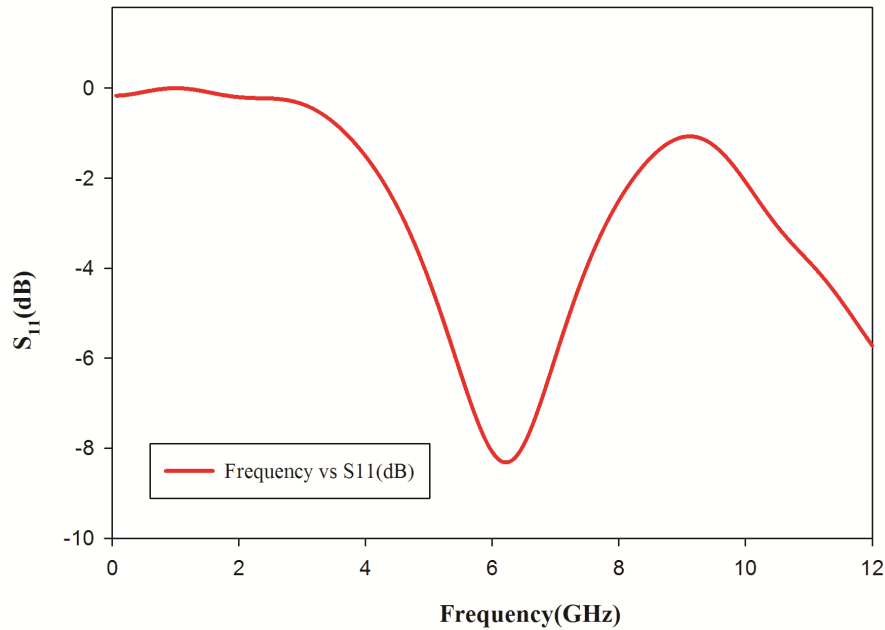
Figure 4.2: Reflection characteristics of basic closed ended slotline

antenna, better matching is to be obtained. For this parametric studies are done, which is discussed in the next section.

4.1.1 Parametric Analysis

The resonance frequencies and matching are always associated with different dimensions of the structure. The use of parametric analysis is to find out the resonance determining parameters and their effect on the reflection and radiation characteristics of the closed ended slot line.

Effect of the parameter L_g on the Reflection Characteristics

Variation of the reflection characteristics with respect to the ground plane length L_g is analyzed, and the results are plotted in Fig 4.3. From the figure, it is seen that resonance frequency and the impedance matching remains nearly the same with the increase in the length Lg. As L_g increases, a slight reduction in the impedance matching is seen from the figure which is due to the change

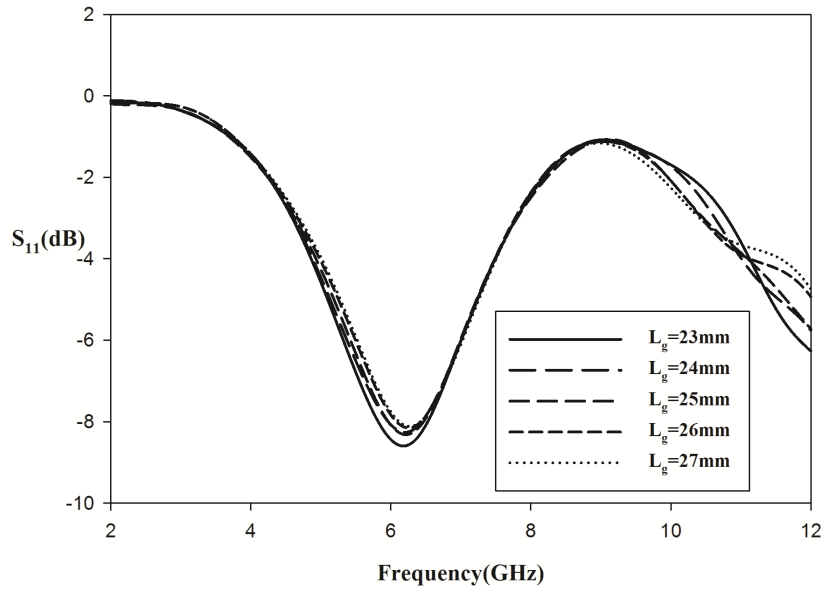in input impedance of the antenna.

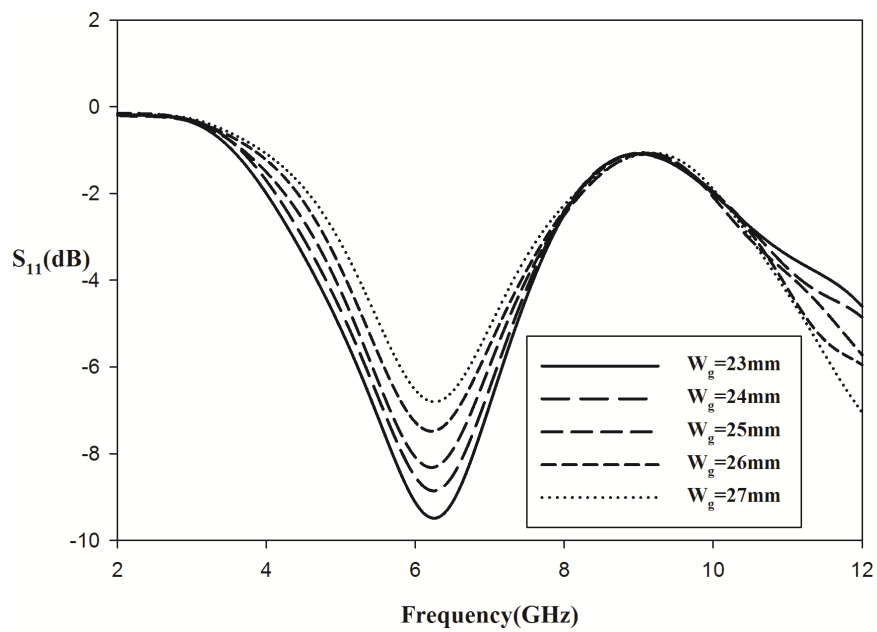*Figure 4.3: Effect of Lg on reflection characteristics*

Figure 4.4: Effect of W_g on reflection characteristics

Effect of the parameter W_g on the Reflection Characteristics

The effect of the parameter W_g on the resonance and the radiation characteristics of the closed ended slot line are analyzed, and the results are shown in fig4.4. It is noted that the resonance frequency remains unaffected due to the variation of the parameter Wg. The impedance matching improves with the increase in W_g.

Effect of the Parameter L_f on the Reflection Characteristics

The effects of L_f on the reflection characteristics are analyzed, and the results are plotted in Fig 4.5. As expected the slot line length increases the resonance comes to a lower value. Thus the parameter L_f is a determinant factor for the resonance. The matching at the resonance frequency decreases as the L_f increases. This is due to the variation in input impedance which results in a change in impedance matching.
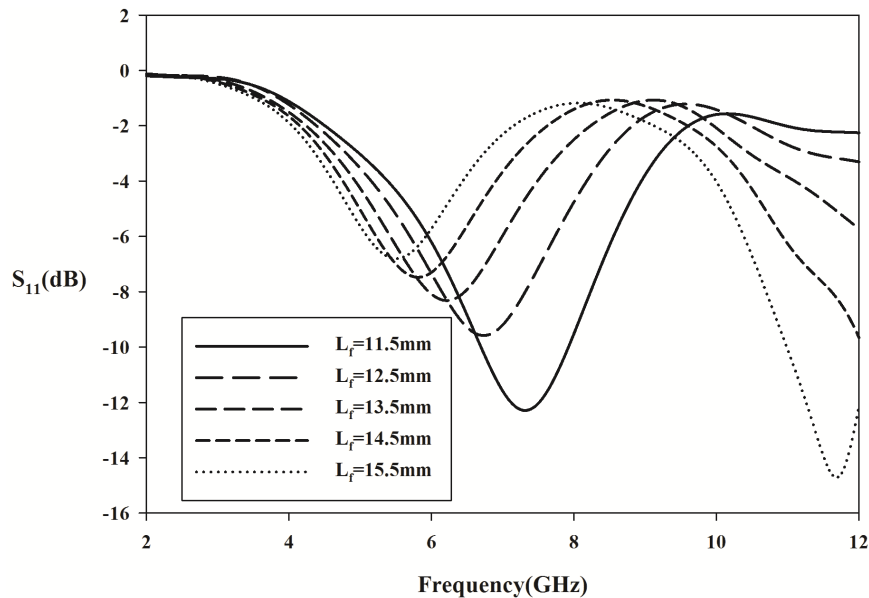

Figure 4.5: Effect of L_f on reflection characteristics

Effect of the Substrate Thickness on the Reflection Characteristics

Substrate thickness hasnt got any significant effect in the closed ended slot line reflection characteristics. The variational study of h is shown in fig4.6. As h is increased the resonance slightly shifts to a lower value. The effective dielectric constant changes with respect to the substrate thickness which changes the guided wavelength causing the resonance to shift. The impedance matching remains the same for all the values of h.
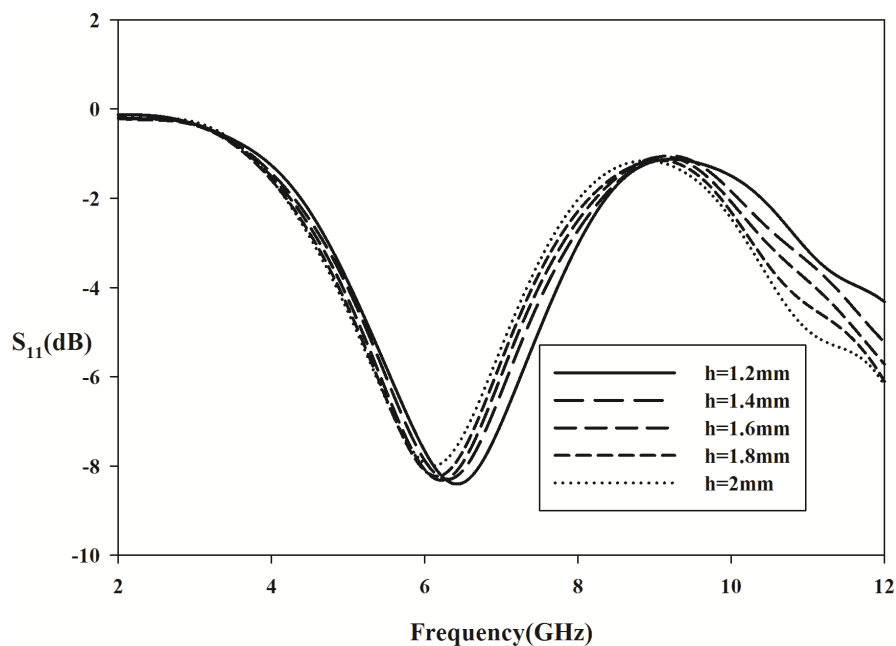
Figure 4.6: Effect of substrate thickness on reflection characteristics

Effect of the ϵ_r on the Reflection Characteristics

The variation of reflection coefficients on different dielectric substrates are analyzed using CST microwave studio, and the results are plotted in Fig **??**fig4.7). From the figure, it is seen that the resonance shifts to a lower value as the permittivity of the substrates increases, which is due to the change in guided wavelength with respect to the permittivity of the substrates. The matching is

reduced with the increase of permittivity. Slotline input impedance is a function of dielectric permittivity also, that is as ϵ_r changes, the input impedance of the slot line changes. This leads to the change in impedance matching.
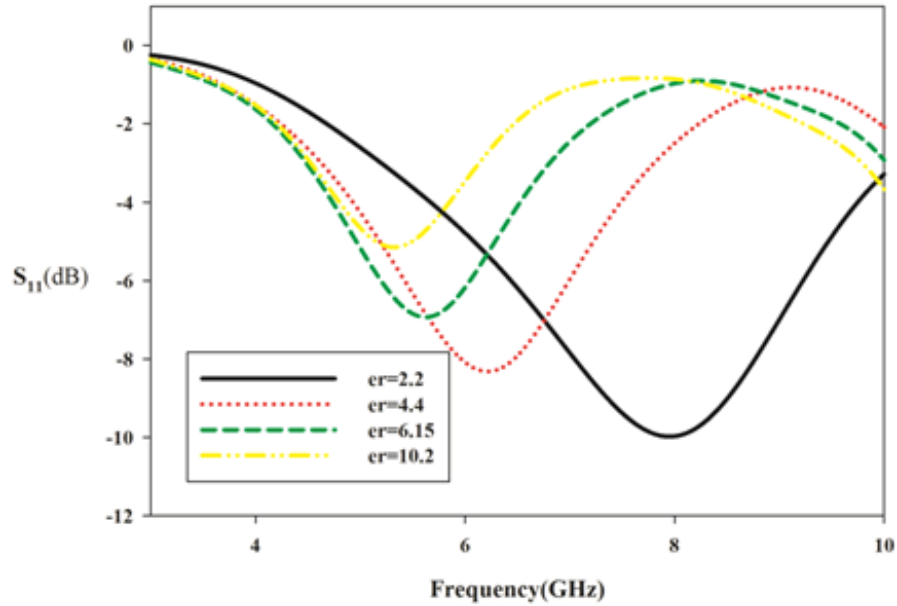

Figure 4.7: Variation of reflection coefficient with ϵ_r

Surface Current Analysis and 3D Radiation Pattern

The simulated surface current distribution of the closed ended slot line at 6.23 GHz is shown in Fig 4.8. From the surface current distribution maximum surface current density is seen across the top end of the slot line and the bottom end. Minima points are near the center of the slot line. A half wave variation is seen along the length L_f. Antenna is linearly polarized along the X direction. The simulated $3D$ radiation pattern of the antenna is shown in Fig 4.9. Directivity is maximum along the Z direction, and the nulls are located in X-axis. The gain of the closed ended antenna is found to be $2.02 dBi$ and efficiency 78%.
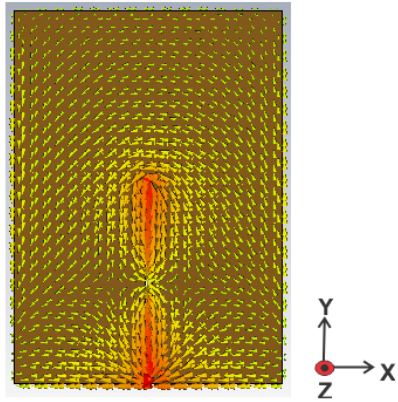
Figure 4.8: Surface current distribution at 6.23 GHz
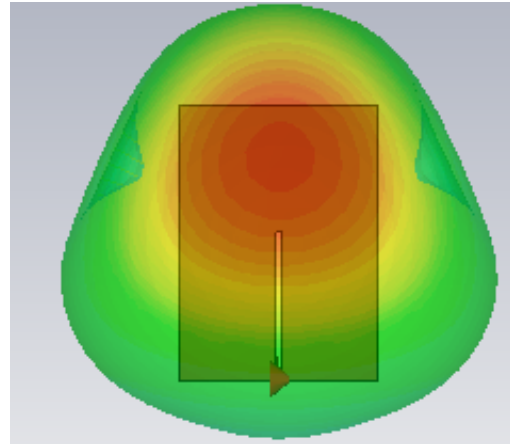

Figure 4.9: Simulated 3D radiation pattern at 6.23 GHz

4.2 Slotline Fed Uniplanar Antenna for 2.4 GHz/ 5.8 GHz WLAN Applications

Slot line fed uniplanar antenna for WLAN applications is presented in this section. It is found from the previous sections that the efficiency of the closed ended slot line is low when compared to that of an open ended slot line. One way to make CES an efficient radiator is to provide a transition from slot line to the rectangular slot which is effectively done in the subsequent sections. Impedance matching has to be improved so as to improve the antenna efficiency. In the subsections, we will be dealing with the evolution of the proposed antenna and its characteristics.

4.2.1 Evolution of the Proposed Design

The proposed antenna is derived from a basic closed ended slot line which we analyzed in the previous section. Developments in the proposed antenna are shown in the Fig 4.10. In the first stage, a closed ended slotline is designed on an FR4 substrate with a slot length of 31.5mm. The simulated reflection characteristics of the first stage are shown in Fig 4.11; it can be seen that a
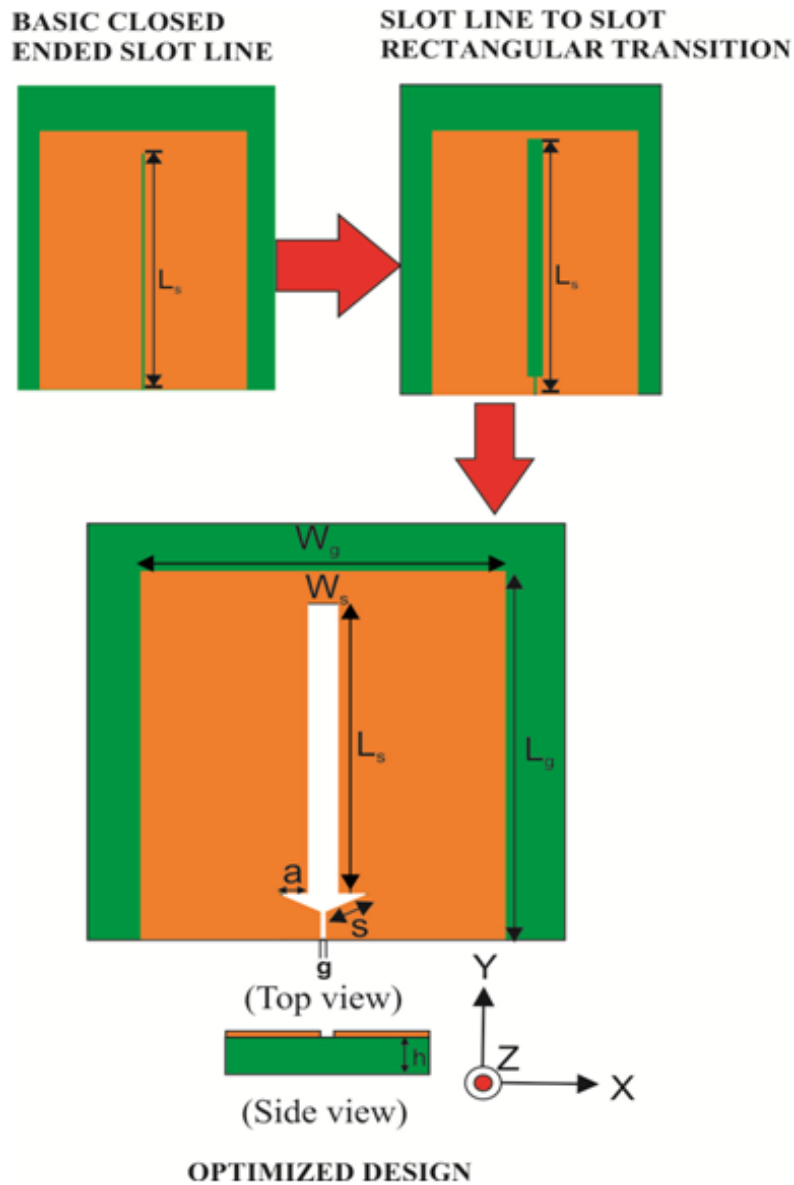
Figure 4.10: Evolution of slot line fed uniplanar antenna

tendency of radiation with poor matching near 2.4 GHz and 6 GHz.

At the second stage of evolution, a transition from slot line to a wider slot is considered which considerably improves the impedance matching, and two resonances are observed at 2.2 GHz and 5.7 GHz. In order to further improve the impedance matching an arrow shaped tapering is used as a transition

from slotline to slot. This improved the impedance matching by an amount of $-15dB$.
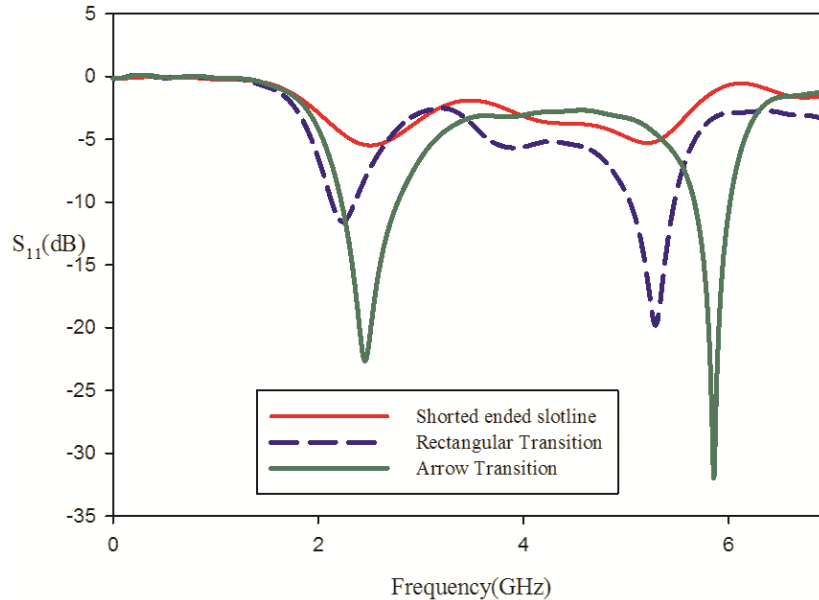

Figure 4.11: Reflection characteristics of the Various designs shown in the Evolution

4.2.2   Parametric Analysis of the Antenna

In order to find out the resonant lengths and radiation characteristics, the parametric analysis of various parameters is performed.

Effect of the length L_g

In order to understand the effect of the parameter L_g on the reflection characteristics, the parametric analysis is performed, and the results are shown in Fig 4.12. It is seen that the resonance frequencies are not at all affected by this variation.

Effect of the Length W_g on the Reflection Characteristics

Effect of the width of the ground on the reflection characteristics is studied, and the results are depicted in Fig 4.13. As the W_g increases, there is no
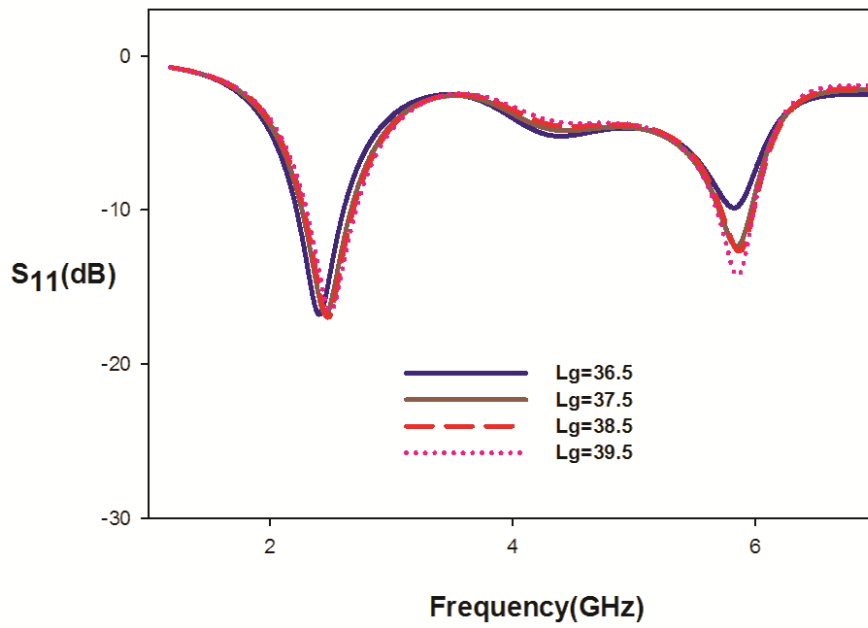
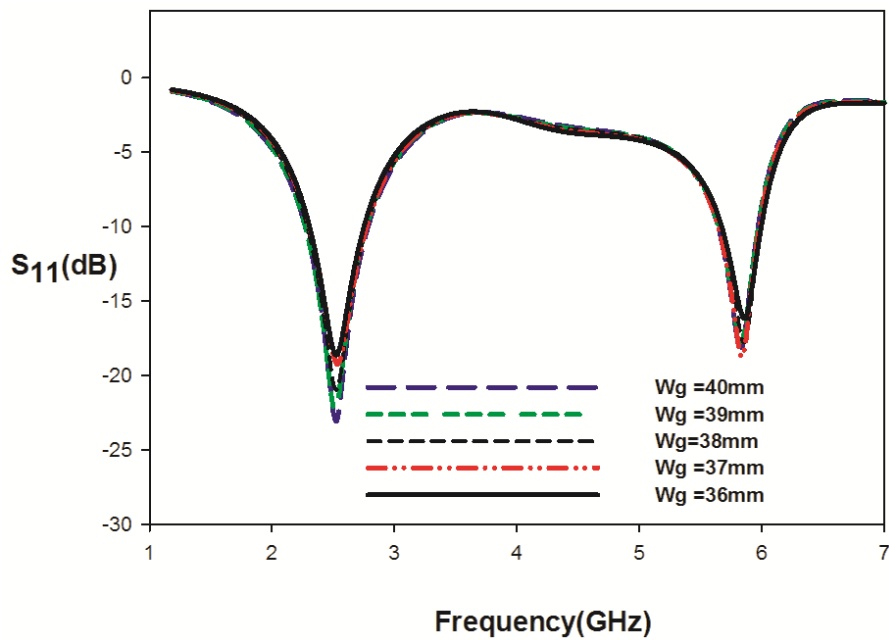*Figure 4.12: Variation of reflection characteristics with L_g*

Figure 4.13: Variation of reflection characteristics with W_g

noticeable change in resonance frequency. Thus the width of the ground has no role in determining the resonance frequency. A slight increase in impedance matching is observed with the increase in W_g. Both the ground dimensions are not at all affecting the reflection characteristics. That means the ground dimensions can be effectively extended to MMIC circuits without affecting the radiation characteristics of the antenna.

Effect of the Length L_s on the Reflection Characteristics

The variation of reflection coefficient with respect to the parameter L_s is shown in Fig 4.14. It is seen from the figure that both the resonance comes down to a lower value as we increase the length of the slot L_s. This indicates that the Length of the slot is a determining factor for both the resonances. Impedance matching for both the resonance frequencies is reduced slightly as we increase the length of the slot. This is due to the change in antennas input impedance .
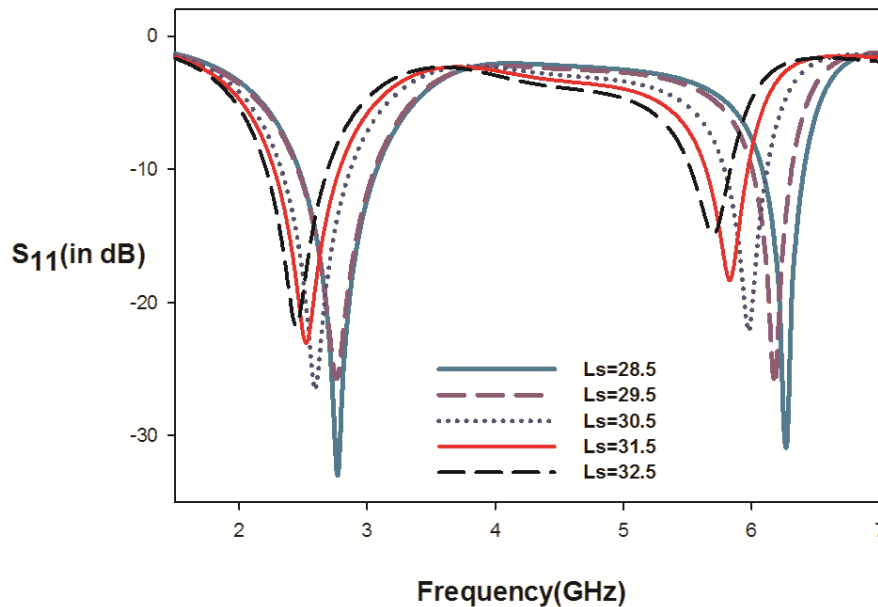

Figure 4.14: Variation of reflection characteristics with L_s

Effect of the Length a on the Reflection Characteristics

The effect of the parameter a on the reflection characteristics is analyzed. The result of the parametric analysis is shown in Fig 4.15. It is seen that both the resonance frequency shifts to a lower value as we increase the parameter a. This indicates that the parameter a is the part of the effective resonant length which controls both the resonances. It is seen that the impedance matching is effected in both the resonances with the increase in the parameter a. In the lower resonant frequency, the impedance matching improves slightly with an increase in a and at the higher frequency impedance matching decreases with increase in a. This is due to the change in reactive part of the input impedance.
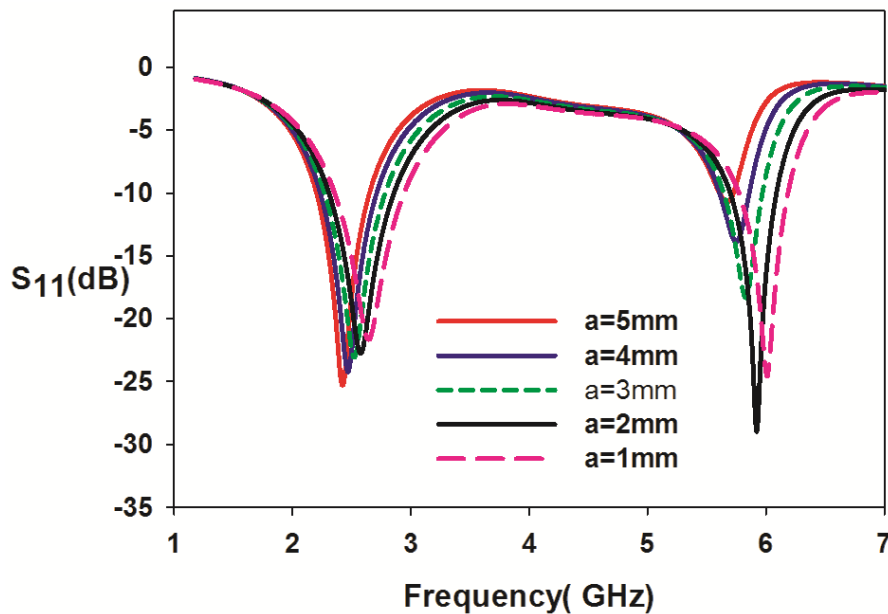

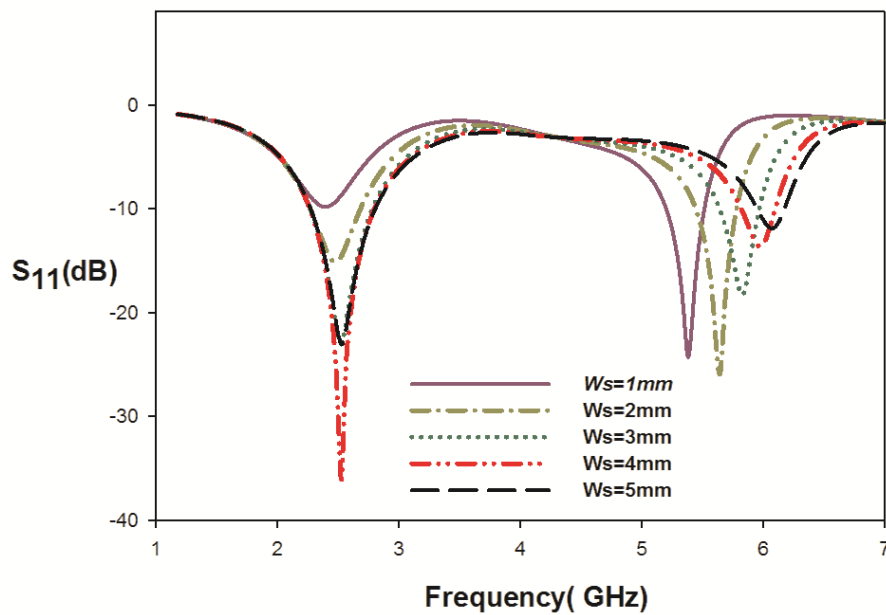*Figure 4.15: Variation of reflection characteristics with a.*

For $a = 1$ mm, $a = 2$ mm and $a = 3$ mm the impedance is inductive and for a greater than 3 mm it becomes capacitive hence the matching is reduced if we increase a beyond 2 mm for the second resonance.

The variation of the input impedance with respect to the parameter a is shown in Table 4.1.

Table 4.1: Variation of the antenna input impedance with respect to the parameter a

$a(mm)$	$F_{r2}(GHz)$	$Z(real)\omega$	$Z(im)\omega$
1	6	36.35	5.38
2	**5.94**	**40.76**	**2.84**
3	5.86	47.7	1.05
4	**5.77**	**56.54**	**-2.34**
5	5.67	67.01	-11.46

Figure 4.16: Variation of the reflection characteristics with W_s

Effect of the Length W_s on the Reflection Characteristics

Effect of slot width, W_s on the resonance and the reflection characteristics is depicted in Fig 4.16.As the slot width increases both the resonances shifts slightly to a higher value.This is because of the reduction in effective reso-

Department of Electronics

nant length. The variation in the impedance matching with respect to W_s can be seen from Fig 4.17a and Fig 4.17b for the first and second resonance respectively.
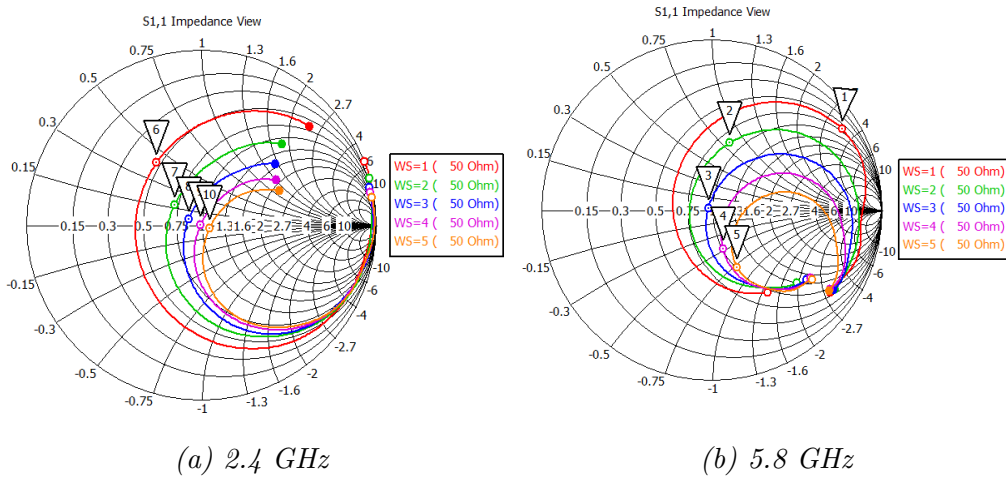

(a) 2.4 GHz   (b) 5.8 GHz

Figure 4.17: Smith chart for various W_s marked
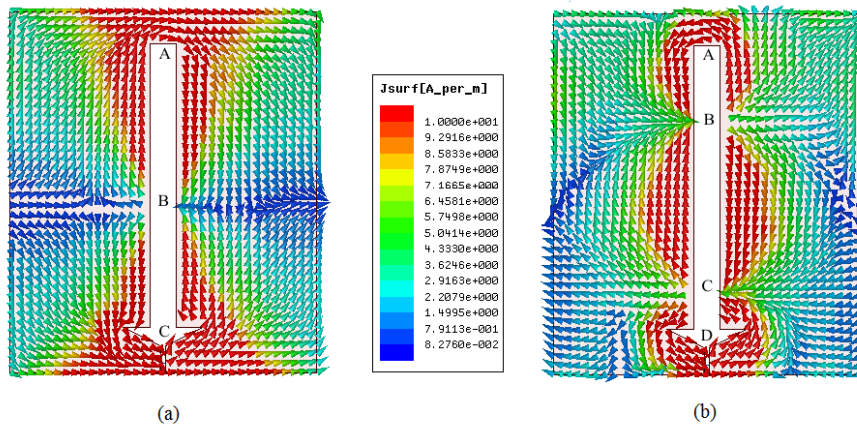

(a)   (b)

Figure 4.18: Simulated surface current distributions at (a) 2.4 GHz (b) 5.8 GHz

4.2.3 Surface Current Analysis and 3D Radiation Pattern

In order to make a clear idea on the parameters which contributes to the effective resonant length that radiates, the surface current distribution of the antenna is obtained from the simulations and is plotted in Fig 4.18. The surface current distribution at 2.4 GHz is shown in Fig 4.18(a). From the figure, it is seen a half wave variation along the path BAB. The minima point located at B and the maximum surface current density at A. Similarly a half wave variation along the path BCB, where B is the minima point, and C is the maxima point. From the figure, it is seen that the surface current present along BA and AC are equal and opposite which cancels outs in the far field. The radiation is contributed by the horizontal current density at above A and below C which adds up in the far field. Thus at 2.4 GHz the antenna is polarized linearly along the X-direction.

For 5.8 GHz the surface current distribution is plotted in Fig 4.18(b). Three half wave variations are seen across the slot length (along with the path ABCD). Along the point BAB a half wave variation is observed, B being the minima point and A the maxima point of surface current density. Half wave variation is seen from B to C with minima points at B and C and the maxima points in between them. It is seen from the figure that the currents in the both sides of the slot are equal and opposite which cancels out. At the bottom end of the slot a half wave variation is seen along the path CDC with the maximum current density seen at D and minima points at C. At the top end and bottom end of the slot there is a horizontal current distribution which adds in the far field and contributes to the radiation. Thus it is seen that at both the resonant frequencies the antenna is polarized linearly along the X-direction. Although the second resonance is a higher order mode of first resonance, due to the cancellation of the surface current at the middle part of slot results in almost similar radiation characteristics. Both the resonances can be controlled by varying similar parameters. The polarizations in both the bands are same.

The simulated 3D radiation patterns at both the frequency bands are shown in Fig 4.19. For the 2.4 GHz band, the bore sight radiation is towards

the Z-direction with the nulls located at the X-axis. In the case of a 5.8 GHz band, the direction of maximum radiation is towards the Y-axis with null located in X-axis. Radiation towards the Z-axis is very low due to the cancellation of the fields as shown in fig4.18(*b*).
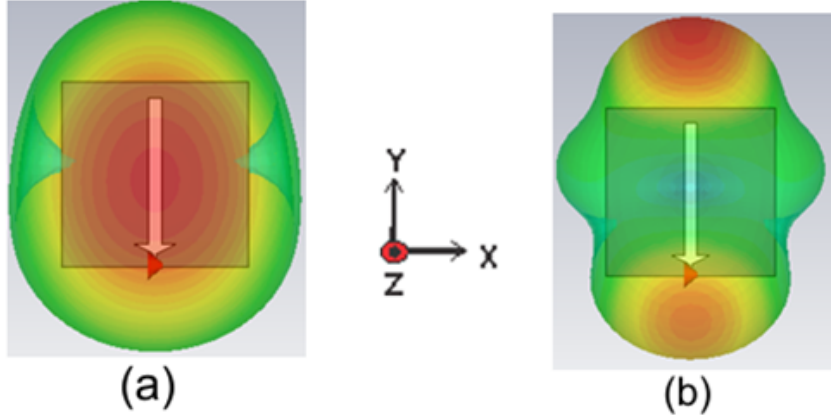

Figure 4.19: Simulated 3D radiation pattern (a) at 2.4 GHz (b) at 5.8 GHz

4.2.4 Antenna Design

Based on the parametric analysis and surface current distributions the empirical design equation of the antenna is derived, and the optimum geometry and the parameters of the antenna are shown in the Fig 4.20.The antenna is designed on FR4 substrate with $\epsilon_r = 4.4$, $h = 1.6$ mm and $tan\delta = 0.016$. The gap g is optimized for 50Ω. From the parametric analysis, it is seen that the parameters which affect the resonance are mainly a and L_s and the overall slot dimensions which were verified in the surface current analysis. The empirical relation which decides the resonance frequency is shown in equation 4.1.

$$L_s + a + s = 0.51\lambda_g \tag{4.1}$$

Where, λ_g is the guided wavelength and ϵ_{reff} is the effective permittivity and are given by equation 4.2 and equation 4.3 respectively.

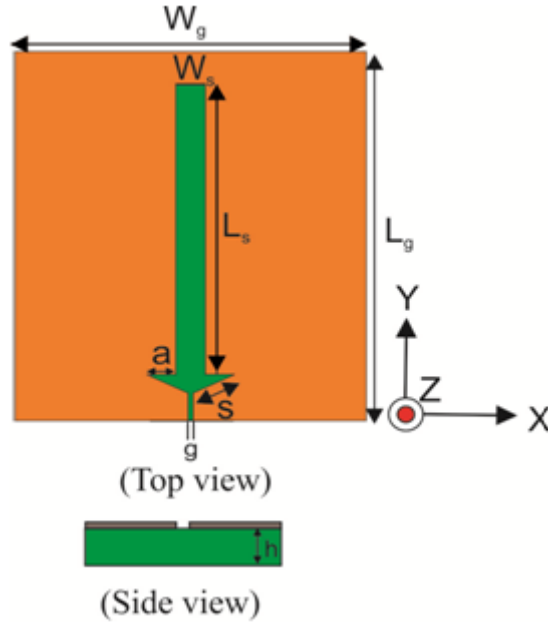$$\lambda_g = \frac{\lambda_0}{\sqrt{\epsilon_{reff}}} \tag{4.2}$$

Figure 4.20: Antenna geometry ($L_s = 31.5$ mm, $a = 3$ mm, $W_g = 35$ mm, $L_g = 38$ mm, $s = 4.7$ mm, $W_s = 3$ mm, $g = 0.5$ mm)

$$\epsilon_{reff} = \frac{\epsilon_r + 1}{2} \tag{4.3}$$

In order to verify these equations, the antenna parameters are computed on 3 different substrates and are simulated using CST microwave studio. The computed parameters are shown in Table 4.2(all the lengths are in mm) and the reflection characteristics of the corresponding antennas are analyzed using CST Microwave Studio . From Fig 4.21 it is seen that the antennas fabricated on different substrates show similar reflection characteristics. Thus design equations are validated on four different substrates.

4.2.5   Experimental Results

The prototype of the antenna is fabricated on the FR4 substrate, and the measurements are taken using R&S zvb20 network analyzer . The reflections coefficients obtained from the simulation and experiment are plotted in 4.22.

From the figure both the simulation and the experimental results shows good agreement. SMA connectors were not modeled in simulations instead

Table 4.2: Computed Antenna parameters

	Antenna A	Antenna B	Antenna C	Antenna D
Substrate	ROGERS 5880	FR4	ROGERS RO3006	ROGERS 6010LM
h	1.57	1.6	1.28	0.635
ϵ_r	2.2	4.4	6.25	10.2
a	3	3	3	3
g	0.1	0.5	0.65	0.775
S	4.7	4.7	4.7	4.7
Ls	41.71	31.5	25.355	18.711
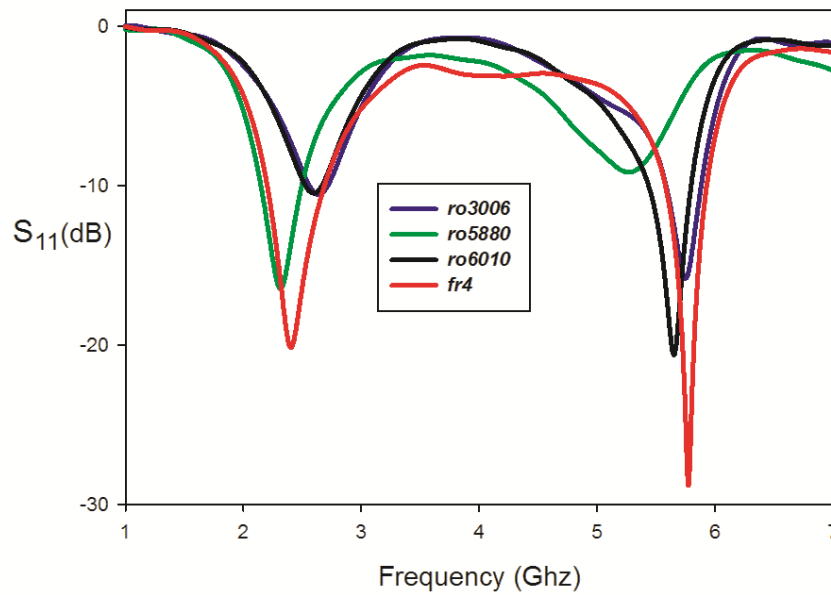
Figure 4.21: Reflection characteristics on different Substrate

default ports were used. The effect of connectors are predominant in the higher frequencies since their wavelength and size are comparable.Slight variation in the resonance frequency is due to these reasons. Two resonances are seen
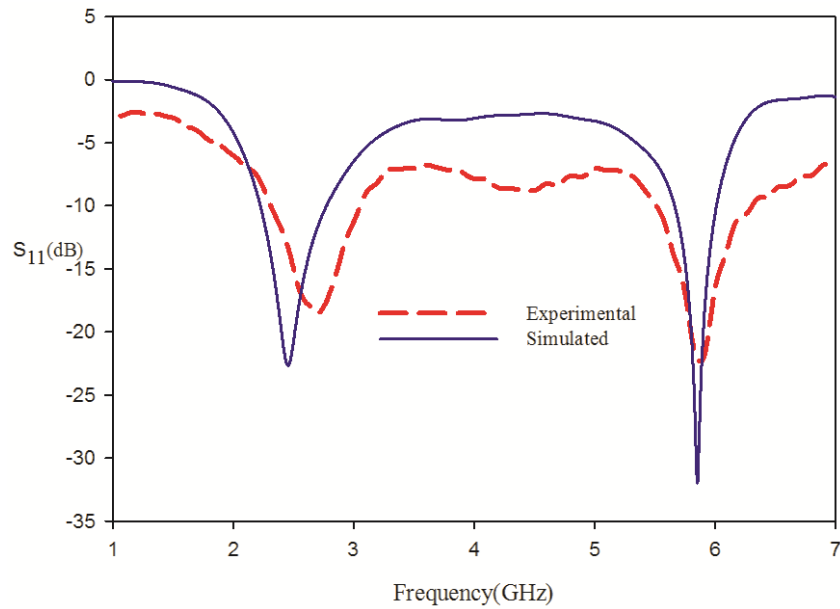
covering 2.4 GHz and 5.8 GHz WLAN bands.

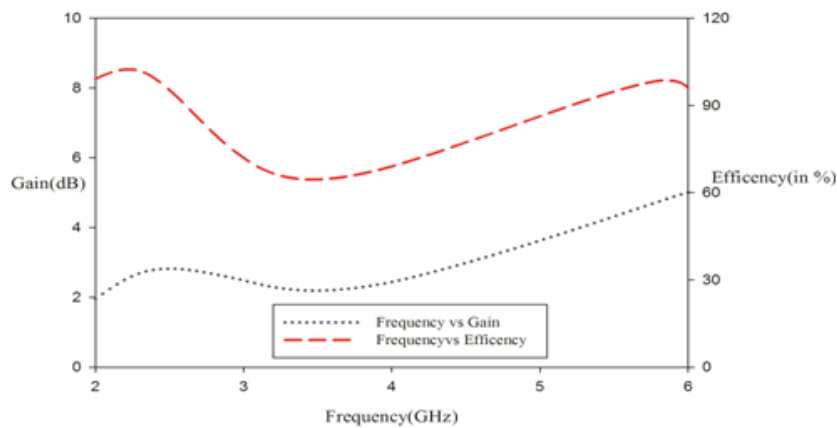*Figure 4.22: Reflection characteristics Experiment and Simulated*

Figure 4.23: Gain and Efficiency

The measured gain at 2.4 GHz is 2.79 dBi and that at 5.8 GHz is 4.74 dBi . The efficiency of the antenna is found to be 91% for lower resonance and 88% for upper band. The gain and efficiency of the antenna are plotted in Fig 4.23.
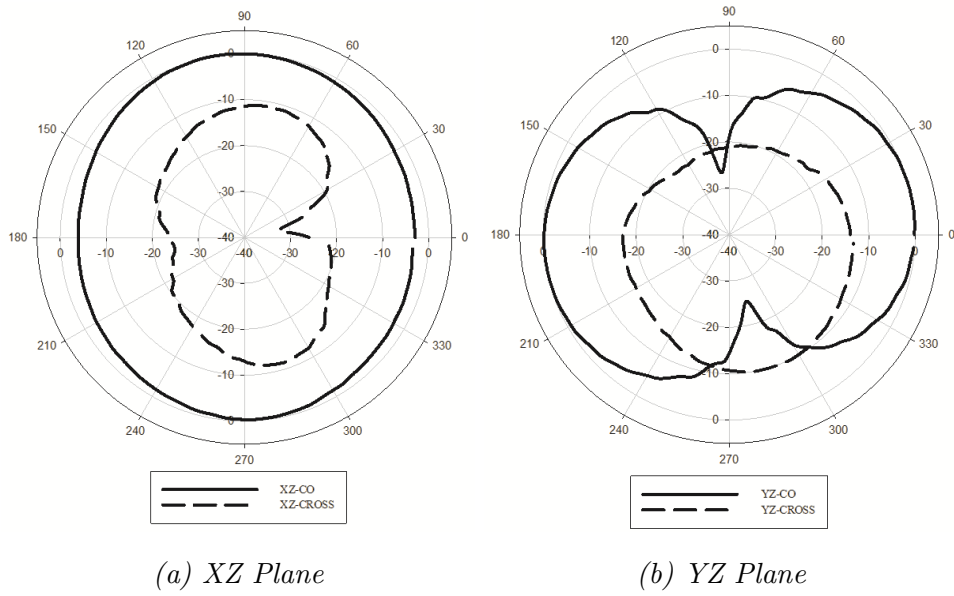
(a) XZ Plane   (b) YZ Plane

Figure 4.24: Measured Radiation pattern at 2.4 GHz

(a) XZ Plane   (b) YZ Plane
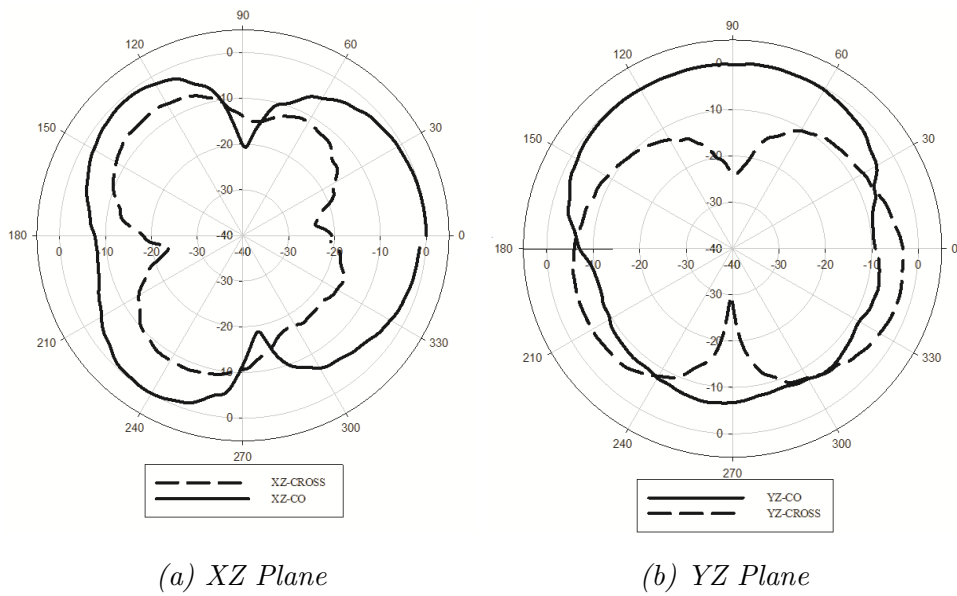
Figure 4.25: Measured radiation pattern at 5.8 GHz

The distinctive feature of the antenna is that the efficiency and the gain of the antenna can be improved further by increasing the metallization width.

This doesnt affect the Frequency of operation.

The measured radiation pattern of the antenna is plotted and is shown in Fig 4.24 for 2.4 GHz and Fig 4.25 for 5.8 GHz. The maximum radiation is along the Z direction in both the frequencies. The maximum radiated power is along the Z-axis in the case of 2.4 GHz. The maximum radiated power is along the Y-axis for 5.8 GHz.Maximum cross polar isolation of -20 dB is obtained at the boresight of the antenna.

4.3 Slotline Coupled Wideband Slot Radiator for 5.2/5.8 GHz WLAN Communications

In the previous sections, we analyzed the closed ended slotline. Slot line fed slot antenna is also analyzed. In this section, a new method of excitation is proposed for effectively radiating a closed ended slot line. Slot line coupled slot radiator for 5.2/5.8 GHz WLAN bands are presented in this section. The evolution of the antenna is discussed.

4.3.1 Evolution of the Proposed Design

The evolution of the proposed antenna is shown in Fig 4.26. The First stage is a basic closed ended slot line with length (L_f) 13.5 mm. A basic closed ended slotline has a tendency to radiate when fabricated on a low permittivity substrate. From section 4.1.1 a half wave variation is seen across the length of the closed ended slotline. The impedance of a closed ended slotline is capacitive, which has to be minimized for better impedance matching and efficiency. So as to improve the gain and efficiency, an additional slot is placed near to the closed ended slotline, which increases the inductive reactance [1] of the antenna. This resulted in resonance with proper impedance matching at 5.7 GHz with a simulated efficiency of 87.5%. Adding an additional slot on the right side of the closed ended slotline with equal length results in improved efficiency, bandwidth, and gain. The comparative studies of the S_{11} , gain, and efficiency, are plotted in Fig 4.27 , Fig 4.28 and fig4.29.
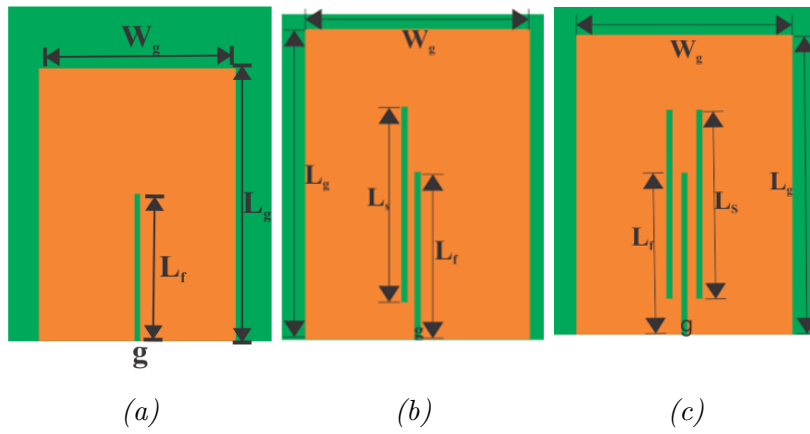
Figure 4.26: Evolution of the proposed design(a) A basic closed ended slotline (b)Slotline coupled slot radiator single slot (c) Final design
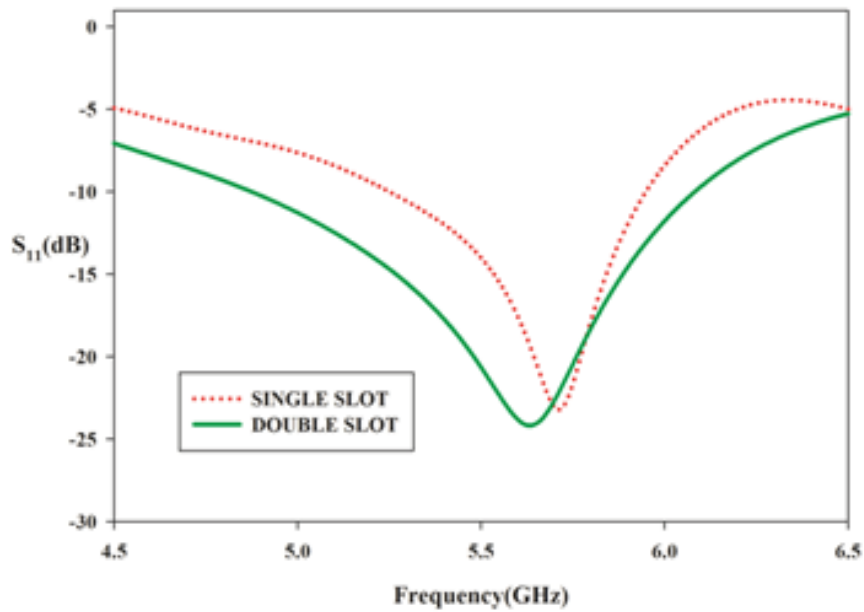

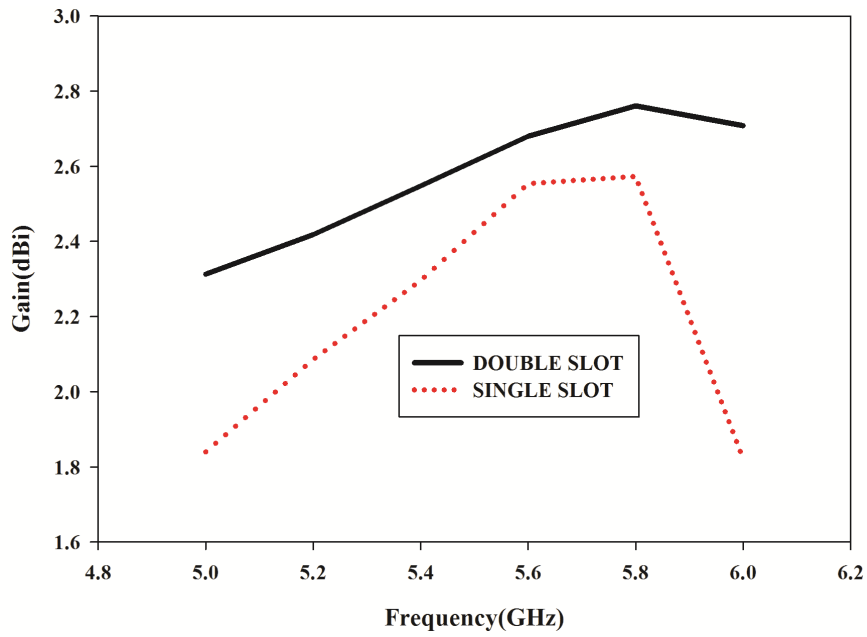*Figure 4.27: Reflection characteristics comparison*
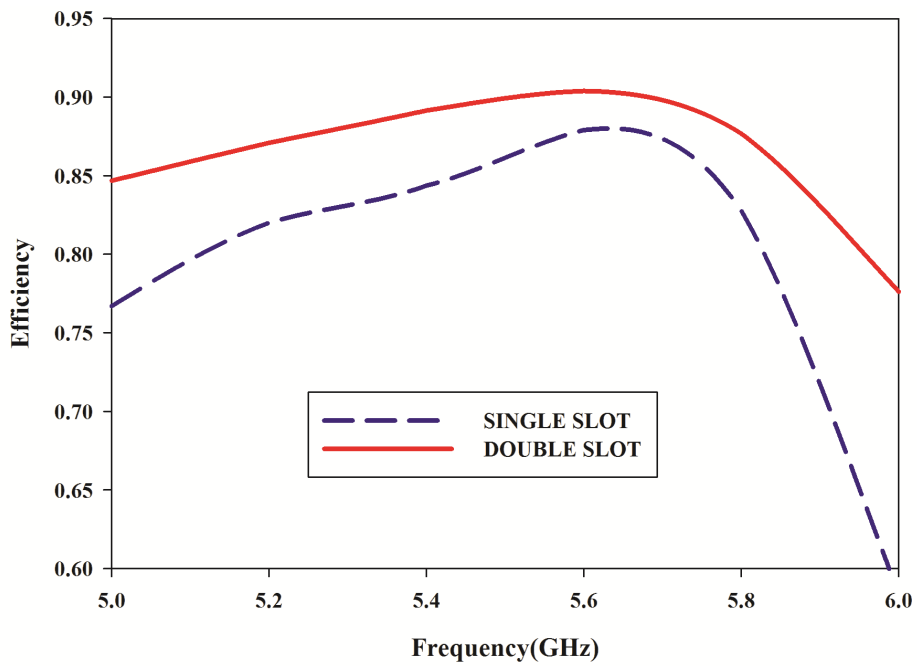
Figure 4.28: Gain comparison

Figure 4.29: Efficiency comparison

4.3.2 Parametric Analysis

In order to obtain a clear insight into the radiation mechanism and the parameters contributing towards the resonance path, the variation studies of the parameters are performed

Effect of W_g on the Reflection Characteristics

The effect of the width of the metallization on the reflection characteristics of the antenna is performed, and the results are shown in Fig 4.30.As we vary the width, the resonance and the matching remains the same.
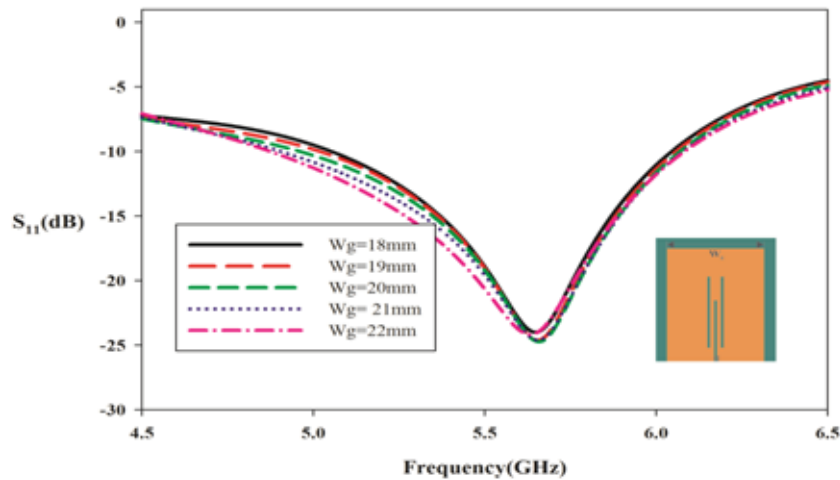
Figure 4.30: Variation of reflection characteristics with W_g

Effect of L_g on the Reflection Characteristics

The reflection characteristics of the antenna for various metallization lengths (L_g) are studied using simulation, and the results are plotted in Fig 4.31. As L_g increases, the resonances are shifted to a higher value slightly. As the L_g increases the capacitive reactance is reduced, and the imaginary part of the impedance is shifted to inductive. But this change is very minimal. The selection of the Lg for the design is made on a compromise between the size and matching. The impedance matching is improved with the increase in

metallization length which is contributed by the inductive reactance. Further increase in L_g results in the reduction of matching. The resonance frequency is shifted to a lower value. This happens due to the increase in inductive reactance.
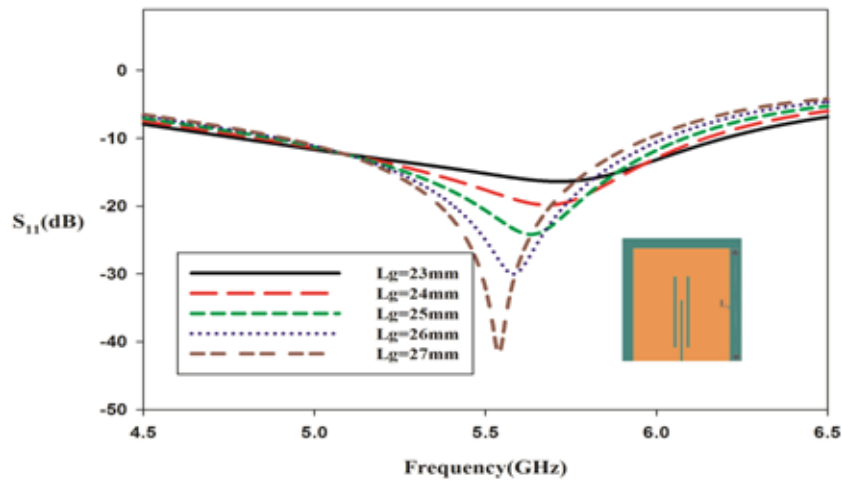

Figure 4.31: Effect of L_g on the reflection characteristics

Effect of L_f on the Reflection Characteristics

Variation in the reflection characteristics with the parameter L_f is analyzed, and the results are plotted in Fig 4.32. As L_f increases, the resonant frequency is slightly shifted to a higher value. It is seen that the impedance matching also improves. The input impedance of the antenna changes with the length L_f. At optimum input impedance, maximum fields are coupled to the adjacent slots. Beyond this optimum value, the impedance matching reduced since the inductive reactance increases from this point. As L_f increases the effective resonance length is reduced, and the resonance is shifted to a higher value. This frequency shift is on a small scale and can be omitted from the discussion of resonance mechanism of the antenna.
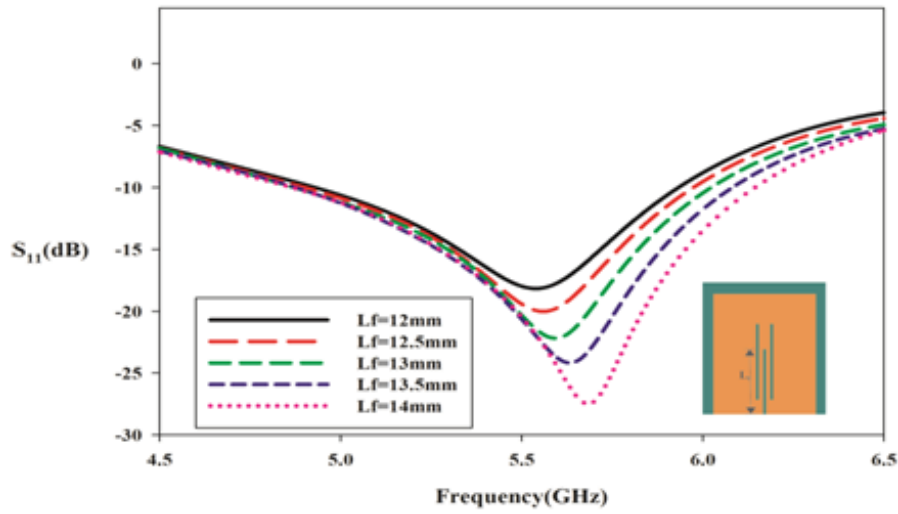
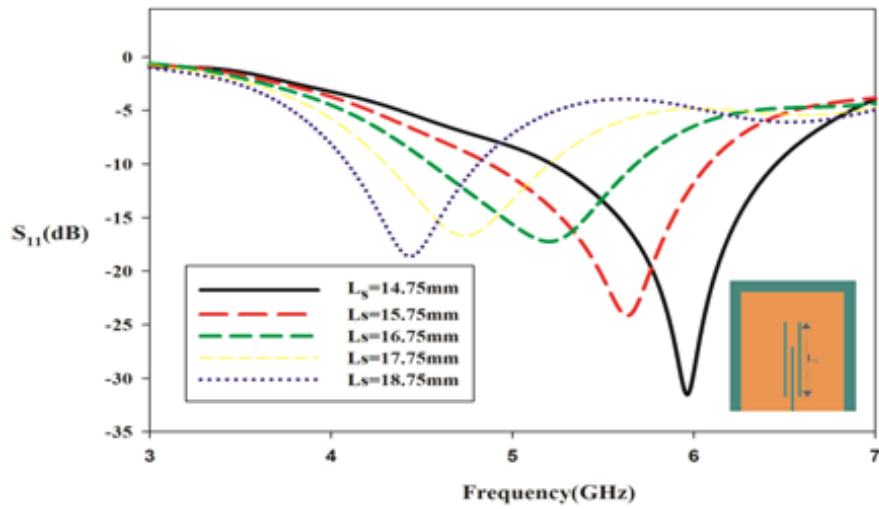*Figure 4.32: Effect of Lf on the reflection characteristics*

Figure 4.33: Effect of L_s on the reflection characteristics

Effect of L_s on the Reflection Characteristics

The effect of L_s on the reflection characteristics is shown in Fig 4.33. As the length, L_s increases the resonance are shifted to a lower value. This indicates that the length L_s contributes towards the effective resonance path. The impedance matching is reduced with the increase in L_s. As Ls increases the

real part of the input impedance is increased, thus changing the impedance matching. The fields are coupled from the closed ended slot line to the adjacent slots. As the length of the adjacent slots are increased the point where the maximum coupling of electromagnetic field occurs changes. Thus it also affects the impedance matching. The same can be verified by section 4.2.1.3. The length of the slot contributes a half wave resonant mode which is causing the shift of resonance.

Effect of the Separation Between Slotline and Slot (the parameter dis) on the reflection characteristics

The effect of the separation between the slotline and slots are analyzed, and the results are shown in Fig 4.34. From the figure, it is seen that as the separation increases the impedance matching reduces in a large scale. This is due to the reduction of electromagnetic coupling which reduces with increase in separation.The optimum separation for effective coupling of the electromagnetic fields from the slotline to the slot is found to be 0.75 mm, which is taken as the value $dis = 0$ mm.
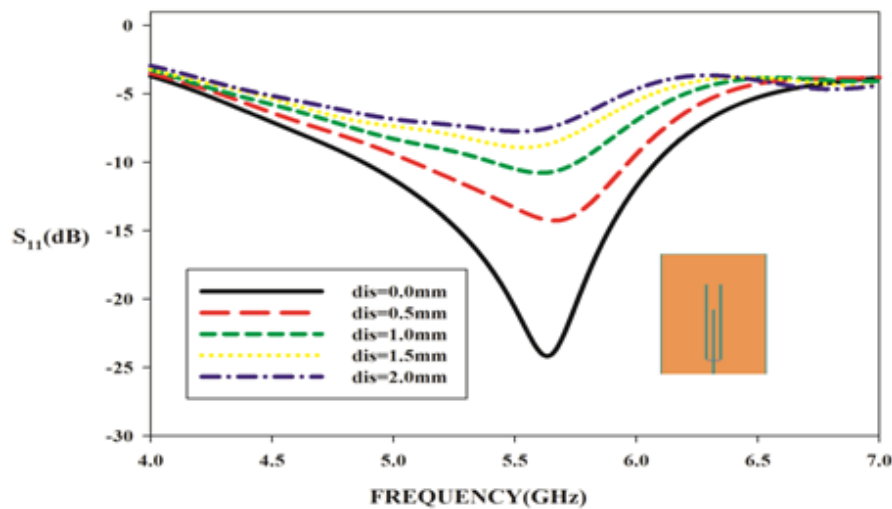

Figure 4.34: Effect of separation between the slotline and the slots on reflection characteristics(dis = 0 corresponds to the optimum separation, i.e., 0.75 mm)

4.3.3 Analysis of Surface Current and 3D Radiation Pattern

For obtaining the reason for resonance and the radiation mechanism the surface current distribution of the antenna is analyzed. The surface current distribution of a basic closed ended slot line is shown in Fig 4.8. A half wave variation along the slot is observed at the resonant frequency. The simu-
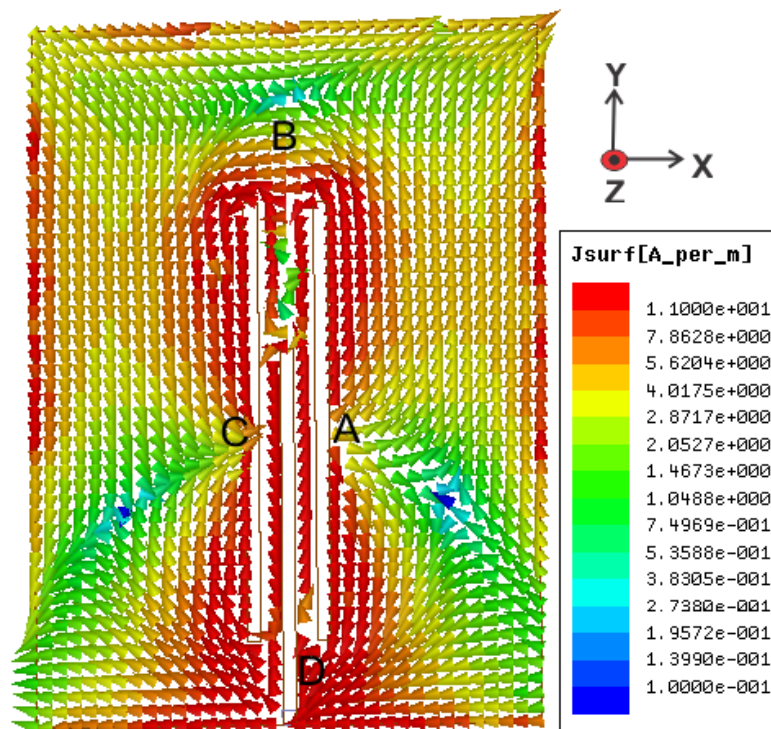

Figure 4.35: Surface current distribution at 5.65 GHz

lated surface current distribution at 5.65 GHz is provided in Fig 4.35. A half wave variation is seen across the path ABC. A and C are the minima points, and the maximum surface current density is observed between these points. Similarly, another half wave variation is seen across ADC. A and C are the minima point, and the maximum surface current density is observed near D. As a whole the total length L_s and L_f contribute towards the resonance. The outer edge of the slots contributes towards the resonant current path. The

inner edge cancels out since they are anti-parallel. The simulated 3D radiation pattern of the antenna is shown in Fig 4.36. The maximum directivity is along the Z-axis, and the nulls of the antenna are located on the X-axis. From the surface current distribution, it is seen that the effective surface current density that adds up in the far field is along the X-axis. Thus the antenna is linearly polarized along the X-axis. Since the same elements are contribution the resonance and radiation in the entire band, the polarization in the entire band remains the same.
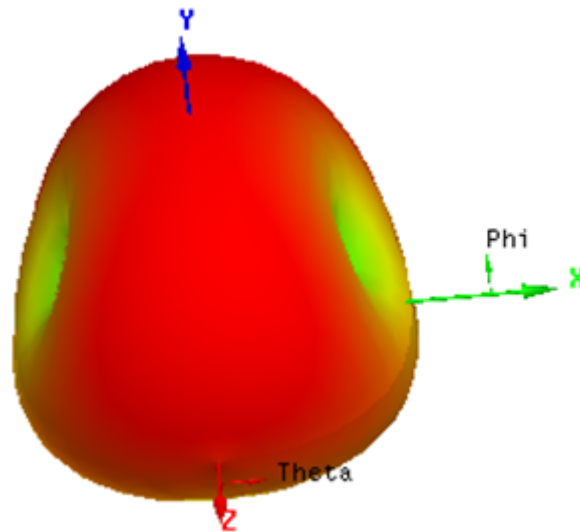

Figure 4.36: Simulated 3D radiation pattern at 5.65 GHz

4.3.4   Antenna Design

Based on the above parametric analysis and the surface current distributions the empirical design equations of the antenna are developed. Two parameters which affect the resonance are L_f and L_s.

$$L_s = 0.485 * \lambda_g \tag{4.4}$$

$$L_f = 0.416 * \lambda_g \tag{4.5}$$

Table 4.3: Computed Antenna parameters

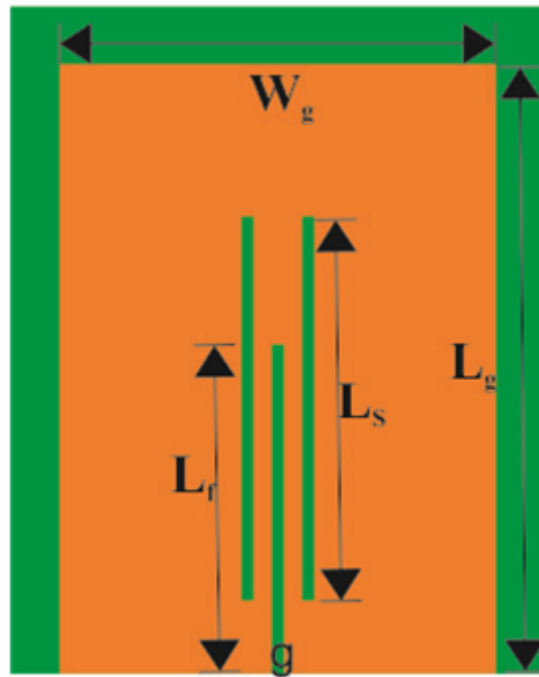|	Antenna A	Antenna B	Antenna C
$h(mm)$	1.6	1.28	0.635
ϵ_r	4.4	6.15	10.2
ϵ_{reff}	2.7	3.575	5.6
L_s	15.75	13.75	10.95
L_f	13.5	11.7	9.37
L_g	25	25	25
W_g	18	18	18
g	0.5	0.65	0.775

Figure 4.38: Antenna geometry with optimized parameters($L_s = 15.75$ mm, $L_f = 13.5$ mm, $g = 0.5$ mm, $W_g = 18$ mm, $L_g = 25$ mm)
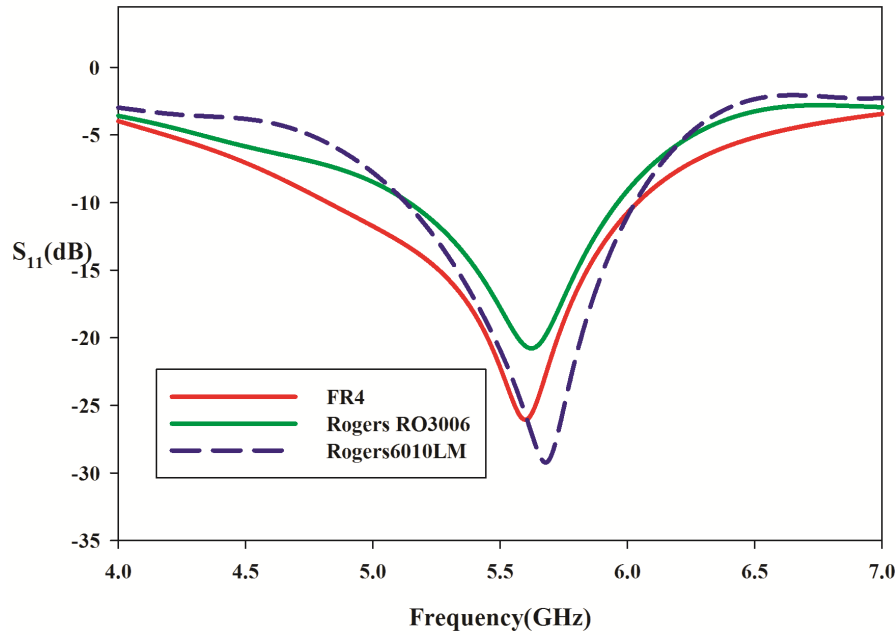
Figure 4.37: Simulated Reflection characteristics on different Substrates

where $\lambda_g = \frac{\lambda_0}{\sqrt{\epsilon_{reff}}}$ and $\epsilon_{reff} = \frac{\epsilon_r + 1}{2}$ Parameters for the antennas are computed based on the above design equation on three different substrates which are shown in table 4.3. These designs are simulated in CST microwave studio and the results are plotted in Fig 4.37.

Figure shows similar responses for all the three substrates. Hence the design equations are validated. The optimized parameters for the antenna and the antenna geometry are shown in Fig 4.38. The antenna is designed on an FR4 substrate with input impedance optimized for 50 Ω.

4.3.5 Experimental Results

The proposed antenna is fabricated on the FR4 substrate, and its characteristics are analyzed using HP8510C network analyzer. The reflection characteristics of the antenna are measured and are found to be in good agreement with the simulated one. The comparison of the reflection characteristics is shown in Fig 4.39. The measure reflection characteristics show good matching and a bandwidth of around 1 GHz. The measured gain and efficiency of the an-

tenna are plotted in Fig 4.40. It is seen that both the gain and efficiency have uniform valued along the entire band. The average gain in the whole
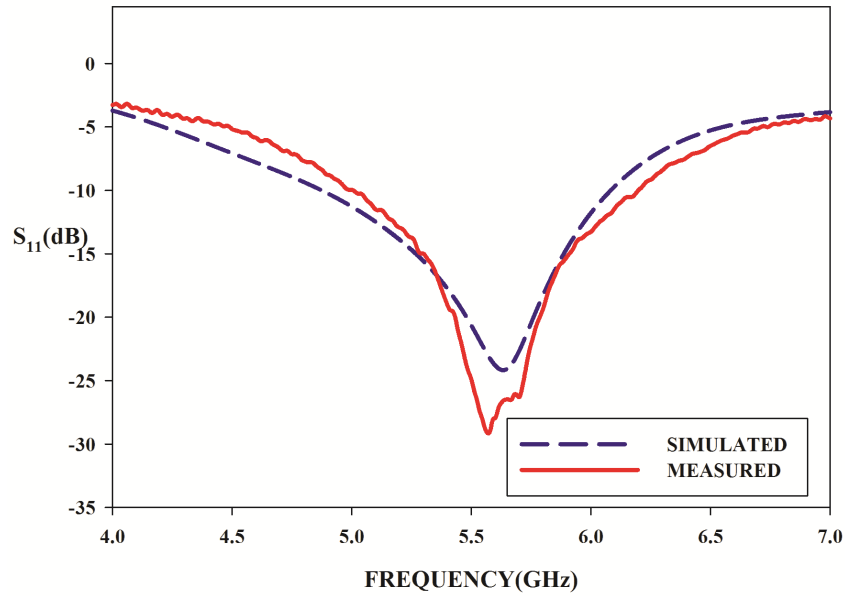

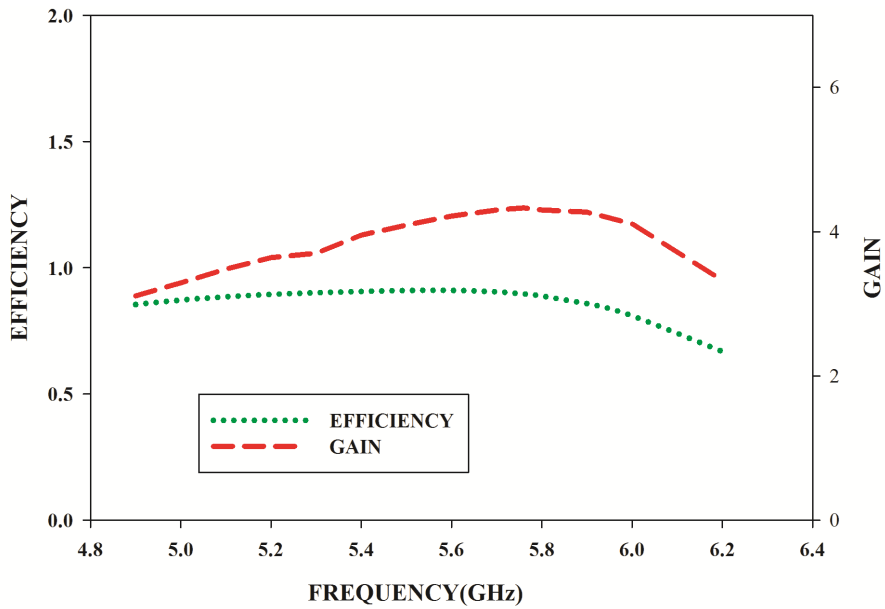*Figure 4.39: Reflection characteristics (measured and simulated)*

Figure 4.40: Measured gain and efficiency

band is found to be 3.46 dBi, and the average efficiency is 86.82 %. The measured radiation pattern of the antenna for the frequency 5.6 GHz is shown in Fig 4.41.
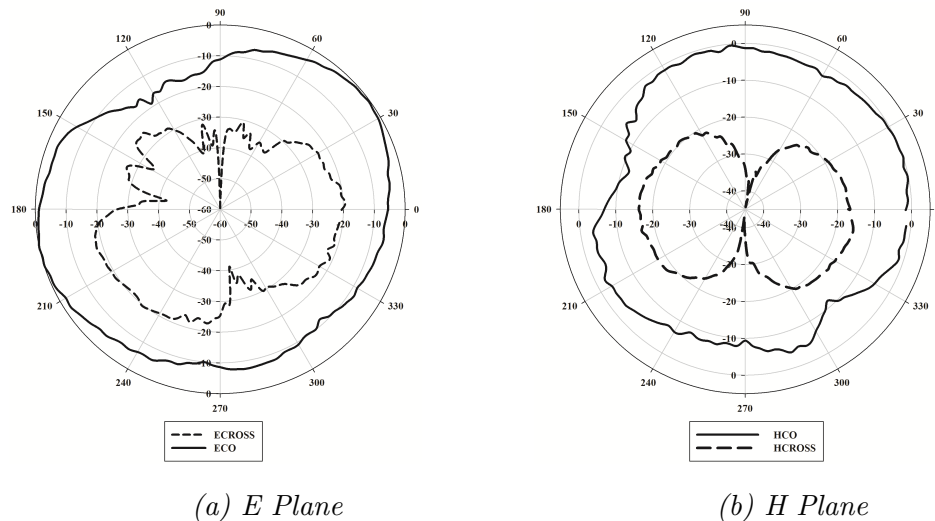

(a) E Plane

(b) H Plane

Figure 4.41: Measured Radiation pattern at 5.6 GHz

In the E-plane the maximum power is seen where $\theta = 45\,$deg. The maximum cross polar isolation at bore sight is -23 dBi in the E-plane and in H-plane it is found to be -19 dBi. Both the E-plane and H-plane radiation patterns are symmetrical. The antenna is linearly polarized along the X-direction

4.3.6 Chapter Conclusion

Finally, it can be concluded that the closed ended slotline can be made to radiate effectively with slight modifications. The first design was a transition from slotline to slot with an arrow shaped transition which resulted in an efficient radiator for the fundamental and the higher order mode of the slot with moderate gain (2.79 dBi, 4.74 dBi) and good efficiency(91%, 88%). The fabricated prototype of the antenna is shown in Fig 4.42 (a).

Table 4.4: Comparison of proposed antennas with Literature antennas

Parameter	ANT1 [2]	ANT2 [3]	ANT3 [4]	ANT4 [5]	Design1	Design2
Resonance Frequencies	2.45GHz, 5.35GHz, 5.8GHz	2.5GHz, 3.5GHz, 5.5GHz	2.4GHz, 5.4GHz	2.45GHz, 5.25GHz, 5.75GHz	2.4GHz, 5.8GHz	5.2GHz , 5.8GHz
Size	50mm × 50mm	35mm × 40mm	40mm × 40mm	60mm × 60mm	38mm × 33mm	18mm × 25mm
Gain	3.74dBi, 4.12dBi, 5.25dBi	2.15dBi, 2.47dBi, 4.13dBi	–	4.6dBi, 5dBi, 4.9dBi	2.79dBi, 4.74dBi	3.46dBi
Efficiency	90%	–	62%, 78%	–	91%, 88%	86.82%
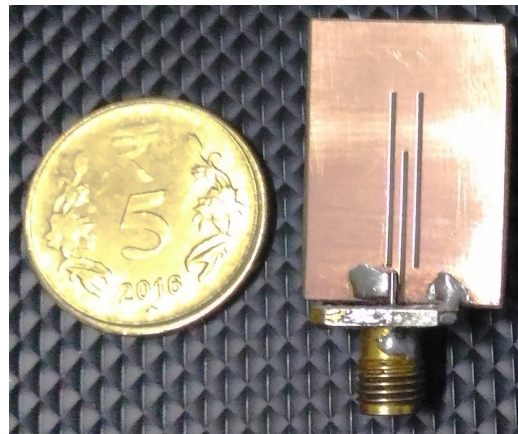
(a)   (b)

Figure 4.42: Fabricated prototype of the antenna (a) slotline fed uniplanar antenna for 2.4/5.8 GHz WLAN applications.(b)Slotline coupled wideband slot radiator for 5.2/5.8 GHz WLAN applications

In the case of the second antenna, two slots which have the same width of that of the closed ended slot line is placed near at the two vertical edges of the slotline. The fields from the slot lines are coupled to the adjacent slots to make it radiate effectively. The length of the slotline is properly selected so as to achieve maximum coupling between slot line and slots. This antenna resulted in a bandwidth of 1 GHz covering the 5.2/5.8 GHz WLAN bands. The antenna has an average gain of 3.46 dBi and efficiency of 86.82%. The fabricated prototype of the antenna is shown in Fig 4.42(b).

REFERENCES

[1] S. Sierra-Garcia and J. J. Laurin, "Study of a cpw inductively coupled slot antenna," *IEEE Transactions on Antennas and Propagation*, vol. 47, no. 1, pp. 58–64, Jan 1999.

[2] T. Lee, J. Jung, H. Lee, and Y. Lim, "Modified annular ring slot antenna for dual wlan band application," in *2008 International Conference on Microwave and Millimeter Wave Technology*, vol. 1, April 2008, pp. 410–412.

[3] H. W. Liu, C. H. Ku, and C. F. Yang, "Novel cpw-fed planar monopole antenna for wimax/wlan applications," *IEEE Antennas and Wireless Propagation Letters*, vol. 9, pp. 240–243, 2010.

[4] M. J. Chiang, S. Wang, and C. C. Hsu, "Compact multifrequency slot antenna design incorporating embedded arc-strip," *IEEE Antennas and Wireless Propagation Letters*, vol. 11, pp. 834–837, 2012.

[5] J. Tao, C. H. Cheng, and H. B. Zhu, "Compact dual-band slot-antenna for wlan applications," *Microwave and Optical Technology Letters*, vol. 49, no. 5, pp. 1203–1204, 2007. [Online]. Available: http://dx.doi.org/10.1002/mop.22395

Chapter 5

CPW FED COMPACT BENT MONOPOLE ANTENNAS FOR UWB APPLICATIONS

This chapter aims at the design of CPW fed compact bend monopole Antenna for UWB applications. The antenna evolution from a basic quarter wave monopole antenna is discussed. The reflection characteristics of the antenna and the radiation properties are discussed. Since UWB antennas aim at short range transient pulse communications, the time domain properties of the antenna such as pulse response, transfer function, fidelity and the group delay are analyzed. The empirical design equation for the antenna is derived and validated on different substrates.

Contents

5.1   Review on Planar UWB Antennas

UWB technology is having a greater interest in the modern day world. UWB aims at high-speed communication using short transient pulses. Plenty of antennas are designed for this purpose [1–7]. This chapter focuses on the development of uniplanar UWB antenna using CPW feed. The proposed antenna is derived from an basic CPW fed monopole antenna. Monopole antennas are the prime choice of an antenna designer of modern communication era because of its simplicity and ease of design. Monopole antennas offer Omni-directional radiation pattern, and the bandwidth can be enhanced quite easily. In the earlier days, the monopole antennas are placed perpendicular to the ground plane. Thus it was too complex to use in planar compact electronics gadgets. The total size and the complexity of the system are increased because of this.

This created a space for the printed monopole antenna [8,9]. They can be fabricated along with the microwave integrated circuits on the same dielectric substrate. Since the thesis is investigating on the small uniplanar antennas, the aim is to build a uniplanar UWB antenna with the ground plane and the signal strips fabricated in the same plane. Thus the integration of circuits components will become easy as the antenna ground will be connected to the circuit ground. This antenna is compact with low fabrication cost. Thus printed monopole antennas are the excellent choice for UWB applications.

The bandwidth of a monopole antenna can be enhanced either by modifying the ground edge, radiator edge or the feed transitions. In the case of microstrip antennas truncating the ground plane results in a wide bandwidth. Various designing techniques for enhancing the bandwidth of a basic square monopole [10] are shown in Fig 5.1. In all the design methods we can see the level of complexity involved.

The proposed antenna is different from the above mentioned design techniques. The evolution of the proposed design is explained in the next section. A basic quarter wave monopole antenna is transformed into the compact UWB antenna.
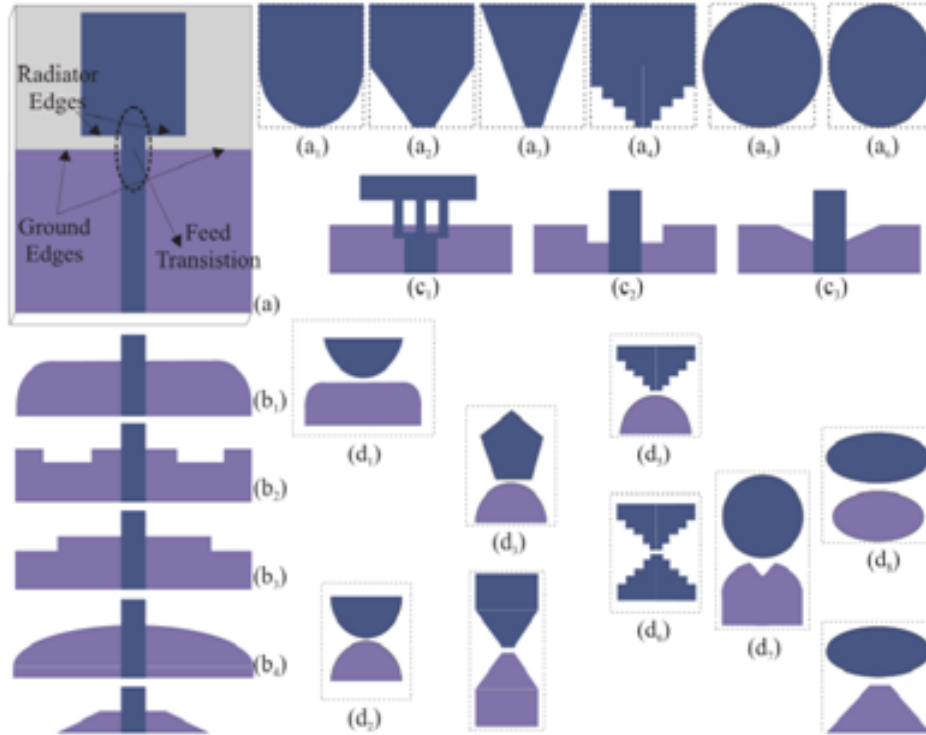
Figure 5.1: Modifications on planar monopole antennas for obtaining UWB response (Picture courtesy: Deepti Das Krishna,"Investigations on broadband planar monopole and slot radiators and their suitability for UWB Applications)

5.2   Evolution of the Proposed Design

The first stage of the design is a CPW fed monopole antenna with a length of 15 mm (L_m = 15 mm). The length L_m is quarter wave approximate of the guided wavelength. The monopole antenna is bent in the form of an inverted L shape by adding a strip with length L_2. This resulted in two resonances one at 3.4 GHz and other at 10 GHz. This resulted in two resonances with moderate matching. The gap between the horizontal strip and ground is reduced which resulted in better impedance matching for a wide band of frequencies. The gap g_2 and the left ground dimensions are optimized to obtain the final design and the UWB response. All the geometrical evolution is shown in Fig 5.2, and the corresponding reflection characteristics are shown in Fig 5.3.
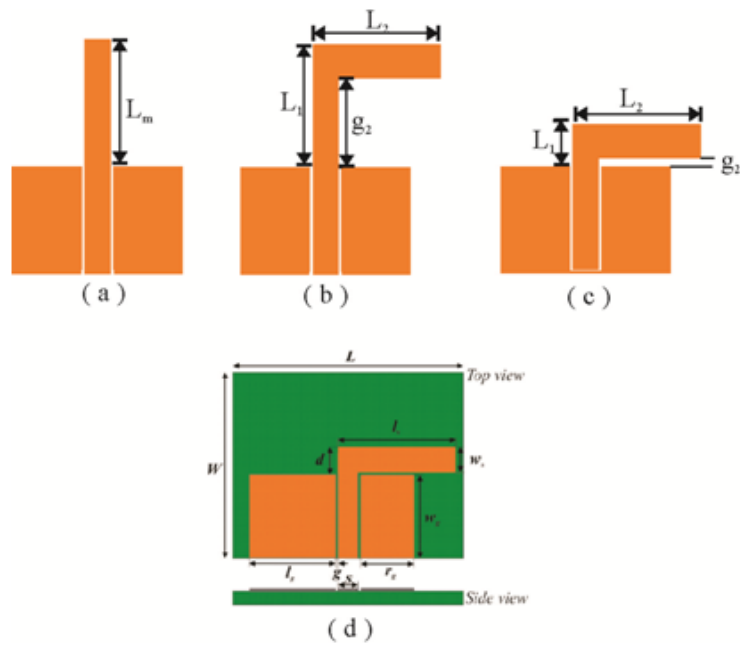
Figure 5.2: Evolution of the proposed antenna.(a) monopole (b)bent monopole (c)bent monopole with reduced gap.(d) final design
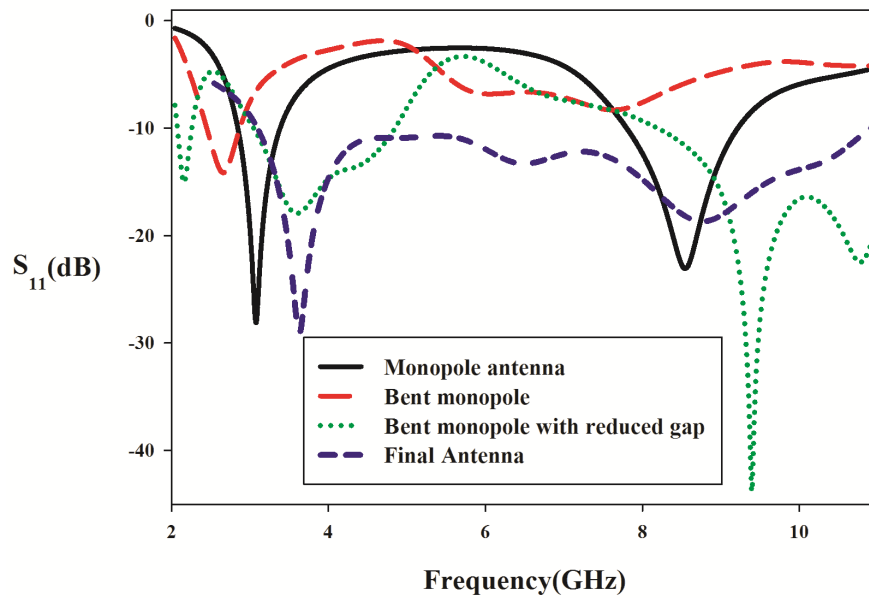

Figure 5.3: Reflection characteristics of the various stages of Evolution

5.3   Parametric Analysis

Parametric analysis of the antenna of the antenna is performed to obtain a clear view of the cause of resonance and the effect of various parameters on the radiation characteristics. The reason for impedance matching can also be identified.
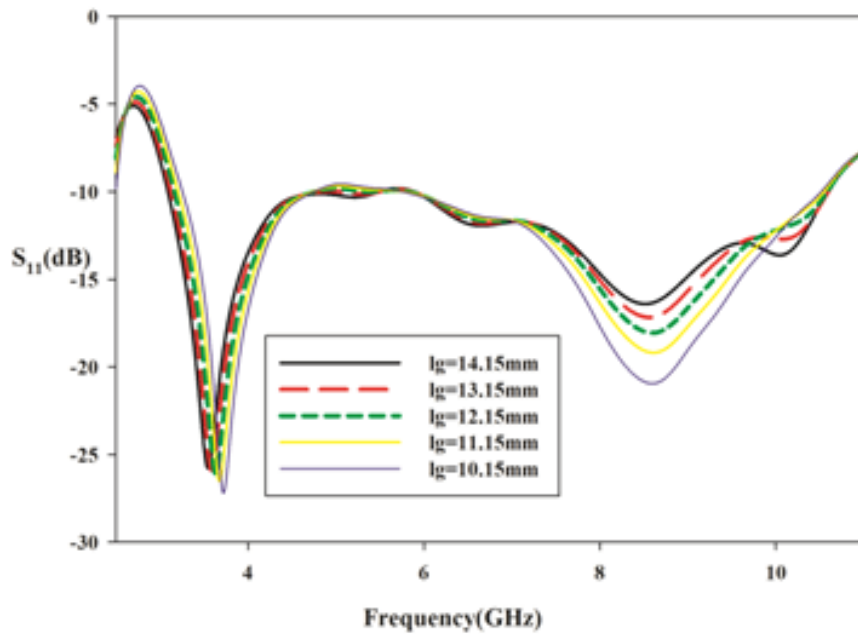
5.3.1   Effect of the parameter l_g

Figure 5.4: Effect of l_g on the reflection characteristics

The reflection characteristics of the antenna for various l_g are analyzed. The results of this study are plotted in Fig 5.4. From the fig, it is seen that the first resonance shifts to a lower value as the length l_g is increased without much change in the impedance matching. The second resonance at 8.6 GHz is not at all affected by the variation of the parameter l_g.

5.3.2 Effect of the Parameter W_g.

The dependence of W_g on the reflection characteristics are simulated and the results are shown in Fig 5.5. From the figure, it is clear that the first resonance frequency remains the same without any shift. Thus the first resonance is independent of the length W_g, but the impedance matching of the first resonance is affected. As W_g increases the capacitive reactance is reduced, and the imaginary part of the impedance approaches to zero. Thus the antenna impedance is nearly the 50Ω. Hence proper impedance matching is obtained. The second resonance at 8.5 GHz is shifted to a lower value as we increase the W_g. The impedance matching at this resonance also is enhanced as we increase W_g. This is due to the change in antenna input impedance towards a real value.
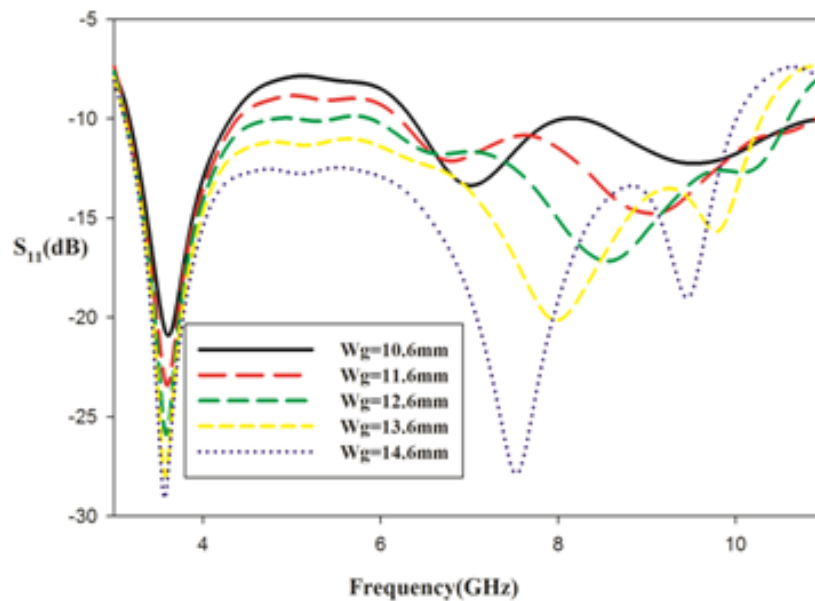
Figure 5.5: Effect of Parameter W_g on the reflection characteristics

5.3.3 Effect of the Parameter l_s.

The variation in reflection characteristics with respect to the change in the length l_s is analyzed, and the results are shown in Fig 5.6.From the fig, it is
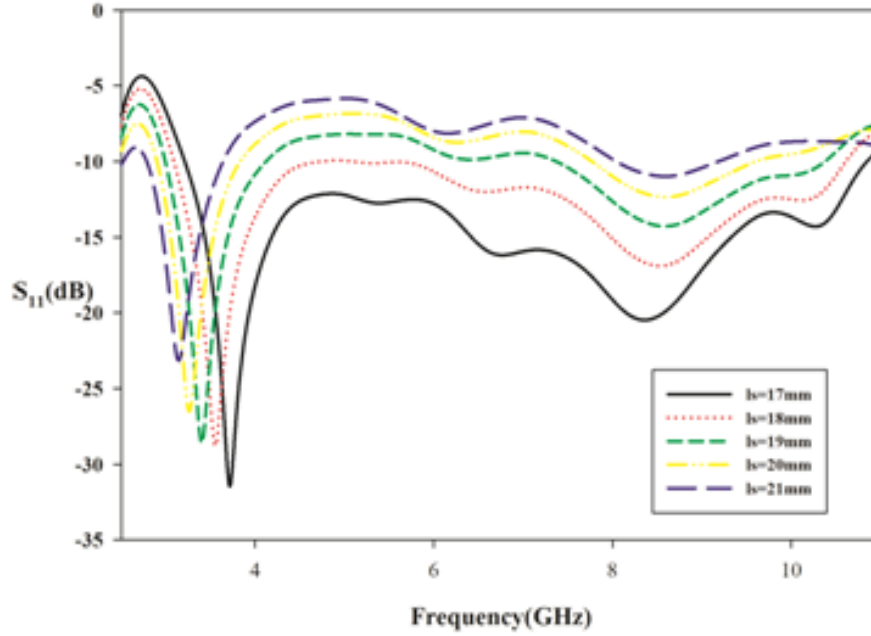
Figure 5.6: Effect of Parameter l_s on the reflection characteristics

seen that the first resonance centered at 3.6 GHz comes to a lower value as we increase the strip length. The impedance matching at the first resonance is not much affected by this variation. The second resonance at 8.6 GHz is also slightly changed with an impedance variation.

5.3.4   Effect of the Parameter W_s on the Reflection Characteristics

The effect of W_s on the reflection characteristics is shown in Fig 5.7. First resonance remains the same as we vary this parameter. The second resonance at 8.6 GHz is also not affected by this variation study. There is a slight reduction in the impedance matching as we increase the W_s. This is due to the change in the reactive impedance of the antenna.
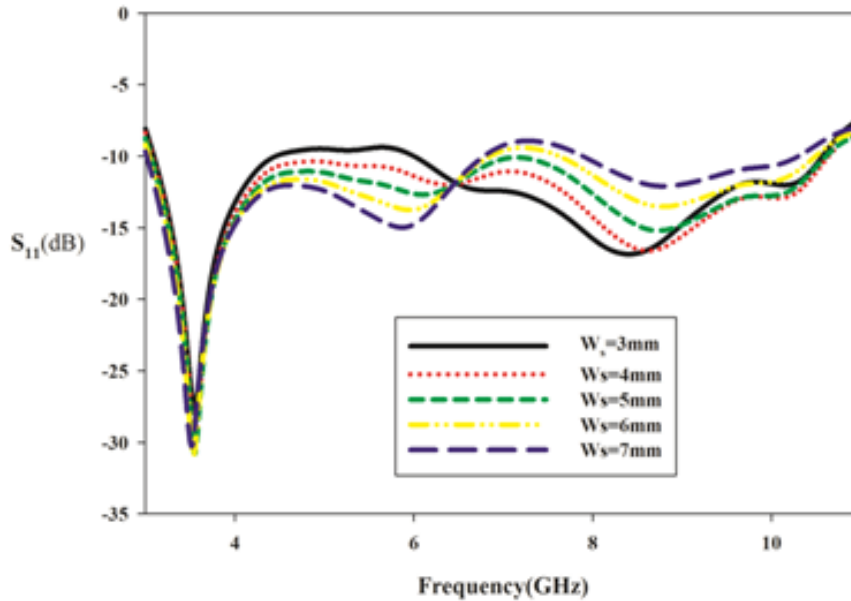
Figure 5.7: Effect of Parameter W_s on the reflection characteristics

5.4 Surface Current Analysis and 3D Radiation Pattern of the Antenna

It is seen from the parametric studies that the merging of two resonances gives rise to the UWB performance of the antenna. The reason for the resonance is analyzed using the simulated surface current distributions. The antenna lengths which are the part of the effective resonance path are figured out using this analysis. The simulated surface current distributions are examined in the following sections. The surface current distribution at 3.6 GHz is shown in Fig 5.8 . From the figure, it is seen that a dipole like current distribution is seen along the path ABC, with minima points at A and C and the maxima points between them(B). The lengths ls and lg are the lengths along the path ABC.
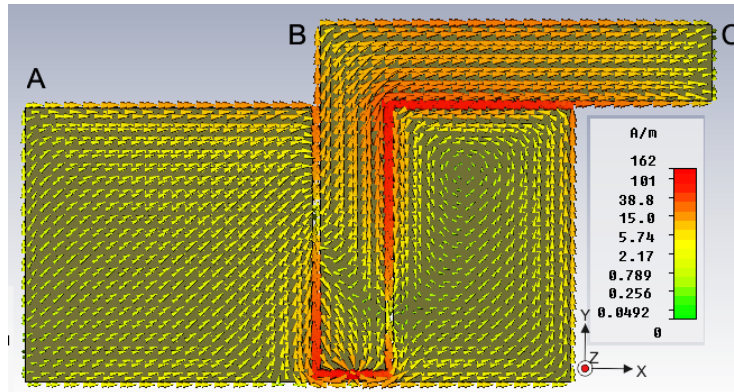
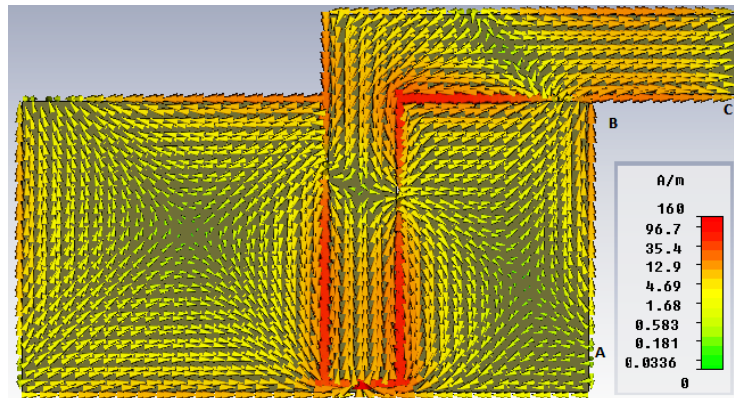*Figure 5.8: Simulated Surface current distribution at 3.6 GHz*

Figure 5.9: Simulated Surface current distribution at 8.6 GHz

Hence the parametric results are validated. Surface current distribution at 8.6 GHz is shown in Fig 5.9. From the figure, a half wave variation is seen across the path ABC. The minimal surface current density is observed at A and C. The maximum surface current density is viewed along the length W_g. Thus the parametric analysis of W_g is validated. These two resonances are merged to form the UWB characteristics. The simulated 3D radiation pattern of the antenna at 3.6 GHz is shown in the Fig 5.10. From the figure, it is seen that the maximum radiation is towards the Y-axis which is perpendicular to the direction of the maximum surface current density. The pattern is tilted by an angle 45°. This is due to the asymmetry in the ground. The left ground width is 5 mm larger than the right ground width. Null is placed in the X-axis
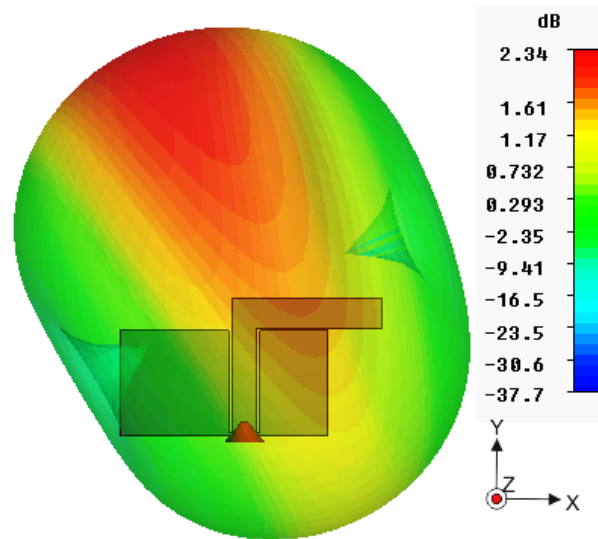
with the slight twilt.

Figure 5.10: Simulated 3D radiation pattern at 3.6 GHz

The simulated 3D radiation pattern at 8.6 GHz is shown in Fig 5.11. The maximum radiation is seen along the Y-axis with a tilt. The null of the pattern is along the X-axis. The pattern seems to be more directional along the Y direction.

5.5   Antenna Design

The characteristics of the antenna are analyzed from the surface current distributions and the parametric studies. The reasons for the two resonance were identified and the from the various parametric studies, the optimum antenna parameters are identified, and the design is shown in Fig 5.12 along with the optimized parameters. Commercially availuable Fr4 is used for the design of the antenna.

The various parameters of the antennas are related with respect to the wavelength of the first resonance is discussed in the following section. The antenna parameters on different dielectric substrates are computed using the
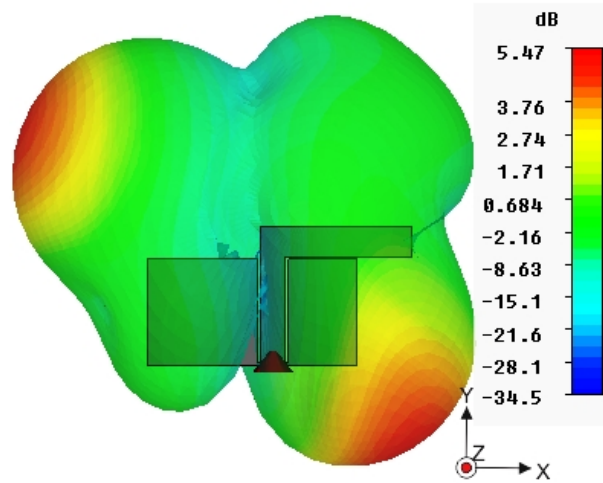
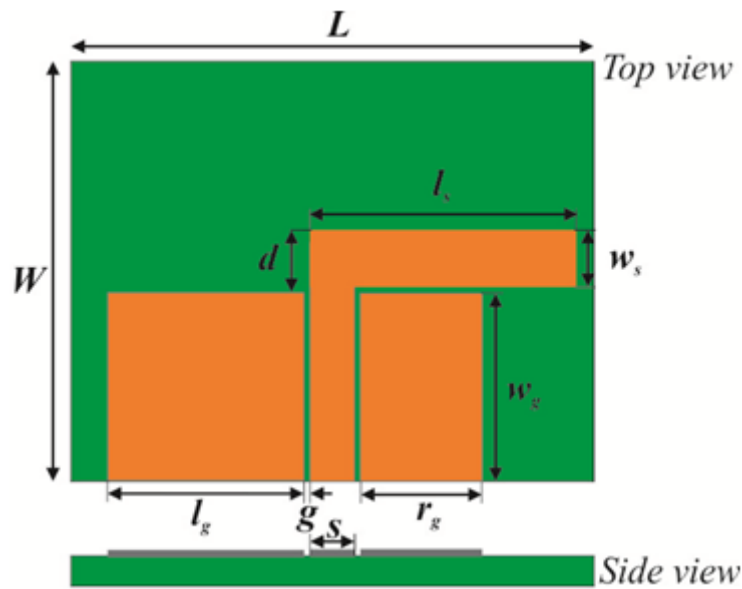*Figure 5.11: Simulated 3D radiation pattern at 8.6 GHz*

Figure 5.12: Antenna design with the optimized parameters. ($l_s = 18$ mm, $W_s = 4$ mm, $l_g = 13.15$ mm, $r_g = 8.15$ mm, $W_g = 12.6$ mm, $s = 3$ mm, $g = 0.35$ mm)

equations 5.1 to equation 5.5 and shown in table 5.1. These designs are simulated in CST and the results are plotted in Fig 5.13. All the three simulated results show UWB response with good impedance matching.

$$l_s = 0.350\lambda_{g1} \tag{5.1}$$

$$l_g = 0.259\lambda_{g1} \tag{5.2}$$

$$W_s = 0.079\lambda_{g1} \tag{5.3}$$

$$W_g = 0.248\lambda_{g1} \tag{5.4}$$

$$r_g = 0.160\lambda_{g1} \tag{5.5}$$

Table 5.1: Computed antenna parameters from the design equations

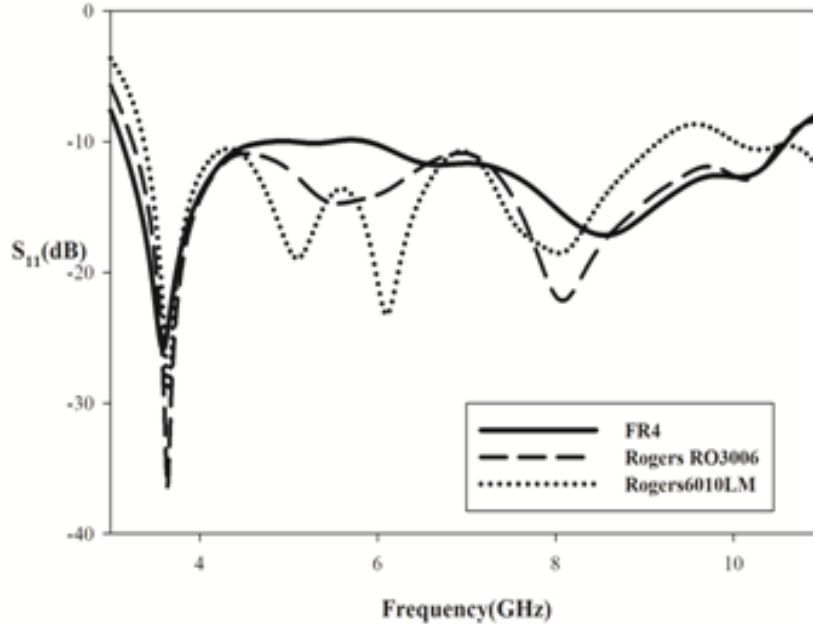|	Antenna 1	Antenna 2	Antenna 3
Substrate	FR4 EPOXY	ROGERS RO 3006	ROGERS 6010 LM
h	1.6	1.28	0.635
ϵ_r	4.4	6.15	10.2
ϵ_{re}	2.7	3.575	5.6
s	3	2.58	2.05
g	0.35	0.45	1.28
L_s	18	15.64	12.5
l_g	13.15	11.43	9.13
r_g	8.15	7.09	5.67
W_g	12.6	10.95	8.75
W_s	4	3.48	2.78

Figure 5.13: Reflection characteristics of the Antennas for computed parameters on different substrates

The CPW strip width and the gap are designed for 50Ω impedance. The effective permittivity (ϵ_{re}) of the substrate is calculated using, $\epsilon_{re} = (\epsilon_r + 1)/2$. As all the simulations showed similar responses, the antenna design equations are considered to be validated. The proposed antenna is easy to fabricate since it is uniplanar and there are a few geometrical parameters.

5.6 Experimental Results in the Frequency Domain

The proposed antenna is fabricated on an FR4 substrate using photolithography process . The measurements are taken using $HP8510c$ Network analyzer. The measured reflection characteristics of the antenna are plotted along with the simulated one, which is shown in Fig 5.14. It can be seen that both are
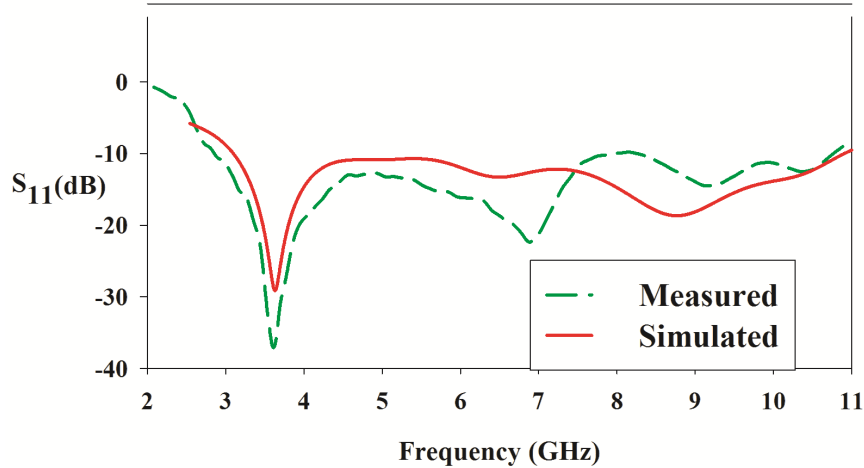
in good agreement.

Figure 5.14: Reflection characteristics of the antenna

The gain and efficiency of the antenna is measured in the entire frequency band and plotted in Fig 5.15. The proposed antenna has an average gain of 3.09 dBi. The efficiency of the antenna is calculated using Wheeler cap method. The antenna has an average efficiency of 87.5% over the entire band. The measured radiation pattern of the antenna in XZ-plane and YZ-plane are shown in Fig 5.16. It is seen that the radiation patterns are almost identical in all the chosen frequencies. The parameter l_s and l_g forms an arbitrary dipole at the lower resonant frequency. This results in an approximate figure of eight radiation pattern at the YZ-plane. The Omni-directional pattern is obtained in the XZ-plane for all the chosen frequencies.

5.7   Time Domain Analysis of the Antenna.

UWB antennas are used for transmitting short transient pulses. The frequency domain studies of the antenna are done in the previous sections. It is equally important to examine the time domain characterizations of the antenna which is done in the following sections.
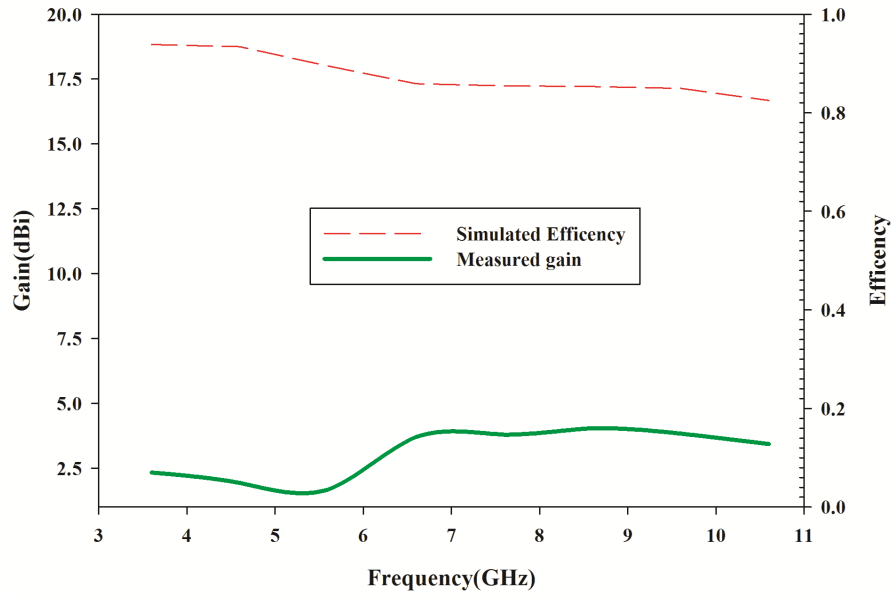
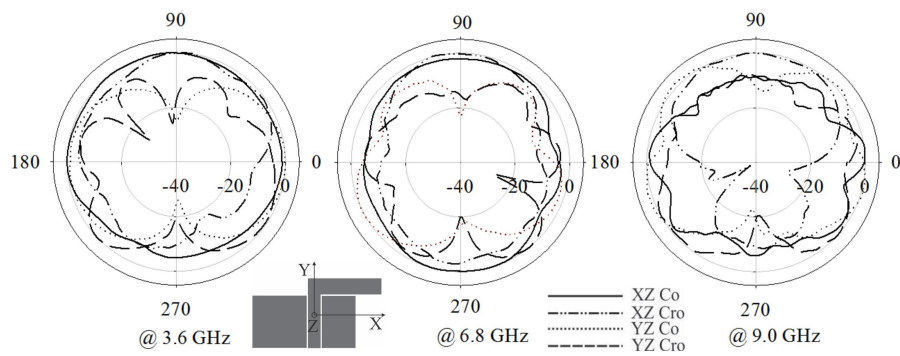*Figure 5.15: Gain and efficiency of the proposed antenna over the entire band*

Figure 5.16: Measured Radiation pattern of the proposed antenna

5.7.1 Group Delay

Group delay is an important parameter to be considered while transmitting short pulses. It is the negative angular frequency derivative of phase. Group delay is used to measure the dispersive nature of the antenna. Since UWB antenna can be considered as a filter, when an input pulse enters it, pulse undergoes different phase shifts for different frequency components. This leads to the spreading of the pulse and distortions take place. The group delay has to be minimum in the case of a UWB antenna. The group delay for the CPW fed compact bent monopole antenna is shown in Fig 5.17 for both the face to face and side by side orientations.
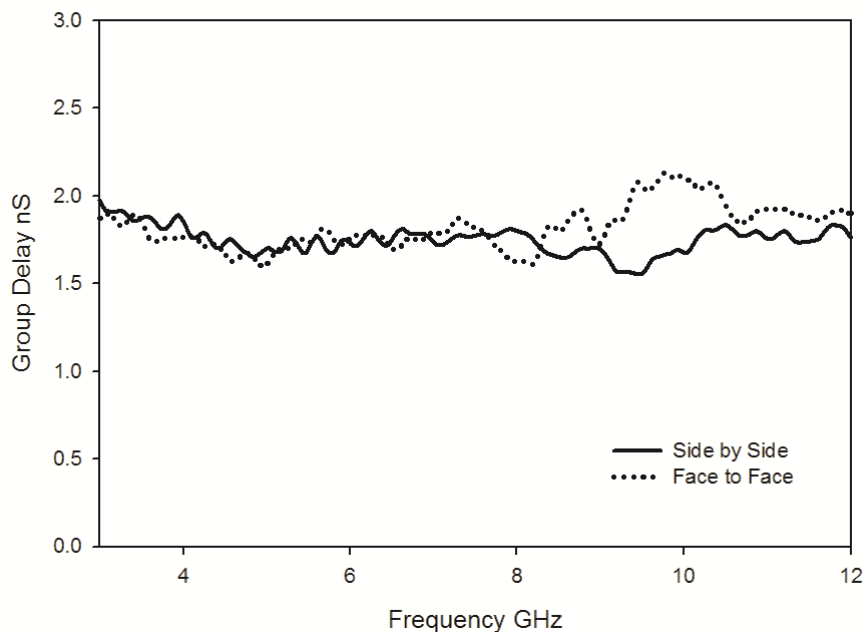

Figure 5.17: Measured group delay of the antenna

The measured group delay of the antenna comes between $1nsec$. This shows the linear phase characteristics of the antenna and the pulse handling the capacity of the antenna is excellent which is essential in communication systems.
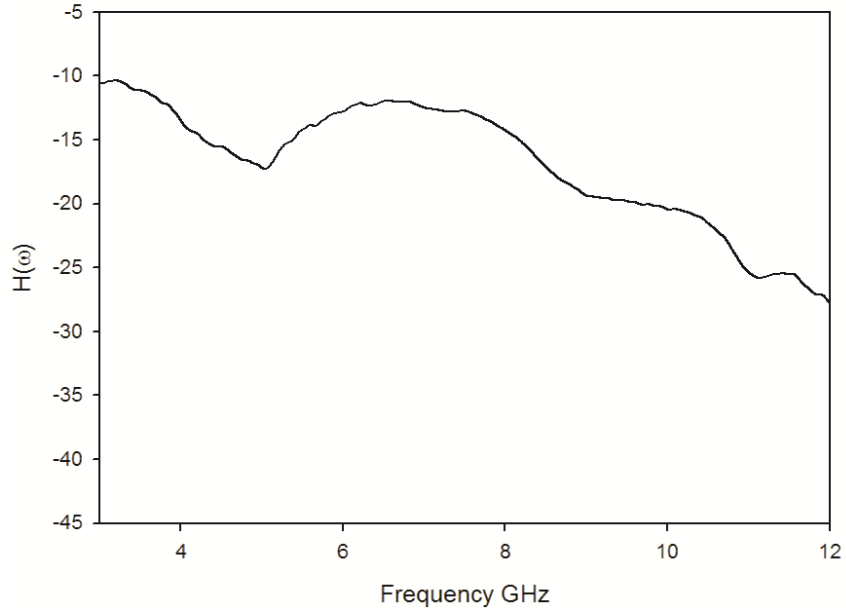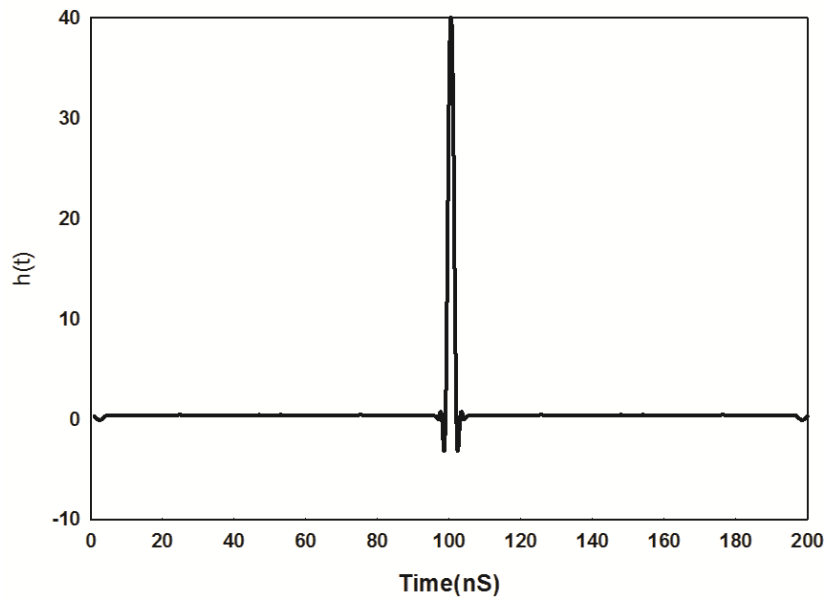
Figure 5.18: Measured transfer function of the antenna

Figure 5.19: Impulse response of the proposed antenna

5.7.2 Transfer Function

The transfer function of the UWB antenna is the Fourier transform of the impulse response. The transfer function of the antenna is measured as per the procedure explained in the methodology section. The measured transfer function of the antenna is shown in Fig 5.18. A decrease in transfer function is seen at the high frequency. The transfer function of the antenna measured here is in the direction of maximum radiation.

5.7.3 Impulse Response

The impulse response of a UWB antenna system may be defined as the output of the system when its input is an impulse signal. It can be obtained by converting the frequency domain transfer function measured in the direction of maximum radiation to the time domain. The impulse response is obtained by performing the inverse Fourier transform of the transfer function, and the result is shown in Fig 5.17. From the fig, it is seen that the ringing is minimum for the proposed UWB antenna. Thus it is a good candidate for UWB impulse transmission.

5.7.4 Received Pulse Waveforms

UWB communication systems use pulse signals as input. In this case, we use fourth order Gaussian derivative as our input. The input pulse given to the transmitting antenna should match with the pulse received by the receiving antenna. Useful information is carried by the signal envelope so the distortions should be minimum. The response of any system can be obtained by convoluting the input signal and the response of the system when it is given an impulse input. Here we convolute the fourth order Gaussian derivative input signal to the impulse response which is obtained by taking the inverse Fourier transform of the transfer function for both the face to face and side by side orientations. The transfer function is calculated from the measured S_{21} using Eqn 2.18. The pulse response for the antenna face to face and the side by side orientations are plotted in Fig 5.20.
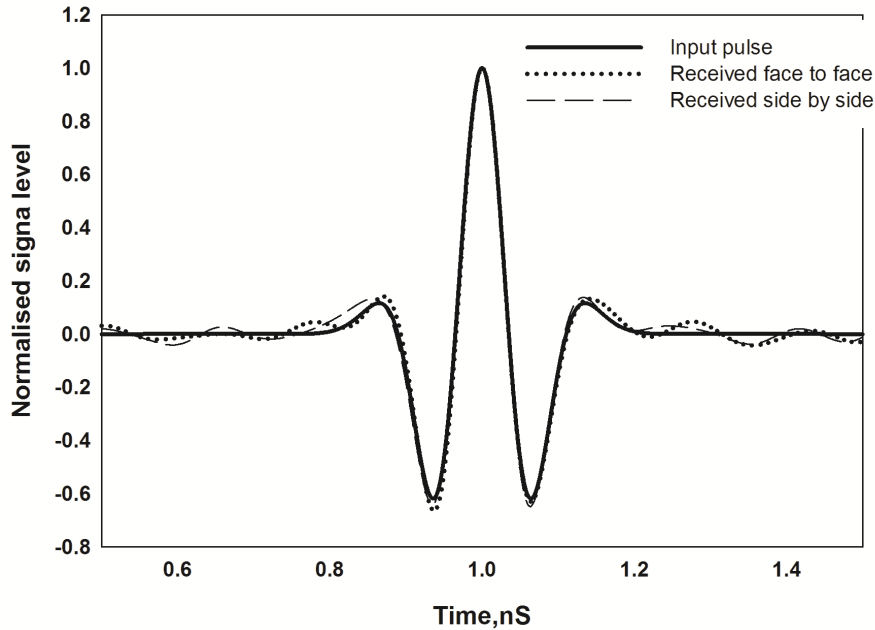
Figure 5.20: Input and received pulse waveforms

From the Fig 5.20, it is seen that the shape of the input pulse and the received pulse at face to face orientation and side by side orientation are same. This ensures the lossless reception of the transmitted data. There is a small amount of ringing present in the received waveforms which arise due to the channel noise.

5.7.5   Fidelity Factor

Fidelity is a parameter which is used to express the similarity between the transmitted pulse and the received pulse in a UWB communications system. It can be defined as the normalized cross-correlation of the reference signal and the measured signal. High fidelity is what is required in the UWB communication systems. The fidelity took from the simulation by placing probes for various azimuth and elevation angles as shown in Fig 5.21.

The fidelity along the azimuth plane is shown in Fig 5.22a. A peak fidelity factor of 0.96 is obtained. Average fidelity factor over the entire angles varied from 0° to 360° is obtained as 0.88. The simulated fidelity factor along the
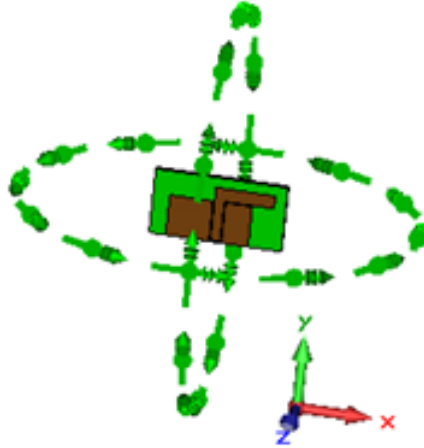
Figure 5.21: Fidelity measurement using probes (Simulation)

elevation plane is shown in Fig 5.22b. Peak fidelity of 0.914 is obtained, and the average fidelity over the elevation plane with 45° separation is 0.87.
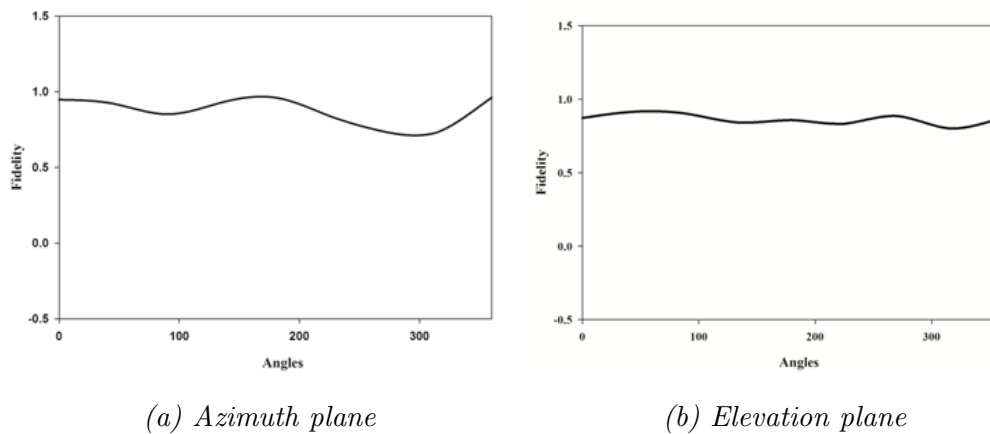

(a) Azimuth plane   *(b) Elevation plane*

Figure 5.22: Fidelity along

The similarity in the fidelity factors in both the azimuth and elevation plane shows that the antenna has good pulse handling capability. The input pulse and the transmitted pulse are having similar shapes at various angles.
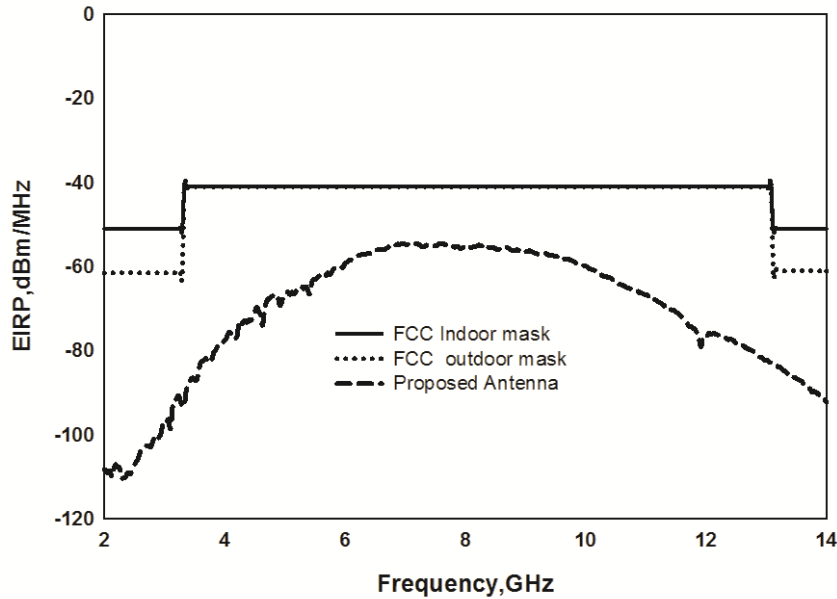
Figure 5.23: EIRP of the UWB antenna

5.7.6 EIRP (Effective Isotropic Radiated Power)

The UWB frequency range communication has power limited transmission as imposed by FCC. The EIRP of a UWB antenna should be less than the indoor and outdoor mask proposed by FCC. Fig 5.23 shows the EIRP for the fourth order Gaussian derivative input which is well within the FCC-imposed limits.

5.8 Chapter Conclusion

CPW fed compact bent monopole antenna for UWB applications is presented in this chapter. The antenna is a modification of the basic monopole

antenna. The proposed antenna has a wide operating bandwidth from 3.1 GHz to 10.8 GHz. The fabricated prototype of the antenna is shown in Fig 5.24 Design simplicity is the most attractive feature of the antenna along with the good pulse handling capacity and excellent frequency domain responses
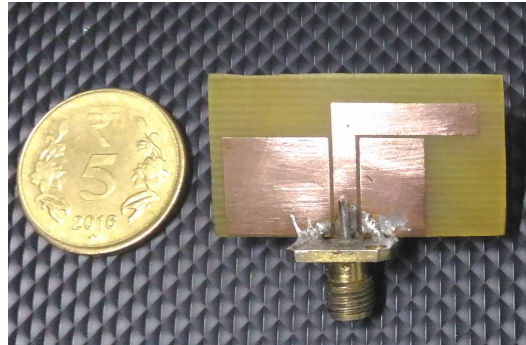
Figure 5.24: Fabricated prototype of the Antenna

REFERENCES

[1] J. D. Taylor, *Introduction to ultra-wideband radar systems.* CRC press, 1994.

[2] N. Behdad and K. Sarabandi, "A compact antenna for ultrawide-band applications," *IEEE Transactions on Antennas and Propagation*, vol. 53, no. 7, pp. 2185–2192, 2005.

[3] J. Jung, W. Choi, J. Choi *et al.*, "A small wideband microstrip-fed monopole antenna," *IEEE Microwave and Wireless Components Letters*, vol. 15, no. 10, pp. 703–705, 2005.

[4] C.-C. Lin, Y.-C. Kan, L.-C. Kuo, and H.-R. Chuang, "A planar triangular monopole antenna for uwb communication," *IEEE Microwave and Wireless Components Letters*, vol. 15, no. 10, pp. 624–626, 2005.

[5] J. Kim, T. Yoon, J. Kim, and J. Choi, "Design of an ultra wide-band printed monopole antenna using fdtd and genetic algorithm," *IEEE Microwave and Wireless Components Letters*, vol. 15, no. 6, pp. 395–397, 2005.

[6] D. Lamensdorf and L. Susman, "Baseband-pulse-antenna techniques," *IEEE Antennas and Propagation Magazine*, vol. 36, no. 1, pp. 20–30, 1994.

[7] H. G. Schantz, "Radiation efficiency of uwb antennas," in *IEEE Conference on Ultra Wideband Systems and Technologies*, vol. 2002, 2002, pp. 351–355.

[8] L. Guo, J. Liang, C. Parini, and X. Chen, "A time domain study of cpw-fed disk monopole for uwb applications," in *2005 Asia-Pacific Microwave Conference Proceedings*, vol. 1. IEEE, 2005, pp. 4–pp.

[9] Y. J. Cho, K. H. Kim, D. H. Choi, S. S. Lee, and S.-O. Park, "A miniature uwb planar monopole antenna with 5-ghz band-rejection filter and the time-domain characteristics," *IEEE transactions on antennas and propagation*, vol. 54, no. 5, pp. 1453–1460, 2006.

[10] D. Das Krishna, "Investigations on broadband planar monopole and slot radiators and their suitability for uwb applications," *PhD thesis*, 2012.

Chapter 6

CONCLUSION

> *This chapter brings up the total outcome of the research carried out by the author and highlights the achievements of the research work. This is followed by few suggestions for future work.*

Contents

6.1 Thesis Summary and Conclusions

The thesis focused on the design and development of compact uniplanar antennas for wireless communications. The various uniplanar antenna configurations are reviewed. Methods are proposed for creating efficient radiation. The uniplanar feeding methods such as Coplanar strips/slotline and coplanar waveguides are used. The whole thesis concentrated on designing simple antennas. The detailed study of CPS/slotline fed antennas both in the open ended configuration and closed ended configurations are studied using simulation and experiment.

The thesis focuses on compact uniplanar antenna structures designed using different methods. They are the open ended slotline fed antenna, closed ended slotline fed antennas and finally CPW fed antenna used for UWB applications. Exciting multiple resonances in the slot line resulted in dual band antenna configuration.CPS fed dual band antenna for PCS/WLAN applications are designed and the basic evolution is detailed. The proposed antenna

has almost symmetrical radiation pattern at both the frequency bands. The characteristics such as gain, efficiency, return loss, and radiation pattern are measured. The gain of the antenna measured is found to be 2.38 dBi and 3.4 dBi for lower and higher band respectively. Measured efficiency is found to be 88.6% and 92% respectively. The design equations of the antenna are formed and verified. The fourth chapter detailed the closed ended slot line fed antennas.Two different methods are proposed in this thesis so as to generate efficient radiation from a closed ended slotline. The first method adopts a transition from a slotline to a slot using an arrow shaped tapering at the bottom end. The slot mode resonance and the higher order resonance are excited hence resulted in a dual band antenna that radiated at 2.4 GHz and 5.8 GHz. The second method introduced for generating radiation is a novel one, which includes the coupling of the electromagnetic field from the slot line to the adjacent slots which resulted in an efficient radiator. Both the antennas possess excellent radiation properties. Various parametric studies are performed to identify the dependency of the antenna parameters on the resonances. In the first method, slotline fed uniplanar antenna for 2.4 GHz/5.8 GHz is designed and tested. Slot line coupled wideband slot radiator for 5.2 GHz/5.8 GHz is the antenna designed using the second method. The study on the evolution of the two antennas is done in detail. The design equations of both the antennas are developed and verified on different substrates. The fifth chapter describes the CPW fed compact bent monopole antenna for UWB applications. A basic CPW fed Quarter wave monopole antenna is transformed into a compact UWB antenna. Bending and properly optimizing the ground dimensions and the gap between the bent monopole and the ground resulted in UWB response. Two resonances at 3.6 GHz and 8.6 GHz are merged to give the UWB response. The frequency domain parameters of the antenna such as the radiation pattern, gain and the efficiency are measured. The antenna also posses excellent time domain characteristics which are essential for the pulse communication. In all the design methods the reason for the radiation is identified using the surface current distributions obtained from CST Microwave Studio. The importance of the uniplanar antenna is directly associated with the microwave circuit component integration.

6.2   Suggestions for Future Work

The following are some of the prospects for future work: All the antennas designed in this thesis are tested in an ideal noise-free environment. The effect of the interference of the electromagnetic waves which are present in the practical cases can be studied. Antennas can be tested along with the associated circuits as a complete working model.The antennas can be fabricated on an LTCC substrate so as to integrate directly with the MMIC circuits. The fabrication of the antennas on the flexible substrates allows it in the use of wearable antennas.More compact UWB antennas can be developed which can be used for the medical diagnosis and therapy purposes such as imaging and hyperthermia. UWB antenna arrays can be used for this purpose. The effect of the feeding cable and the surface waves has to be considered in designing an antenna for industrial use. UWB antenna arrays can be designed for beam forming.

Author's Resume

Education

May 2008–ongoing **PhD**, *From Department of Electronics, Cochin University of Science and Technology*, Kochi, Kerala , India, .
Specialization in Microwave Engineering

2004–2006 **Master of Science (MSc)**, *From University of Calicut*, Kerala, India, .
Specialized in Electronics science

2001–2004 **Bachelor of Science (BSc)**, *From University of Calicut*, Kerala, India, .
Specialized in Electronics Science

1999–2001 **PLUS TWO**, *NHSS VELLIYOOR*, Kerala , India, .
Maths, Physics,Chemistry and Biology

1999 **Secondary School Leaving Certificate (SSLC)**, *Board of Public Exams*, Kerala , India, .

Teaching Experience

Jun 2007 -March 2008 **Guest Lecturer**, College Of applied Science, IHRD, Kerala, India.
During this tenure, I taught Microprocessor, Digital Electronics, Electronics Circuits, Communication Engineering, Digital Communication, Electromagnetic Theory, Microwave Theory and Techniques . . . etc.Conducted practicals for Microprocessor, Electronic circuits, Communication, Digital Electronics

Industrial Experience

SEP 2009 -till **Junior Engineer**, BSNL Calicut SSA,Kerala, India.
During this tenure, I work with Broad band equipments maintanance,5ESS switch Maintanance,Leased Line Fault trouble shooting

Achievements

Junior Research fellowship and NET(JRF-2011) by UGC

KSCSTE Research Fellowship for the year 2007

First Rank for MSc Electronics ,Calicut University,Kerala

Publications

1. **S Sreenath**, P Ashkarali, P Thomas, R Dinesh, and CK Anandan, *"CPW-FED compact bent monopole antenna for UWB applications"*, Microwave and Optical Technology Letters 55 (1), 56-58, 2012.

(91) 8547591003 • (0496) 2673339
✉ sreenathatholi@gmail.com

2. **S Sreenath**, P Ashkarali, Nair M Sreejith, T Paulbert and Chandroth Aanandan, *"Slot Line Fed Uniplanar Antenna for 2.4/5.8 GHz WLAN Applications"*, European Journal of Advances in Engineering and Technology , 2(5): 7-11, 2015.

3. P Ashkarali, **S Sreenath**, R Sujith, R Dinesh, DD Krishna, and CK Aanandan, *"A compact asymmetric coplanar strip fed dualâĂŘband antenna for DCS/WLAN applications"*, Microwave and Optical Technology Letters 54 (4), 1087-1089, 2012.

4. P Ashkarali, **S Sreenath**, RK Raj, and C.K. Aanandan, *"Asymmetric Coplanar Strip Fed Pattern Reconfigurable Antenna"*, European Journal of Advances in Engineering and Technology, 2(6): 43-46, 2015.

5. Dibin Mary George, Libimol V. A., **Sreenath S**, Sreekala P.S and Aanandan C. K, *"High Gain Circular Sector Microstrip Patch Antenna for Millimeter Wave WLAN Applications"*, European Journal of Advances in Engineering and Technology, 3(9), 67-70, 2016.

6. Sreejith M. Nair, Shameena V.A, **Sreenath S** and P.Mohanan, *"Slotline fed Ultra Compact Antenna for Wide Band Applications"*, Microwave and Optical Technology letters,Vol.55, Issue 3, pp.526-529, March 2013.

7. Paulbert Thomas, G. K. Ullas, V. P. Sarin, **S. Sreenath**, and C. K. Aanandan, *"Microwave Characterization of Polyaniline Prepared via Agitation-Free Self-Stabilized Dispersion Polymerization"*, Advanced Carbon Vol. 1, 1âĂŞ6, 2014.

8. Neeraj K Pushkaran, Libimol V. A, Sreekala P. S, **Sreenath S**, Aanandan C. K. and Tessamma Thomas, *"Polyaniline Based Monopole Antenna for Broadband Applications"*, IJLRET International Journal of Latest Research in Engineering and Technology (IJLRET), 02(10),41 -44, 2016.

Technical Skills

Development Languages	MATLAB	Operating System	LINUX, WINDOWS
	VHDL,VERILOG		
Documentation	LaTeX, OPEN OFFICE		

Personal Vitae

Date Of Birth	30.05.1984
Contact Address	**Sreenath S**

Senior Research Scholar,	Sathyanivas (H)
Department of Electronics,	Atholi (PO)
Cochin University of Science and Technology,	Calicut-673315

Index